

AD _____

Award Number: DAMD17-97-1-7082

TITLE: Novel Mechanisms of Mammary Oncogenesis by Human
Adenovirus Type 9

PRINCIPAL INVESTIGATOR: Ronald Javier, Ph.D.

CONTRACTING ORGANIZATION: Baylor College of Medicine
Houston, Texas 77030

REPORT DATE: July 2000

TYPE OF REPORT: Annual

PREPARED FOR: U.S. Army Medical Research and Materiel Command
Fort Detrick, Maryland 21702-5012

DISTRIBUTION STATEMENT: Approved for Public Release;
Distribution Unlimited

The views, opinions and/or findings contained in this report are those of the author(s) and should not be construed as an official Department of the Army position, policy or decision unless so designated by other documentation.

REPORT DOCUMENTATION PAGE			Form Approved OMB No. 074-0188	
Public reporting burden for this collection of information is estimated to average 1 hour per response, including the time for reviewing instructions, searching existing data sources, gathering and maintaining the data needed, and completing and reviewing this collection of information. Send comments regarding this burden estimate or any other aspect of this collection of information, including suggestions for reducing this burden to Washington Headquarters Services, Directorate for Information Operations and Reports, 1215 Jefferson Davis Highway, Suite 1204, Arlington, VA 22202-4302, and to the Office of Management and Budget, Paperwork Reduction Project (0704-0188), Washington, DC 20503				
1. AGENCY USE ONLY (Leave blank)	2. REPORT DATE July 2000	3. REPORT TYPE AND DATES COVERED Annual (14 Jun 99 - 13 Jun 00)		
4. TITLE AND SUBTITLE Novel Mechanisms of Mammary Oncogenesis by Human Adenovirus Type 9		5. FUNDING NUMBERS DAMD17-97-1-7082		
6. AUTHOR(S) Ronald Javier, Ph.D.				
7. PERFORMING ORGANIZATION NAME(S) AND ADDRESS(ES) Baylor College of Medicine Houston, Texas 77030 E-MAIL: rjavier@bcm.tmc.edu		8. PERFORMING ORGANIZATION REPORT NUMBER		
9. SPONSORING / MONITORING AGENCY NAME(S) AND ADDRESS(ES) U.S. Army Medical Research and Materiel Command Fort Detrick, Maryland 21702-5012		10. SPONSORING / MONITORING AGENCY REPORT NUMBER		
11. SUPPLEMENTARY NOTES				
12a. DISTRIBUTION / AVAILABILITY STATEMENT Approved for public release; distribution unlimited			12b. DISTRIBUTION CODE	
13. ABSTRACT (Maximum 200 Words) The adenovirus E4 region-encoded open reading frame 1 (9ORF1) transforming protein is the major oncogenic determinant of human adenovirus type 9 (Ad9), a virus that generates exclusively estrogen-dependent mammary tumors in rats. We have found that 9ORF1 complexes with four different cellular PDZ-domain proteins (MUPP1, MAGI-1, ZO-2, and DLG) and that these interactions are essential for its transforming activity. The fact that three of these 9ORF1-associated PDZ-domain proteins also complex with high-risk papillomavirus E6 oncoproteins provides further evidence that these cellular factors are relevant to transformation. Prompted by the knowledge that PDZ domain-containing proteins generally function in cell signaling, we recently showed that 9ORF1 transforms cells, in part, by activating the phosphoinositide 3-kinase (PI 3-K)/protein kinase B (PKB) signaling pathway and, in addition, that this activity depends on the ability of 9ORF1 to complex with its cellular PDZ-domain protein targets. We report here that the 9ORF1-associated protein MAGI-1 complexes with the tumor suppressor protein PTEN, a lipid phosphatase that antagonizes PI 3-K/PKB signaling in cells. We postulate that MAGI-1 may be an essential co-factor for PTEN and that activation of PI 3-K/PKB signaling by E4-ORF1 may be due in part to its ability to inactivate this PDZ protein in cells.				
14. SUBJECT TERMS Breast Cancer, CDA Award			15. NUMBER OF PAGES 133	
			16. PRICE CODE	
17. SECURITY CLASSIFICATION OF REPORT Unclassified	18. SECURITY CLASSIFICATION OF THIS PAGE Unclassified	19. SECURITY CLASSIFICATION OF ABSTRACT Unclassified	20. LIMITATION OF ABSTRACT Unlimited	

NSN 7540-01-280-5500

Standard Form 298 (Rev. 2-89)
Prescribed by ANSI Std. Z39-18
298-102

FOREWORD

Opinions, interpretations, conclusions and recommendations are those of the author and are not necessarily endorsed by the U.S. Army.

 Where copyrighted material is quoted, permission has been obtained to use such material.

 Where material from documents designated for limited distribution is quoted, permission has been obtained to use the material.

 Citations of commercial organizations and trade names in this report do not constitute an official Department of Army endorsement or approval of the products or services of these organizations.

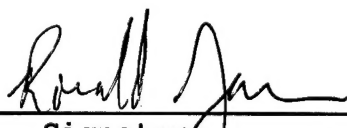
X In conducting research using animals, the investigator(s) adhered to the "Guide for the Care and Use of Laboratory Animals," prepared by the Committee on Care and use of Laboratory Animals of the Institute of Laboratory Resources, national Research Council (NIH Publication No. 86-23, Revised 1985).

N/A For the protection of human subjects, the investigator(s) adhered to policies of applicable Federal Law 45 CFR 46.

X In conducting research utilizing recombinant DNA technology, the investigator(s) adhered to current guidelines promulgated by the National Institutes of Health.

X In the conduct of research utilizing recombinant DNA, the investigator(s) adhered to the NIH Guidelines for Research Involving Recombinant DNA Molecules.

N/A In the conduct of research involving hazardous organisms, the investigator(s) adhered to the CDC-NIH Guide for Biosafety in Microbiological and Biomedical Laboratories.



PI - Signature Date

Table of Contents

Cover 1
SF 298 2
Foreword 3
Table of Contents 4
Introduction 5
Body6-9
Key Research Accomplishments10
Reportable Outcomes11
Conclusions12
References13
Appendices13

INTRODUCTION

One of my research career goals is to decipher a novel cellular pathway which, when perturbed, leads to the development of breast neoplasms. The proposed research focuses on a unique viral oncogenic determinant encoded by human adenovirus type 9 (Ad9), a virus that elicits exclusively mammary tumors in rats. Following infection of newborn rats with Ad9, female animals develop estrogen-dependent mammary tumors (primarily fibroadenomas) within multiple mammary glands after a three-month latency period, whereas no tumors of any type form in infected male rats. In contrast to other adenoviruses, Ad9's major oncogenic determinant is its E4 region-encoded open reading frame 1 (9ORF1) transforming protein. Results obtained to date suggest that the abilities of 9ORF1 to bind a select group of cellular proteins and to activate the phosphoinositide 3-kinase (PI 3-K)/protein kinase B (PKB) signaling pathway correlate well with its transforming function. Therefore, studies of this model system may reveal a completely new route for breast cancer development. The main goal of this project is to elucidate a detailed molecular model of 9ORF1 oncoprotein function. The two objectives of the proposed work are: (1) To identify the 9ORF1-associated cellular proteins and (2) To reveal the mechanism whereby 9ORF1 activates the PI 3-K/PKB signaling pathway in cells (revised objective).

BODY

TECHNICAL OBJECTIVE 1: Identify the 9ORF1-associated cellular proteins.

As we have succeeded in identifying the four major 9ORF-associated cellular proteins, this objective is now completed. Manuscripts describing the PDZ proteins MUPP1 and MAGI-1 as cellular targets of both 9ORF1 and high-risk papillomavirus E6 oncoproteins have recently been accepted for publication (see Appendices for attached preprints). Additionally, a manuscript identifying the PDZ protein ZO-2 as a specific cellular target for 9ORF1 is also now in preparation.

TECHNICAL OBJECTIVE 2 (REVISED): Reveal the mechanism whereby 9ORF1 activates the phosphoinositide 3-kinase (PI 3-K)/protein kinase B (PKB) signaling pathway in cells.

In the previous annual report, we presented preliminary evidence that 9ORF1 activates the PI 3-K/PKB signaling pathway (Fig. 1) in cells and that interactions of 9ORF1 with its cellular PDZ protein targets are required for this activity. In the current annual report, we present results extending these findings. Our results with 9ORF1 transformation-defective mutant proteins are summarized in Fig.2. The findings with 9ORF1 proteins having mutations within C-terminal Region III (the PDZ domain-binding motif) or Regions I and II (unknown functions) indicate that interactions of 9ORF1 with its PDZ protein targets are necessary, although not sufficient, for the transforming and tumorigenic potentials of this viral oncoprotein.

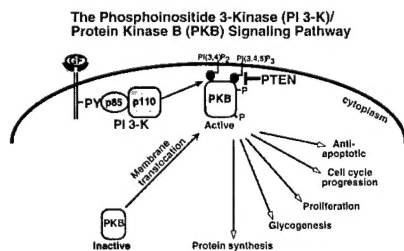


Fig. 1. Illustration summarizing the current model for activation of the PI 3-K/PKB signaling cascade by growth factors. In this model, PI 3-K associates with an activated growth factor receptor at the membrane, where it phosphorylates lipid substrates to generate D3-phosphoinositides. After translocation to the membrane by binding to these D3-phosphoinositide second messengers, PKB is subsequently activated by protein kinases such as PDK1 (not shown). Activated PKB regulates a variety of cellular processes, including apoptosis and cell cycle progression. The PTEN tumor suppressor protein antagonizes this signaling pathway by dephosphorylating the D3 phosphate of D3-phosphoinositides.

	Region I	Region II	Region III	Binding to PDZ proteins	Focus forming activity: Ad9 E4-ORF1	Transformation with Refs. BEE cells	Promoting mammary tumors
wild-type E4-ORF1	+	+	+	+++++	+++++	+++++	+++++
IA	+	+	+	+++++	-	+++	-
IIA	+	+	+	+++++	-	+++	-
IIB	+	+	+	+++++	-	+++	-
IIIA	+	+	+	-	-	-	-
T123D	+	+	+	-	-	-	-
V123A	+	+	+	-	-	-	-
IIIC	+	+	+	++	+	+	-
IIID	+	+	+	++	+	+	-
T108S	+	+	+	++++	+++++	+++++	+++++

Fig. 2. Protein binding and transforming properties of mutant Ad9 E4-ORF1 proteins.

The relative capacities of mutant Ad9 E4-ORF1 proteins (i) to bind the four E4-ORF1-associated cellular PDZ proteins, (ii) to induce transformed foci on CREF fibroblasts or primary rat embryo fibroblasts (REFs), or (iii) to promote Ad9-induced rat mammary tumors compared to the wild-type Ad9 E4-ORF1 protein are indicated. The transformation-proficient T108S E4-ORF1 mutant was included as a control in these assays. The facts that transformation-defective Region I and II mutants retain wild-type binding to PDZ proteins whereas the Region III mutants either fail or show reduced binding to these cellular factors suggest that these interactions are necessary but not sufficient for transformation by the Ad9 E4-ORF1 oncoprotein.

To initially show that 9ORF1 activates PKB in cells, we transfected COS7 cells with a 9ORF1 expression plasmid and subsequently measured the activity of PKB in these cells. The results showed that 9ORF1 activated PKB but not ERK2 in the cells, whereas Ras activated both of these signaling proteins (Fig. 3).

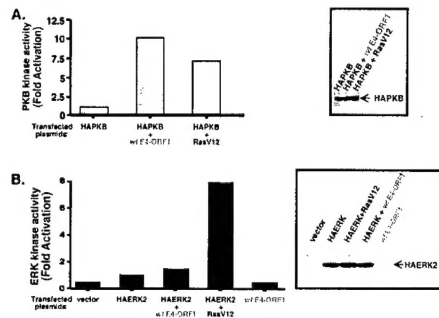


Fig. 3. Ad9 E4-ORF1 specifically activates PKB in COS7 cells. (A) COS7 cells on 60 mm dishes were lipofected with 1.6 μ g of pSG5-HAPKB plasmid and 6.4 μ g of either empty GW1 plasmid (vector) or a GW1 plasmid expressing wild-type E4-ORF1 or activated RasV12. Cells serum-starved for 16 h were harvested at 48 h post-transfection. Cell proteins (200 μ g) in lysis buffer were first immunoprecipitated with α -HA antibodies and then subjected to an *in vitro* PKB kinase assay using H2B as substrate (*left panel*). The right panel shows that similar amounts of HAPKB protein were used in these *in vitro* kinase assays. (B) COS7 cells were lipofected with pCEP-HAERK2 plasmid and either wild-type E4-ORF1 or activated RasV12 plasmid and then harvested as described in (A) above. Cell proteins (200 μ g) in lysis buffer were first immunoprecipitated with α -HA antibodies and then

subjected to an *in vitro* ERK2 kinase assay using MBP as substrate (*left panel*). The right panel shows that similar amounts of HAERK2 protein were used in these *in vitro* kinase assays.

To confirm and extend these findings, we performed similar assays in CREF cell lines stably expressing wild-type or mutant 9ORF1 proteins. The results showed that wild-type 9ORF1, but not the transformation-defective mutant 9ORF1 proteins, was able to activate PKB in these cell lines (Fig. 4). Similar results were obtained after transient expression of these 9ORF1 proteins in CREF cells (Fig. 5). These findings demonstrate that the oncogenic potential 9ORF1 is intimately linked to its ability to activate PKB in cells.

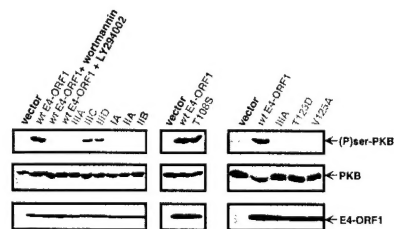
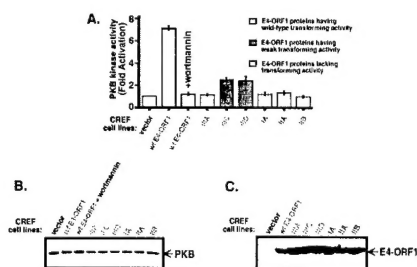


Fig. 4. Impaired PKB activation by Ad9 E4-ORF1 mutants in stable CREF cell lines. (A) Normal CREF cells or CREF cells stably expressing wild-type or mutant E4-ORF1 were serum-starved for 16 h. Cell proteins (1 mg) in lysis buffer were first immunoprecipitated with PKB antibodies (Upstate) and then subjected to an *in vitro* PKB kinase assay using histone 2B (H2B) as substrate. Phosphorylated H2B was detected by autoradiography and quantified with a phosphorimager. (B) Similar amounts of PKB protein were utilized in the *in vitro* kinase assays shown in (A) above. (C) The different CREF cell lines express similar amounts of E4-ORF1 protein.

Fig. 5. Impaired PKB activation by Ad9 E4-ORF1 mutants in transient expression assays in CREF cells. CREF cells were lipofected with 2 μ g of empty GW1 plasmid (vector) or a GW1 plasmid expressing wild-type or the indicated mutant E4-ORF1 protein. Cell proteins (100 μ g) in sample buffer were separated by SDS-PAGE and then immunoblotted with α -phospho-Akt(Ser473) [(P)ser-PKB], α -Akt, or α -E4-ORF1 antibodies.

Our results with Region III 9ORF1 mutants presented in Figs. 4 and 5 above further suggested that interactions of 9ORF1 with one or more of the four 9ORF1-associated PDZ proteins is required for activation of PKB. This finding prompted us to assess whether any of the 9ORF1-associated PDZ proteins may complex with components of the PI 3-K/PKB signaling-pathway. One such protein that we examined was the tumor suppressor protein PTEN, which is a lipid phosphatase that antagonizes PI 3-K in cells (see Fig. 1). Interestingly, like 9ORF1, PTEN has a PDZ domain-binding motif at its C-terminus. We found that PTEN co-immunoprecipitated with the 9ORF1-associated PDZ protein MAGI-1 from cell lysates (Fig. 6A). This interaction was mediated by four of the five MAGI-1 PDZ domains (Fig. 6B). Results with PTEN mutant V403A having a disrupted PDZ domain-binding motif further indicated that interaction of PTEN with three of the MAGI-1 PDZ domains (PDZ2, PDZ3, PDZ5) was dependent on the PTEN PDZ domain-binding motif whereas interaction of PTEN with MAGI-1 PDZ4 did not require this motif (Fig. 6B). The latter observation is likely to be the reason that the PTEN-V403A mutant retained approximately wild-type binding to MAGI-1 in co-immunoprecipitation assays (see Fig. 6A).

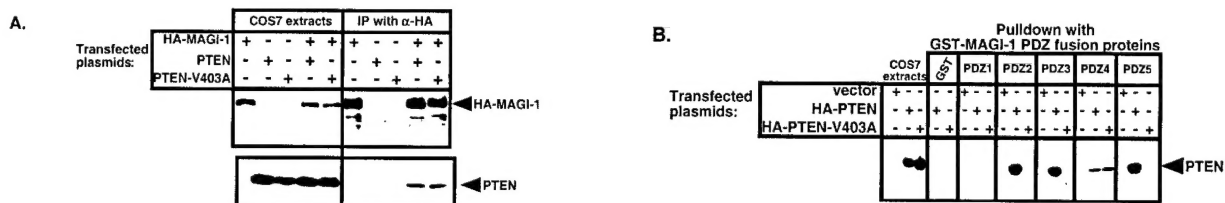


Fig. 6. PTEN binds to MAGI-1. (A) COS7 cells were transfected with an HA-MAGI-1 expression plasmid and a plasmid expressing either wild-type PTEN or mutant PTEN-V403A, which has a disrupted PDZ domain-binding motif. Cell proteins were immunoprecipitated with α -HA antibodies and then immunoblotted with the same antibodies or α -PTEN antibodies. (B) COS7 cells were transfected with a plasmid expressing either wild-type PTEN or mutant PTEN-V403A, and cell proteins were subjected to pull-down assays using GST fusion proteins containing each of the five MAGI-1 PDZ domains. These assays revealed that wild-type PTEN binds four of five MAGI-1 PDZ domains. Results with PTEN-V403A further show that the PDZ domain-binding motif of PTEN mediates binding to three such MAGI-1 PDZ domains.

In an attempt to specifically link the interaction between 9ORF1 with MAGI-1 to the ability of this viral oncoprotein to activate PKB in cells, we examined the consequences of MAGI-1 protein over-expression on 9ORF1-induced PKB activation. The results showed that overexpression of two different wild-type isoforms of MAGI-1, 1b and 1c, were able to block activation of PKB by 9ORF1 in CREF cells (Fig. 7). This effect was specific as MAGI-1 mutant Δ PDZ1&3, which fails to bind 9ORF1, was unable to diminish PKB activation by 9ORF1 in these assays.

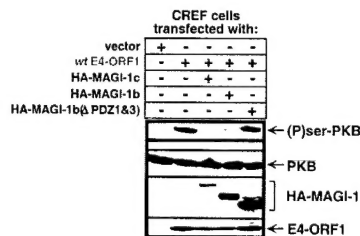


Fig. 7. Overexpression of MAGI-1 diminishes E4-ORF1-induced PKB activation. CREF cells were lipofected with 0.2 μ g of GW1-E4-ORF1 plasmid and 3 μ g of either empty GW1 plasmid or a GW1 plasmid expressing wild-type HA-MAGI-1b isoform, wild-type HA-MAGI-1c isoform, or mutant HA-MAGI-1b Δ PDZ1/3 (Δ PDZ1/3), which fails to bind to the E4-ORF1 protein. Cells lipofected with 3 μ g of empty GW1 plasmid (vector) were included as a negative control. Cell proteins (100 μ g) in sample buffer were immunoblotted with α -HA, α -phospho-Akt(Ser473), α -Akt, or α -E4-ORF1 antibodies.

From the results presented in this annual report, we postulate that MAGI-1 is an essential co-factor for PTEN and that activation of PI 3-K/PKB signaling by E4-ORF1 is due in part to its ability to inactivate this PDZ protein in cells.

Proposed Revised Statement of Work (SOW) for Final Year of Grant

(I am currently attempting to get approval for these SOW changes)

Technical Objective 2: Reveal the mechanism whereby 9ORF1 activates the phosphoinositide 3-kinase (PI 3-K)/protein kinase B (PKB) signaling pathway in cells.

Task 6: Months 36-48: Determine whether MAGI-1 and other 9ORF1-associated proteins enhance the function of PTEN in cells.

Task 7: Months 36-48: Assess whether the interaction of 9ORF1 with MAGI-1 blocks the function of PTEN.

Task 8: Months 36-48: Determine whether 9ORF1 can activate PKB in PTEN⁻ cells.

Task 9: Months 36-48: Assess whether 9ORF1 activates PI 3-K in cells.

Task 10: Months 36-48: Test whether 9ORF1 activates signaling proteins both upstream and downstream of PKB.

Key Research Accomplishments

- The Ad9 E4-ORF1 oncoprotein, which promotes mammary tumors in animals, selectively and potently activates the phosphoinositide 3-kinase (PI 3-K)/protein kinase B (PKB) signaling pathway in cells.
- Stimulation of PI 3-K/PKB signaling by E4-ORF1 is intimately associated with its ability to transform cells *in vitro* and to promote mammary tumors *in vivo*.
- Activation of PI 3-K/PKB signaling by E4-ORF1 is also dependent on its interactions with cellular PDZ proteins, most notably MAGI-1.
- MAGI-1 forms a complex with the PTEN tumor suppressor protein, a lipid phosphatase that antagonizes PI 3-K in cells.
- These findings suggest that Ad9 E4-ORF1 stimulates the PI 3-K/PKB signaling pathway by a novel mechanism of action.

Reportable Outcomes

Manuscripts

1. Pim, D., Thomas, M., Javier, R., Gardiol, D. and Banks, L. (2000). HPV E6 Targeted Degradation of the Discs Large Protein: Evidence for the Involvement of a Novel Ubiquitin Ligase. *Oncogene* 19:719-725.
2. Barritt, D., Pearn, M., Zisch, A., Lee, S., Javier, R., Pasquale, E. and Stallcup, W. (2000). The multi-PDZ domain protein MUPP1 is a cytoplasmic ligand for the membrane-spanning proteoglycan NG2. *J. Cellular Biochem.*, in press.
3. Lee, S., B. Glaunsinger, F. Montavani, L. Banks, R. Javier. (2000). The Multi-PDZ Domain Protein MUPP1 Is a Cellular Target for Both Adenovirus E4-ORF1 and High-Risk Papillomavirus E6 Oncoproteins. *J. Virol.*, in press.
4. Glaunsinger, B., S. Lee, M. Thomas, L. Banks, and R. Javier. (2000). Interactions of the PDZ-Protein MAGI-1 with Adenovirus E4-ORF1 and Papillomavirus E6 Oncoproteins. *Oncogene*, in press.

Abstracts/Presentations

R. Javier. Mammary Tumorigenesis by Human Adenovirus Type 9: A Role for Cellular PDZ Domain Proteins. Oral presentation for Symposium on Virus/Host Interactions in Pathogenesis at The American Society for Microbiology Meeting. May 30 - June 3, 1999.

R. Javier. A Role for Cellular PDZ Proteins in Tumorigenesis by Viral Oncoproteins. Oral presentation for The Special Interest Subgroup Meeting MAGUKs and PDZs at The American Society for Cell Biology 39th Annual Meeting. December 11 - 15, 1999.

R. Javier, S. Lee, B. Glaunsinger, R. Weiss, D. Thomas. The Adenovirus E4-ORF1 Oncoprotein Activates the PI 3-K/PKB Signaling Pathway by a Mechanism Involving Cellular PDZ Proteins. Poster presentation for The Era of Hope Meeting in Atlanta, Georgia. June 8-11, 2000.

Conclusions

Although the functions of the Ad9 E4-ORF1-associated PDZ proteins are not currently known, the domain structures of these polypeptides suggest that they function as adaptor proteins in cell signaling. In light of this observation, we tested here whether E4-ORF1 activates any known signaling pathways. Our results indicated that the tumorigenic potential of E4-ORF1 is intimately linked to its ability to activate the phosphoinositide 3-kinase (PI 3-K)/protein kinase B (PKB) signaling pathway in cells. Other results further showed that the capacity of wild-type E4-ORF1 to stimulate this signaling pathway can be blocked either by disruption of its PDZ domain-binding motif or by overexpression of the E4-ORF1-associated PDZ protein MAGI-1. These findings argue that activation of PI 3-K/PKB signaling by the Ad9 E4-ORF1 oncoprotein depends on its ability to complex with MAGI-1, and perhaps also with other E4-ORF1-associated cellular PDZ proteins. Significantly, we also showed that MAGI-1 forms a complex with the tumor suppressor protein PTEN, a lipid phosphatase that antagonizes PI 3-K/PKB signaling in cells.

"So What Section"

Our results suggest that MAGI-1 may be an essential co-factor for tumor suppressor protein PTEN and that activation of PI 3-K/PKB signaling by E4-ORF1 may be due in part to its ability to inactivate this PDZ protein in cells. Therefore, studies of the Ad9 E4-ORF1 oncoprotein are expected to reveal novel mechanisms for disregulating PI 3-K/PKB signaling in cells. Such findings would be significant considering that uncontrolled stimulation of this signaling pathway is associated with the development of a wide range of human malignancies, including breast cancer.

References

None cited.

Appendices

Manuscripts

1. Pim, D., Thomas, M., Javier, R., Gardiol, D. and Banks, L. (2000). HPV E6 Targeted Degradation of the Discs Large Protein: Evidence for the Involvement of a Novel Ubiquitin Ligase. *Oncogene* 19:719-725.
2. Lee, S., B. Glaunsinger, F. Montavani, L. Banks, R. Javier. (2000). The Multi-PDZ Domain Protein MUPP1 Is a Cellular Target for Both Adenovirus E4-ORF1 and High-Risk Papillomavirus E6 Oncoproteins. *J. Virol.*, in press.
3. Glaunsinger, B., S. Lee, M. Thomas, L. Banks, and R. Javier. (2000). Interactions of the PDZ-Protein MAGI-1 with Adenovirus E4-ORF1 and Papillomavirus E6 Oncoproteins. *Oncogene*, in press.



HPV E6 targeted degradation of the discs large protein: evidence for the involvement of a novel ubiquitin ligase

David Pim¹, Miranda Thomas¹, Ron Javier², Daniela Gardiol³ and Lawrence Banks^{*1}

¹International Centre for Genetic Engineering and Biotechnology, Padriciano 99, I-34012 Trieste, Italy; ²Division of Molecular Virology, Baylor College of Medicine, One Baylor Plaza, Houston, Texas, TX 77030, USA; ³Instituto de Biología Molecular y Celular de Rosario, Departamento de Microbiología, Facultad de Ciencias Bioquímicas, Suipacha 531, 2000 Rosario, Argentina

The Discs Large (DLG) tumour suppressor protein is targeted for ubiquitin mediated degradation by the high risk human papillomavirus (HPV) E6 proteins. In this study we have used a mutational analysis of E6 in order to investigate the mechanism by which this occurs. We first show that the differences in the affinities of HPV-16 and of HPV-18 E6 proteins for binding DLG is reflected in their respective abilities to target DLG for degradation. A mutational analysis of HPV-18 E6 has enabled us to define regions within the carboxy terminal half of the protein which are essential for the ability of E6 to direct the degradation of DLG. Mutants within the amino terminal portion of E6 which have lost the ability to bind the E6-AP ubiquitin ligase, as measured by their ability to degrade p53, nonetheless retain the ability to degrade DLG. Significant levels of DLG degradation are also obtained using wheat germ extracts which lack E6-AP. Finally, we show that the transfer of the DLG binding domain onto the low risk HPV-6 E6 confers DLG binding activity to that protein and, most significantly, allows HPV-6 E6 to target DLG for degradation. These results indicate that E6 mediated degradation of DLG does not involve the E6-AP ubiquitin ligase and, in addition, shows that the high and low risk HPV E6 proteins most likely share a common cellular intermediary in the ubiquitin pathway. *Oncogene* (2000) 19, 719–725.

Keywords: HPV E6; DLG; ubiquitin

Introduction

Human Papillomaviruses (HPVs) are the principal aetiological agent of cervical cancer (zur Hausen and Schneider, 1987; zur Hausen, 1991). The two viral types most frequently found in cervical tumours, HPV-16 and HPV-18, encode two oncoproteins, E6 and E7, which are largely responsible for the viruses' malignant potential. Both E6 and E7 interact with key components of the cellular regulatory machinery, in particular with the tumour suppressor proteins p53 and pRb respectively (Werness *et al.*, 1990; Dyson *et al.*, 1989). Although both E6 and E7 are retained and continually expressed in cervical tumours and derived cell lines (Schwarz *et al.*, 1985; Smotkin and Wettstein, 1986; Androphy *et al.*, 1987; Banks *et al.*, 1987), and both will co-operate with cellular oncoproteins in a variety of transformation systems (Matlashewski *et al.*, 1987; Pim *et al.*, 1994), there is now growing evidence that it

is the E6 protein that contributes most significantly to the malignant potential of the virus (Hiraiwa *et al.*, 1993; Song *et al.*, 1999). A major feature of the E6 proteins derived from the high-risk virus types is their ability to target cellular proteins for ubiquitin mediated degradation. This was first shown for p53, where the cellular protein E6-AP and E6 together function as an E3 ubiquitin ligase for the degradation of p53 (Werness *et al.*, 1990; Scheffner *et al.*, 1990; Huibregtse *et al.*, 1991, 1993). Although this activity of E6 is likely to play a role during the development of cervical tumours, it is clear that other functions of the E6 proteins are required for malignant progression. Several mutants of E6 have now been described which have lost the ability to interact with p53 but have retained the ability to transform cells (Pim *et al.*, 1994; Ishiwatari *et al.*, 1994; Nakagawa *et al.*, 1995; Inoue *et al.*, 1998). However, recent studies have defined a new cellular target of the high risk E6 proteins, the discs large (DLG) tumour suppressor protein, interaction with which would appear to be absolutely required for E6's transforming activity (Kiyono *et al.*, 1997).

The DLG protein belongs to a family of proteins called MAGUKs (membrane associated guanylate kinase homologues) (Lue *et al.*, 1994; Muller *et al.*, 1995). These proteins are characterized by having several PDZ domains, repeated throughout the length of the protein, which function as specific protein recognition motifs (Ponting and Phillips, 1995; Saras and Heldin, 1996; Kim, 1997; Kim *et al.*, 1998). Indeed, it is through interaction with these PDZ domains that the HPV-16 and HPV-18 E6 proteins can interact with DLG (Lee *et al.*, 1997; Kiyono *et al.*, 1997; Gardiol *et al.*, 1999). Little is known about the functions of the mammalian DLG protein as most of the studies to date have been performed on the *Drosophila* equivalent. Such studies have shown that knockout of the *dlg-1* locus is lethal, and a characteristic of these mutations is uncontrolled cell proliferation and loss of cell polarity (Woods *et al.*, 1996; Goode and Perrimon, 1997). Mammalian DLG is expressed in a variety of cell types, including epithelia where it has been shown to be located at regions of cell–cell contact (Lue *et al.*, 1994), and has been found in complex with the Shaker channel 4.1 protein and the tumour suppressor protein, APC (Kim *et al.*, 1995; Marfatia *et al.*, 1996; Matsumine *et al.*, 1996). Taking these data together, it is likely that DLG plays an intimate role in the processes that regulate cell polarity and cell growth in response to cell contact.

Recent studies have shown that tumours induced by E6 in transgenic animals are considerably more aggressive than those induced by E7 (Song *et al.*, 1999). In addition, mutational analysis of E6 indicates

*Correspondence: L Banks

Received 6 September 1999; revised 12 November 1999; accepted 23 November 1999

that the association with DLG is critical for its transforming activity in rodent cells (Kiyono *et al.*, 1997). More recently, we have shown that high risk E6 proteins can also target DLG for ubiquitin mediated degradation (Gardioli *et al.*, 1999). Degradation of p53 by E6 is known to involve the cellular ubiquitin ligase, E6-AP (Huibregtse *et al.*, 1991, 1993); however it is presently not known how E6 targets DLG for degradation. In order to address this question we have made use of a panel of HPV-18 E6 mutant proteins. We show that the regions of E6 that are required for degradation of DLG are distinct from those required for the degradation of p53. Using a series of chimaeric E6 molecules we have been able to show that the bulk of the activity lies within the carboxy terminal half of the E6 protein. We also show that the last seven amino acids of HPV-18 E6 (which include the DLG binding motif), when fused to the carboxy terminus of the low risk HPV-6 E6, will enable HPV-6 E6 to interact with DLG and, most significantly, will allow HPV-6 E6 to target DLG for degradation. These results demonstrate that the mechanism by which HPV E6 proteins target DLG for degradation most likely does not involve E6-AP. They also show that the E6 proteins from low risk HPV types can also interact with components of the ubiquitin pathway and suggests that their, as yet unidentified, substrate proteins may also be targets for ubiquitin mediated degradation.

Results

HPV-18 E6 binds DLG more strongly than HPV-16 E6

Previous studies had shown that sequences in the extreme carboxy terminus of HPV-16 and HPV-18 E6 were responsible for binding to the PDZ domains of DLG (Lee *et al.*, 1997; Kiyono *et al.*, 1997). In the case of HPV-16 E6 this appeared to require PDZ domain 2 (Kiyono *et al.*, 1997), whereas HPV-18 E6 was shown to be capable of binding independently to any of the PDZ domains 1, 2 or 3 (Gardioli *et al.*, 1999). This difference was believed to be related to the difference in the consensus PDZ binding motif between HPV-16 and HPV-18 E6. In order to directly compare the relative binding affinities of HPV-16 and HPV-18 E6 proteins for DLG, we first performed a GST pull down assay using GST-DLG and *in vitro* translated HPV-16 and 18 E6 proteins; GST-p53 was also included for comparison. The results are shown in Figure 1a. It is clear that while HPV-16 E6 binds somewhat more strongly to p53 than HPV-18 E6, which is in agreement with previous observations (Werness *et al.*, 1990; Scheffner *et al.*, 1990), HPV-18 E6 binds to DLG significantly more strongly than HPV-16 E6. To determine whether this is reflected in their respective abilities to degrade DLG, *in vitro* and *in vivo* degradation assays were then performed and the results are shown in Figure 1b,c respectively. As can be seen in both *in vitro* and *in vivo* assays HPV-18 E6 induces significantly greater degradation of DLG than HPV-16 E6. Therefore, these results confirm the previous supposition that HPV-18 E6 indeed has a stronger affinity for DLG than HPV-16 E6, and demonstrate that this is reflected in their respective abilities to target DLG for degradation.

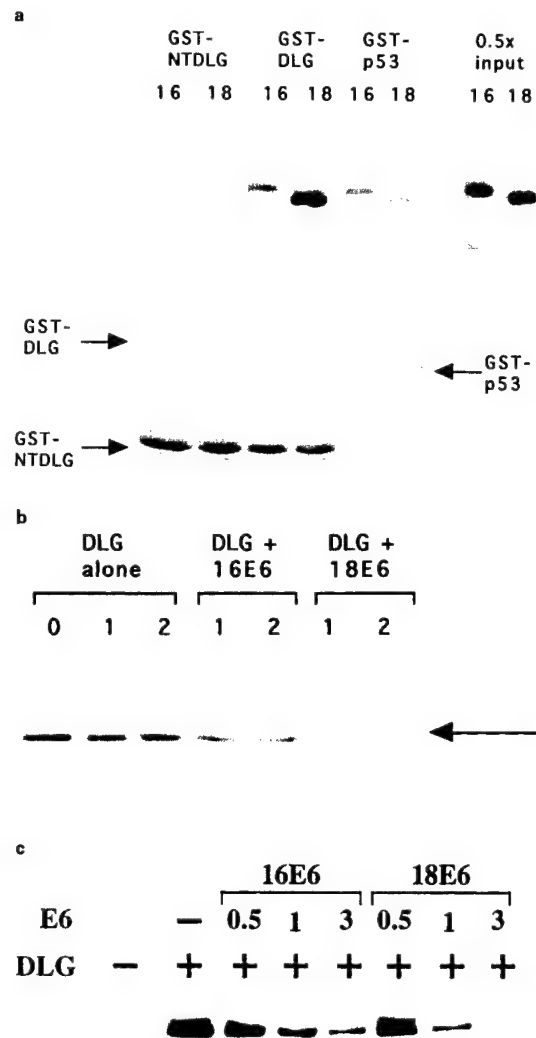


Figure 1 HPV-18 E6 interacts with DLG more strongly than HPV-16 E6. (a) *In vitro* translated HPV-16 and HPV-18 E6 proteins were used in GST-pull down assays with GST-DLG. GST-NTDLG, which lacks the PDZ binding domains, was used as a negative control and GST-p53 was used as a positive control. The lower panel is the Coomassie stained gel and shows equal levels of GST fusion protein loading for each pair of comparisons. The right-hand panel shows equal levels of input E6 proteins. Percentage recoveries were as follows: GST-NT DLG <1% 16E6 or 18E6; GST-DLG 37% 16E6, 82% 18E6; GST-p53 30% 16E6, 24% 18E6. (b) HPV-18 E6 induces a faster degradation of DLG than HPV-16 E6 *in vitro*. *In vitro* translated DLG was incubated, either alone or with HPV-16 or HPV-18 E6 at 30°C for 0, 1 or 2 h. The remaining DLG was detected by immunoprecipitation and autoradiography. (c) HPV-18 E6 degrades DLG more efficiently than HPV-16 E6 *in vivo*. U2OS cells were transfected with 3 µg of the DLG expression plasmid together with 0.5, 1 and 3 µg of either the HPV-16 or HPV-18 E6 expression plasmids as indicated. After 24 h cells were harvested and remaining DLG ascertained by Western blot analysis

Sequences in the carboxy terminal half of E6 are required for the degradation of DLG

Previous studies have defined the regions of E6 required for the binding and degradation of p53

(Crook *et al.*, 1991; Pim *et al.*, 1994; Li and Coffino, 1996). In order to determine whether similar regions of E6 were also involved in the degradation of DLG we made use of a previously characterized panel of HPV-18 E6 mutant proteins (Pim *et al.*, 1994) and these are shown schematically in Figure 2. Degradation assays were performed both *in vitro* and *in vivo* and the results obtained are shown in Figures 3 and 4 respectively. As can be seen, the regions of E6 required for the degradation of DLG encompass large portions of the E6 protein with, in particular, the region from amino acid 101 to amino acid 130, as defined by mutants ΔE , ΔF and ΔG , being particularly important both *in vitro* and *in vivo*. As can be seen from Figure 2, these mutations lie well outside the core DLG binding motif which is located at the extreme carboxy terminus of the E6 protein (residues 155–158). Interestingly, mutant ΔH ($\Delta 144$ –149) which lacks six amino acid residues immediately prior to the DLG binding motif, and thus brings the motif closer to the carboxy terminal loop, has no effect on the ability of E6 to degrade DLG, indicating that the spacing between the putative zinc finger and the DLG binding domain is not an important aspect of this activity. Most interesting are the results with the three amino terminal mutants of E6: M2 (R10S, P11G), ΔM ($\Delta 28$ –31) and ΔA ($\Delta 47$ –49). Both M2 and ΔA are defective with respect to their ability to induce p53 degradation (Pim *et al.*, 1994; Gardiol and Banks, 1998; see also Figure 5c), yet both are active with respect to DLG. Although the ΔA mutant is defective *in vitro*, it is interesting to note that it is active *in vivo*, suggesting significant differences between the two assay systems. This is consistent with previous observations which indicated that this was also the case with p53 degradation assays (Foster *et al.*, 1994; Crook *et al.*, 1996; Gardiol and Banks, 1998). Significant levels of DLG degradation were also obtained with the ΔM mutant which has been shown previously to be greatly reduced in its ability to bind E6-AP (Pim and Banks, 1999). Taken together, these studies demonstrate that the mechanism by which E6 targets DLG for degradation is separate from that used to target p53.

To further investigate any potential role for E6-AP in E6 mediated degradation of DLG we performed *in vitro* degradation assays using proteins translated in wheat germ extracts which lack any E6-AP (Huibregtse *et al.*, 1991). The results obtained are shown in Figure 5. As can be seen, both DLG and p53 are efficiently degraded by HPV-18 E6 when translated using rabbit

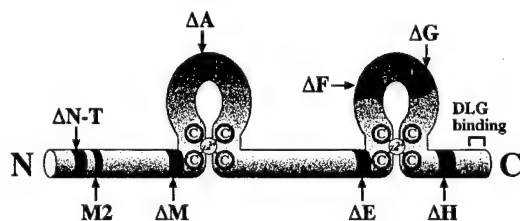


Figure 2 Schematic diagram showing the location of the mutations in HPV-18 E6 used in this study: $\Delta N-T$ ($\Delta 4$ –7), M2 (R10S, P11G), ΔM ($\Delta 28$ –31), ΔA ($\Delta 47$ –49), ΔE ($\Delta 101$ –104), ΔF ($\Delta 113$ –117), ΔG ($\Delta 126$ –130), ΔH ($\Delta 144$ –149). For comparison the position of the core DLG binding domain is also shown (residues 155–158)

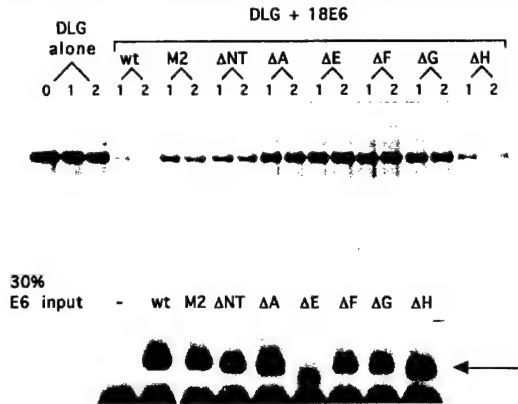


Figure 3 Mutational analysis of the regions of HPV-18 E6 involved in inducing the degradation of DLG *in vitro*. *In vitro* translated DLG was incubated in the presence of the wild type (wt) and mutant HPV-18 E6 proteins for 1 or 2 h as indicated. The remaining DLG was then ascertained by immunoprecipitation followed by SDS-PAGE and autoradiography. The lower panel shows the inputs of the mutant E6 proteins

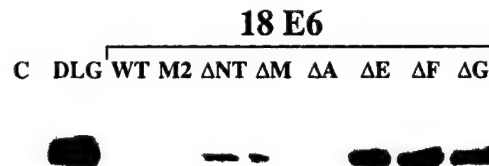


Figure 4 Mutational analysis of the regions of HPV-18 E6 involved in inducing the degradation of DLG *in vivo*. U2OS cells were transfected with 3 μ g of the DLG expression plasmid together with 3 μ g of the wild type (WT) and mutant HPV-18 E6 expression plasmids. After 24 h the cells were harvested and residual DLG ascertained by Western blot analysis. Lane C represents control transfected cells

reticulocyte lysate. In contrast, when wheat germ extracts are used, no degradation of p53 is obtained whereas there is still a significant reduction in the levels of DLG. These results further demonstrate that E6 induced degradation of DLG can occur in the absence of E6-AP.

Low risk E6 proteins also target cellular proteins for ubiquitin mediated degradation

To further define the mechanism by which the HPV E6 proteins target DLG for degradation we generated a number of chimaeric E6 proteins. Previous studies had shown that both the amino terminal and carboxy terminal halves of the high risk E6 proteins were required for the degradation of p53 (Crook *et al.*, 1991; Pim *et al.*, 1994; Li and Coffino, 1996). In particular, the use of HPV-6 and HPV-16 E6 chimaeric proteins showed that sequences in the carboxy terminal half of E6 were largely responsible for binding p53, whereas sequences in the amino terminal half of E6 were responsible for degradation (Crook *et al.*, 1991). However we were particularly interested in determining how these chimaeric proteins would behave with respect to DLG, especially since the HPV-6.16 E6

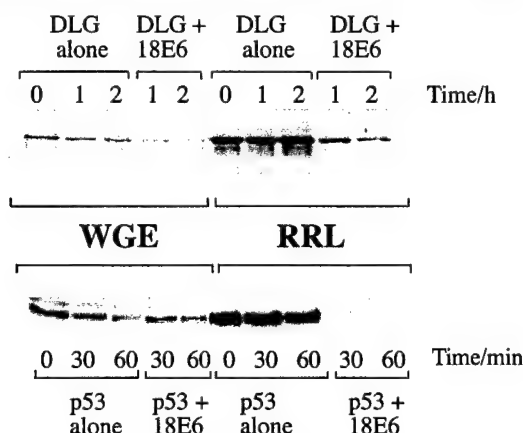


Figure 5 Comparison of HPV-18 E6 induced degradation of DLG in rabbit reticulocyte lysate and wheat germ extracts. HPV-18 E6, p53 and DLG were translated in wheat germ extract (WGE) or rabbit reticulocyte lysate (RRL). The proteins were then mixed in the combinations indicated and incubated at 30°C for the times shown. The remaining p53 and DLG was ascertained by immunoprecipitation followed by PAGE and autoradiography. The upper panel shows the DLG degradation assay and the lower panel shows the p53 degradation assay

chimaera, which comprises the N-terminal 60 amino acids from HPV-6 E6 and the C-terminal 92 amino acids from HPV-16 E6 (Crook *et al.*, 1991), should have all the necessary sequences required for binding DLG. We first performed *in vivo* degradation assays with the HPV-16.6 and HPV-6.16 E6 chimaeric proteins, and the results obtained are shown in Figure 6a. As can be seen, the HPV-16.6 E6 chimaera which comprises the N-terminal 59 amino acids from HPV-16 E6 and the C-terminal 90 amino acids from HPV-6 E6, has only a modest effect on the levels of DLG. In contrast, the HPV-6.16 E6 chimaera is as effective as HPV-16 E6 in targeting DLG for degradation. This is in marked contrast to the effects of these chimaeric proteins on p53 steady state levels which are shown in Figure 6c, where neither protein is capable of degrading p53, and agrees with previous observations (Foster *et al.*, 1994; Li and Coffino, 1996). To further elucidate the mechanism by which DLG was being degraded by E6, we then constructed three smaller chimaeric E6 molecules. These consisted of an HPV-6 E6 backbone with the last 18 amino acids from HPV-18 E6, and the last seven amino acids of HPV-18 E6 or the last eight amino acids of HPV-16 E6 added on to the end of the HPV-6 E6 protein. The reasoning being that, since the HPV-6.16 E6 chimaera could degrade DLG we wished to determine whether the PDZ consensus binding motif alone was sufficient to confer binding, and secondly whether low risk E6 proteins had any significant capacity to target cellular proteins for degradation. The results obtained are also shown in Figure 6a and, strikingly, show that addition of just the last seven or eight amino acids of either HPV-18 (6.18s) or 16 E6 (6.16s) onto the carboxy terminus of HPV-6 E6 results in that protein being capable of degrading DLG *in vivo*. Addition of a further 12 residues onto HPV-6 E6 from HPV-18 E6 (6.18l) did not appear to significantly increase the degradation efficiency. Parallel assays were performed on p53 and,

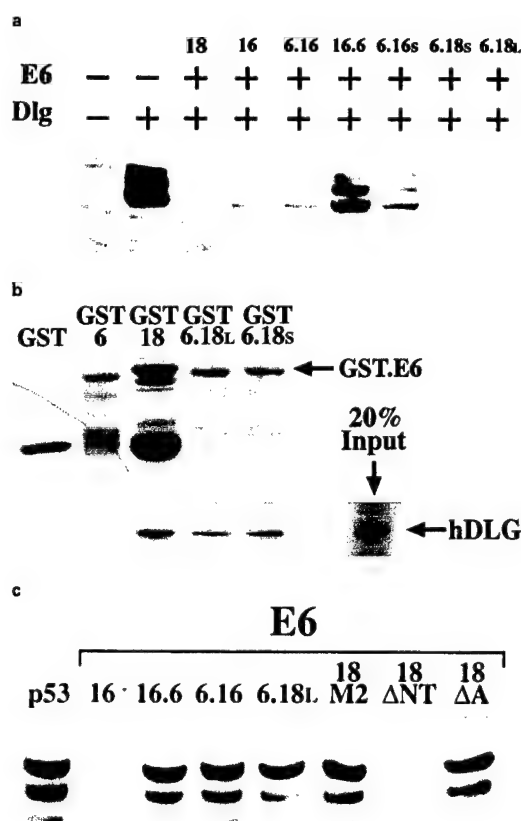


Figure 6 Addition of the extreme carboxy terminal region of HPV-18 E6 onto HPV-6 E6 confers DLG binding and degradation. (a) U2OS cells were transfected with 3 µg DLG expression plasmid together with 3 µg of either the wild type or chimaeric E6 expression plasmids as indicated. After 24 h the cells were harvested and residual DLG was ascertained by Western blot analysis. (b) GST pull down assay of *in vitro* translated DLG with HPV-6 E6, HPV-18 E6, HPV-6.18l (HPV-6 E6 plus the carboxy terminal 19 amino acids of HPV-18 E6) and HPV-6.18s (HPV-6 E6 plus the carboxy terminal 7 amino acids of HPV-18 E6) GST fusion proteins as indicated. Bound DLG was ascertained by SDS-PAGE and autoradiography. The upper panel shows the Coomassie stain of the same gel and shows equal levels of loading of the HPV-6 E6 based GST fusion proteins. (c) Saos-2 cells were transfected with 4 µg of p53 expression plasmid together with 5 µg of the indicated E6 expression plasmids. After 24 h the cells were harvested and remaining p53 ascertained by Western blot analysis

as can be seen from Figure 6c, none of these chimaeric proteins could target p53 for degradation. In order to verify that the addition of the last seven amino acids of HPV-18 E6 onto HPV-6 E6 did indeed confer DLG binding activity, we performed a GST pull down assay with *in vitro* translated DLG. As can be seen from Figure 6b, HPV-6 E6 is completely defective with respect to binding DLG, yet addition of the PDZ binding domain from HPV-18 E6 confers complete binding.

In order to overcome any potential problems associated with differences in the levels of protein expression *in vivo*, the degradation assay was performed with HPV-6 E6 and the HPV-6.18s chimaera *in vitro*. The results obtained are shown in Figure 7. As can be seen,

HPV-6 E6 has no effect upon DLG levels over the course of the assay whereas the HPV-6.18s chimaera induces almost complete degradation of DLG over the same period of time. Taken together, these results demonstrate that the low risk HPV E6 proteins also interact with a component of the ubiquitin pathway and can be induced to bring about the degradation of a cellular target protein. Since these low risk HPV E6 proteins only have a very low affinity for E6-AP (Scheffner *et al.*, 1990, 1993), this activity must be mediated by another, as yet unknown, ubiquitin ligase and this points to another potential target for therapeutic intervention in HPV induced disease.

Discussion

The DLG tumour suppressor protein is intimately involved in processes regulating cell growth in response to external stimuli and cell contact. The demonstration that DLG is regulated by the ubiquitin pathway, which in turn can be used by the high risk E6 proteins, has important implications for the role of this interaction in the development of cervical cancer (Gardioli *et al.*, 1999). In this study we have continued to investigate the mechanism by which E6 induces the degradation of DLG. We show that this activity of E6 is independent of its association with p53 and rule out a direct involvement of the E3 ubiquitin ligase, E6-AP. Rather, the demonstration that the low risk E6 proteins can also target DLG for degradation following the addition of a binding site, together with the demonstration that HPV-18 E6 can degrade DLG in wheat germ extracts, indicates the involvement of another, as yet unknown ligase.

Previous studies had suggested that the mechanism of interaction between HPV-16 and HPV-18 E6 proteins

with DLG was somewhat different. HPV-16 E6 was reported to require PDZ domain 2 on DLG (Kiyono *et al.*, 1997), whereas HPV-18 E6 was shown to bind independently to PDZ domains 1, 2 or 3 (Gardioli *et al.*, 1999); although different assay systems were used in these two studies. Preliminary studies had also suggested that HPV-18 E6 could more readily target DLG for degradation *in vivo* (Gardioli *et al.*, 1999). In order to verify whether this was indeed the case, a series of comparative binding assays were performed which showed that HPV-18 E6 does indeed bind DLG more strongly than HPV-16 E6. This increased level of interaction is also reflected in a higher level of induced degradation both *in vitro* and *in vivo*. This contrasts markedly with the E6-p53 interaction where HPV-16 E6 has consistently been shown to bind and degrade p53 more effectively than HPV-18 E6 (Werness *et al.*, 1990; Scheffner *et al.*, 1990). It is interesting at this point to speculate whether the increased activity of HPV-18 with respect to DLG may be reflected in any pathological outcomes of infection. Certainly, there is an extensive literature which indicates that HPV-18 is generally more active than HPV-16 in a variety of transformation assays (Barbosa and Schlegel, 1989; Villa and Schlegel, 1991). In addition, there are also several reports which indicate that HPV-18-containing cervical tumours have a more aggressive phenotype and are also more prone to recurrence than HPV-16-containing tumours (Barnes *et al.*, 1988; Kurman *et al.*, 1988; Burnett *et al.*, 1992; Zhang *et al.*, 1995). Since the only biochemical activity of HPV-18 which correlates with this trend, so far, is the increased activity of E6 with respect to DLG, it is tempting to speculate that it is this association which is critical for the malignant progression of HPV induced tumours.

HPV E6 induced degradation of p53 requires the interaction with the cellular ubiquitin ligase E6-AP (Huibregtse *et al.*, 1991, 1993). Extensive mutational analysis of E6 indicates that this binds to the amino terminal region of the E6 protein and that only the E6 proteins of high risk HPV types can interact to any significant degree (Huibregtse *et al.*, 1991; Pim *et al.*, 1997). In this study we have used a well-defined panel of E6 mutants (Pim *et al.*, 1994; Pim and Banks, 1999) to investigate the requirements for E6 induced degradation of DLG. It is clear that sequences that are essential for p53 degradation, as defined by mutants M2 (R10S, P11G), Δ M (Δ 28–31) and Δ A (Δ 47–49) which lie within the amino terminal half of the E6 protein, are largely dispensable for the degradation of DLG. This broadly covers the region of E6 which is required for high affinity binding to p53 via E6-AP (Li and Coffino, 1996) and is the first line of evidence that suggests that E6-AP is not involved in the degradation of DLG. In contrast, mutants within the carboxy terminal half of E6, which had previously been shown to be involved in basic binding to p53 (Crook *et al.*, 1991; Li and Coffino, 1996), as defined by mutants Δ E (Δ 101–104), Δ F (Δ 113–117) and Δ G (Δ 126–130), were however found to be required for E6 induced degradation of DLG, again suggesting a lack of E6-AP involvement. It should be emphasized that these mutants are well clear of the DLG binding motif located at residues 155–158. In addition, it is worth noting that the Δ H (144–149) mutation, although much closer to the DLG binding site, has no deleterious effect upon E6 induced degradation of



Figure 7 HPV-6.18s induced degradation of DLG *in vitro*. *In vitro* translated DLG was incubated, either alone or with HPV-18 E6, HPV-6 E6 or the HPV-6.18s chimaera at 30°C for 0, 1 or 2 h as indicated. The remaining DLG was detected by immunoprecipitation and autoradiography. The lower panel shows the inputs of the E6 proteins used

DLG. Further evidence for a lack of E6-AP involvement also comes from the degradation assays performed in the wheat germ extract. This system lacks any E6-AP (Huibregtse *et al.*, 1991), yet HPV-18 E6 is still capable of inducing DLG degradation, albeit not as efficiently as in the rabbit reticulocyte lysate. This is in marked contrast to p53, where no degradation is obtained in the wheat germ system. Obviously we cannot formally rule out a role for E6-AP *in vivo*, however the above results strongly suggest the involvement of at least one other as yet unknown, ubiquitin ligase in E6 mediated degradation of DLG.

We then proceeded to investigate the potential of low risk HPV E6 proteins to interact with the ubiquitin pathway by the use of a chimaeric analysis, a summary of which is shown in Figure 8. Clearly the HPV-6.16 E6 chimaera is capable of directing DLG degradation but the HPV-16.6 E6 chimaera is not; this however could merely be a reflection of lack of binding to DLG with the 16.6 E6 protein. However, addition of just seven amino acids from the carboxy terminus of HPV-18 E6 onto the carboxy terminus of HPV-6 E6 allows that protein to bind DLG. Most strikingly, the HPV-6.18s E6 chimaera can then target DLG for degradation. Since HPV-6 E6 is reported to be largely defective for binding E6-AP this would also appear to rule out any involvement of E6-AP in E6 mediated degradation of DLG. The second important point to be taken from these studies is that this demonstrates that the low risk HPV E6 proteins will also interact with a component of the ubiquitin system. It seems extremely likely that this is the same protein that is being used by the high risk E6 proteins to degrade DLG. It now remains to be determined whether this ligase is also responsible for regulating DLG levels in the absence of E6, and which cellular proteins are normally targeted by the low risk viral E6 proteins.

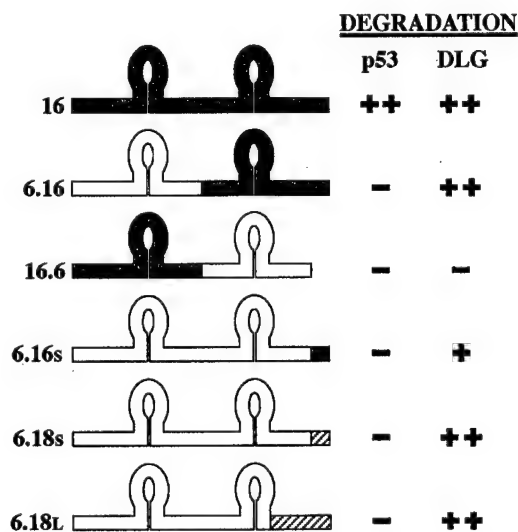


Figure 8 Schematic diagram showing the nature of the chimaeric HPV E6 proteins and their activity with respect to degradation of p53 and DLG. Filled in portions represent HPV-16 E6 derived sequences, open portions represent HPV-6 E6 derived sequences and hatched portions represent HPV-18 E6 derived sequences

Materials and methods

Cells and tissue culture

Human Saos-2 and U2OS cells were grown in DMEM with 10% foetal calf serum. All the transfections were carried out using the calcium phosphate precipitation procedure, as described previously (Matlashewski *et al.*, 1987), and transfection efficiencies were monitored by performing parallel β -galactosidase assays.

Plasmids

Plasmids for expressing DLG *in vivo* and *in vitro* have been described previously (Lee *et al.*, 1997; Gardiol *et al.*, 1999). For GST fusion protein production, DLG and NT-DLG were cloned into pGEX 2 and have also been described previously (Lee *et al.*, 1997; Gardiol *et al.*, 1999).

The HPV-18 E6 mutants used in this study were Δ NT (Δ 4-7), M2 (R10S, P11G), Δ M (Δ 28-31), Δ A (Δ 47-49), Δ E (Δ 101-104), Δ F (Δ 113-117), Δ G (Δ 126-130) and Δ H (Δ 144-149) and have been described previously (Pim *et al.*, 1994; Pim and Banks, 1999). The wild type and mutant E6s were cloned into pSP64 for *in vitro* expression and into pCDNA3 for *in vivo* expression (Pim *et al.*, 1994; Gardiol and Banks, 1998). The two chimaeric constructs, HPV-16.6 E6 and HPV-6.16 E6 have been described previously (Crook *et al.*, 1991), but were subcloned into pCDNA-3 for this study. The HPV-6.18_L, HPV-6.18_s and HPV-6.16_s chimaeras (shown schematically in Figure 7) were produced by PCR amplification and cloned into pCDNA-3 and pGEX-2T and were verified by DNA sequencing.

GST fusion protein binding assays

The *in vitro* binding assays were performed as described previously (Thomas *et al.*, 1995; Gardiol *et al.*, 1999), and bound proteins were washed extensively in PBS containing 1% NP40 before analysing on SDS-PAGE and autoradiography.

Degradation assays

For the *in vitro* assays, proteins were translated using either the TNT coupled rabbit reticulocyte lysate or wheat germ extract systems (Promega) as indicated in the text according to the manufacturer's instructions, in the presence of [³⁵S]-cysteine. The translated E6 proteins were then quantitated by PhosphorImager analysis, and equal amounts of wild type and mutant E6 proteins were added to a constant amount of *in vitro* translated DLG. Following incubation of the E6 proteins with DLG for 1 or 2 h, the remaining DLG was assessed by immunoprecipitation with an antibody raised against the GST-NT-DLG fusion protein (Lee *et al.*, 1997), followed by SDS-PAGE and autoradiography. The *in vivo* degradation assays for p53 and DLG were performed as described previously (Gardioli and Banks, 1998; Gardiol *et al.*, 1999).

Acknowledgments

We are most grateful to Christian Kühne for comments on the manuscript. This work was supported in part by a research grant from the Associazione Italiana per la Ricerca sul Cancro to L Banks and grants from the National Institutes of Health (ROI CA58541), American Cancer Society (RPG-97-668-01-VM) and US Army (DAMD17-97-1-7082) to R Javier.

References

- Androphy E, Hubbert N, Schiller J and Lowy D. (1987). *EMBO J.*, **6**, 989–992.
- Banks L, Spence P, Androphy E, Hubbert N, Matlashewski G, Murray A and Crawford L. (1987). *J. Gen. Virol.*, **68**, 1351–1359.
- Barbosa MS and Schlegel R. (1989). *Oncogene*, **4**, 1529–1532.
- Barnes W, Delgado G, Kurman RJ, Petrilli ES, Smith DM, Ahmed S, Lorincz AT, Temple GF, Jenson AB and Lancaster WD. (1988). *Gynecol. Oncol.*, **29**, 267–273.
- Burnett AF, Barnes WA, Johnson JC, Grendys E, Willett GD, Barter JF and Doniger J. (1992). *Gynecol. Oncol.*, **47**, 343–347.
- Crook T, Ludwig R, Marston N, Willkomm D and Vousden KH. (1996). *Virology*, **217**, 285–292.
- Crook T, Tidy J and Vousden KH. (1991). *EMBO J.*, **11**, 3935–3940.
- Dyson N, Howley PM, Münger K and Harlow E. (1989). *Science*, **243**, 934–936.
- Foster S, Demers W, Etscheid B and Galloway D. (1994). *J. Virol.*, **68**, 5698–5705.
- Gardioli D and Banks L. (1998). *J. Gen. Virol.*, **79**, 1963–1970.
- Gardioli D, Kühne C, Glaunsinger B, Lee SS, Javier R and Banks L. (1999). *Oncogene*, **18**, 5487–5496.
- Goode S and Perrimon N. (1997). *Genes Dev.*, **11**, 2532–2544.
- Hiraiwa A, Kiyono T, Segawa K, Utsumi KR, Ohashi M and Ishibashi M. (1993). *Virology*, **192**, 102–111.
- Huibregtse J, Scheffner M and Howley P. (1991). *EMBO J.*, **10**, 4129–4135.
- Huibregtse J, Scheffner M and Howley P. (1993). *Mol. Cell. Biol.*, **13**, 775–784.
- Inoue T, Oka K, Yong-II H, Vousden KH, Kyo S, Jing P, Hakura A and Yutsoda M. (1998). *Mol. Carcinog.*, **21**, 215–222.
- Ishiwatari H, Hayasaka N, Inoue H, Yutsudo M and Hakura A. (1994). *J. Med. Virol.*, **44**, 243–249.
- Kim E, DeMarco S, Marfatia S, Chishti A, Sheng M and Strehler E. (1998). *J. Biol. Chem.*, **273**, 1591–1595.
- Kim E, Niethammer M, Rothschild A, Nung Jan Y and Sheng M. (1995). *Nature*, **378**, 85–88.
- Kim S. (1997). *Curr. Opin. Cell Biol.*, **9**, 853–859.
- Kiyono T, Hiraiwa A, Fujita M, Hayashi Y, Akiyama T and Ishibashi M. (1997). *Proc. Natl. Acad. Sci. USA*, **94**, 11612–11616.
- Kurman RJ, Schiffman MH, Lancaster WD, Reid R, Jenson AB, Temple GF and Lorincz AT. (1988). *Am. J. Obstet. Gynecol.*, **159**, 293–296.
- Lee SS, Weiss R and Javier R. (1997). *Proc. Natl. Acad. Sci. USA*, **94**, 6670–6675.
- Li X and Coffino P. (1996). *J. Virol.*, **70**, 4509–4516.
- Lue R, Marfatia S, Branton D and Chishti A. (1994). *Proc. Natl. Acad. Sci. USA*, **91**, 9818–9822.
- Marfatia S, Morais Cabral J, Lin L, Hough C, Bryant P, Stolz L and Chishti A. (1996). *J. Cell. Biol.*, **135**, 753–766.
- Matlashewski G, Schneider J, Banks L, Jones N, Murray A and Crawford L. (1987). *EMBO J.*, **6**, 1741–1746.
- Matsumine A, Ogai A, Senda T, Okumura N, Satoh K, Baeg G, Kawahara T, Kobayashi S, Okada M, Toyoshima K and Akiyama T. (1996). *Science*, **272**, 1020–1023.
- Muller B, Kistner U, Veh R, Cases-Langhoff C, Becker B, Gundelfinger E and Garner C. (1995). *J. Neuroscience*, **15**, 2354–2366.
- Nakagawa S, Watanabe S, Yoshikawa H, Taketani Y, Yoshiike K and Kanda T. (1995). *Virology*, **212**, 535–542.
- Pim D and Banks L. (1999). *Oncogene*, **18**, 7403–7408.
- Pim D, Massimi P and Banks L. (1997). *Oncogene*, **15**, 257–264.
- Pim D, Storey A, Thomas M, Massimi P and Banks L. (1994). *Oncogene*, **9**, 1869–1876.
- Ponting C and Phillips C. (1995). *Trends Biochem. Sci.*, **20**, 102–103.
- Saras J and Heldin C. (1996). *Trends Biochem. Sci.*, **21**, 455–458.
- Scheffner M, Huibregtse J, Vierstra R and Howley P. (1993). *Cell*, **75**, 495–505.
- Scheffner M, Münger K, Byrne JC and Howley P. (1990). *Cell*, **63**, 1129–1136.
- Schwarz E, Freese U, Gissmann L, Mayer W, Roggenbuck B, Stremlau A and zur Hausen H. (1985). *Nature*, **314**, 111–114.
- Smotkin D and Wettstein F. (1986). *Proc. Natl. Acad. Sci. USA*, **83**, 4680–4684.
- Song S, Pitot HC and Lambert PF. (1999). *J. Virol.*, **73**, 5887–5893.
- Thomas M, Massimi P, Jenkins J and Banks L. (1995). *Oncogene*, **10**, 261–268.
- Villa LL and Schlegel R. (1991). *Virology*, **181**, 374–377.
- Woods D, Hough C, Peel D, Callaini G and Bryant P. (1996). *J. Cell. Biol.*, **134**, 1469–1482.
- Werness B, Levine A and Howley P. (1990). *Science*, **248**, 76–79.
- Zhang J, Rose BR, Thompson CH, Jarrett C, Russell P, Houghton RS and Cossart YE. (1995). *Gynecol. Oncol.*, **57**, 170–177.
- zur Hausen H. (1991). *Virology*, **184**, 9–13.
- zur Hausen H and Schneider A. (1987). In: *The Papovaviridae*, vol. 2, pp. 245–263.

Interactions of the PDZ-Protein MAGI-1 with Adenovirus E4-ORF1 and Papillomavirus E6 Oncoproteins

Britt A. Glaunsinger¹, Siu Sylvia Lee¹, Miranda Thomas², Lawrence Banks², and Ronald Javier¹

¹Division of Molecular Virology, Baylor College of Medicine, Houston, Texas 77030, USA;

²International Center for Genetic Engineering and Biotechnology, Padriciano 99, I-34012

Trieste, Italy

Running title: Binding of viral oncoproteins to MAGI-1

Keywords: adenovirus E4-ORF1/MAGI-1/papillomavirus E6/PDZ

Corresponding author: Ronald Javier, Division of Molecular Virology, Baylor College of
Medicine, Houston, Texas 77030, USA

Phone: (713) 798-3898

Fax: (713) 798-3586

E-mail: rjavier@bcm.tmc.edu

Abstract

The oncoproteins of DNA tumor viruses promote tumorigenesis by complexing with cellular factors intimately involved in the control of cell proliferation. The major oncogenic determinants for human adenovirus type 9 (Ad9) and high-risk human papillomaviruses (HPV) are the E4-ORF1 and E6 proteins, respectively. These seemingly unrelated viral oncoproteins are similar in that their transforming activities in cells depend, in part, on a carboxyl-terminal PDZ domain-binding motif which mediates interactions with the cellular PDZ-protein DLG. Here we demonstrated that both Ad9 E4-ORF1 and high-risk HPV E6 proteins also bind to the DLG-related PDZ-protein MAGI-1. These interactions resulted in MAGI-1 being aberrantly sequestered in the cytoplasm by the Ad9 E4-ORF1 protein or being targeted for degradation by high-risk HPV E6 proteins. Our findings suggest that MAGI-1 is a member of a select group of cellular PDZ proteins targeted by both adenovirus E4-ORF1 and high-risk HPV E6 proteins and, in addition, that the tumorigenic potentials of these viral oncoproteins are determined, in part, by their ability to inhibit the function of MAGI-1 in cells.

Introduction

Human adenoviruses are associated primarily with respiratory, gastrointestinal, and eye infections in people but, in rodents, some of these viruses have the capacity to induce tumors (Shenk, 1996). Based on the types of tumors elicited and the oncoproteins that determine their tumorigenicity, two different classes of oncogenic human adenoviruses can be distinguished. Human adenoviruses from subgroups A and B induce primarily undifferentiated sarcomas at the site of injection, and the tumorigenic potential of these viruses solely depends on their nuclear E1A and E1B transforming proteins (Shenk, 1996). In contrast, subgroup D human adenovirus type 9 (Ad9) generates exclusively estrogen-dependent mammary tumors (Javier *et al.*, 1991), and the tumorigenic potential of this virus relies on its cytoplasmic Ad9 E4-ORF1 (9ORF1) transforming protein (Javier, 1994; Thomas *et al.*, 1999).

Human papillomaviruses (HPV), on the other hand, are the etiological agents of warts in people. With regard to HPVs that infect the genital tract, high-risk HPVs (types 16, 18, 31, and 45) are strongly associated with cervical cancer whereas low-risk HPVs (types 6 and 11) are weakly or not associated with this disease (Howley, 1996). In addition, the major oncogenic determinants of high-risk HPVs are their E7 and E6 gene products. Interestingly, the tumorigenic potentials of high-risk HPV E7 and E6 and adenovirus E1A and E1B, as well as SV40 large T-antigen, similarly depend, in part, on their capacity to complex with and inactivate the tumor suppressor proteins pRB and p53 (Nevins and Vogt, 1996). Such findings have revealed that seemingly unrelated oncoproteins from DNA tumor viruses often target common cellular factors having critical roles in the control of cellular proliferation.

We and others recently showed that the seemingly unrelated adenovirus E4-ORF1 and high-risk HPV E6 proteins, as well as the human T-cell leukemia virus type I (HTLV-1) Tax protein, likewise target a common cellular factor (Lee *et al.*, 1997). It was found that these viral oncoproteins similarly bind to the cellular PDZ domain-containing protein DLG (Kiyono *et al.*, 1997; Lee *et al.*, 1997), which is a mammalian homolog of the *Drosophila* tumor suppressor protein dlg (Lue *et al.*, 1994; Muller *et al.*, 1995).

PDZ domains are 80-90 amino-acid protein-protein interaction modules most often found within cellular factors that function in signal transduction (Fanning and Anderson, 1999). These domains typically bind specific sequence motifs located at the extreme carboxyl-terminus of target proteins, although they also participate in other types of protein interactions. Three different types of carboxyl-terminal PDZ domain-binding motifs are recognized and, at their extreme carboxyl-termini, adenovirus E4-ORF1, high-risk HPV E6, and HTLV-1 Tax proteins possess a class I motif having the consensus sequence -(T/S)-X-(V/I)-COOH (X, any amino-acid [aa] residue) (Lee *et al.*, 1997). These binding motifs mediate interactions with one or more PDZ domains of DLG and, for the 9ORF1 and high-risk HPV-16 E6 proteins, disruption of this carboxyl-terminal motif abolishes their transforming activity (Kiyono *et al.*, 1997; Lee *et al.*, 1997). These findings suggest that transformation by these viral oncoproteins depends, in part, on their ability to block the function of DLG.

Drosophila dlg has been designated as a tumor suppressor protein because, for larvae carrying homozygous *dlg* mutations, imaginal disc epithelial cells exhibit loss of polarity and neoplastic outgrowth and, in addition, certain neuronal cells of the brain undergo hyperplastic growth (Woods and Bryant, 1991). The fact that DLG rescues the phenotypic defects of *Drosophila* unable to express functional dlg indicates that these two proteins are functionally

homologous (Thomas *et al.*, 1997). These closely-related proteins are members of the membrane-associated guanylate kinase (MAGUK) family of proteins, which typically have a domain structure consisting of one or more amino-terminal PDZ domains, an internal SH3 domain, and a carboxyl-terminal guanylate kinase-homology domain (Craven and Brecht, 1998). In general, this family of polypeptides functions to properly localize membrane and cytosolic proteins to the plasma membrane at specialized regions of cell-cell contact, as well as to organize these targets into large signaling complexes (Fanning and Anderson, 1999). These results, together with our recent finding that high-risk HPV E6 proteins target DLG for degradation in cells (Gardioli *et al.*, 1999), suggest a model whereby the proposed cell signaling regulatory activities of DLG function to suppress inappropriate proliferation of cells.

Our previous findings with the 9ORF1 oncoprotein suggest that its oncogenic potential depends not only on interactions with DLG (Lee *et al.*, 1997), but also with other unidentified cellular PDZ proteins (p220, p180, p160, p155) (Weiss *et al.*, 1997a). In this paper, we screened a panel of large cellular PDZ proteins for an ability to bind the 9ORF1 protein in order to identify additional cellular factors that contribute to 9ORF1-induced transformation. We found that 9ORF1, as well as high-risk HPV E6 oncoproteins, selectively complex with the widely-expressed cellular PDZ-protein MAGI-1, a MAGUK protein related to DLG. Additional results showed that MAGI-1 is aberrantly sequestered in the cytoplasm of cells by the 9ORF1 protein and is targeted for degradation in cells by high-risk HPV E6 proteins, suggesting that the transforming potentials of two unrelated viral oncoproteins depend, in part, on an ability to inactivate this cellular PDZ protein.

Results

9ORF1 complexes with the PDZ-protein MAGI-1 in cells

The transforming activity of the 9ORF1 oncoprotein depends on its carboxyl-terminal PDZ domain-binding motif (Table 1) (Lee *et al.*, 1997), which mediates binding to multiple large cellular polypeptides (p220, p180, p160, p155, and p140/p130) (Weiss *et al.*, 1997a). Whereas 9ORF1-associated protein p140/p130 has been identified as the PDZ-protein DLG (Lee *et al.*, 1997), the identities of the remaining 9ORF1-associated proteins have not been determined. Reasoning that, like DLG, these unidentified 9ORF1-associated polypeptides contain PDZ domains and also considering their predicted sizes (155 kD - 220 kD), we examined a group of cellular PDZ-proteins that included FAP-1 (273 kD) (Sato *et al.*, 1995), ZO-1 (220 kD) (Willott *et al.*, 1993), AF-6 (182 kD) (Prasad *et al.*, 1993), hINADL (167 kD) (Philipp and Flockerzi, 1997), MAGI-1 (152 kD) (Dobrosotskaya *et al.*, 1997), and ZO-3 (130 kD) (Haskins *et al.*, 1998) for binding to 9ORF1. Using a variety of assays, we demonstrated that 9ORF1 bound to the widely-expressed PDZ-protein MAGI-1 (Fig. 1) (see below), but not to the other PDZ-proteins tested (data not shown).

Although its function is not known, MAGI-1 is a MAGUK protein related to DLG (Dobrosotskaya *et al.*, 1997). MAGI-1 is structurally inverted relative to DLG, however, as MAGI-1 has a guanylate kinase-homology domain at its amino-terminus and five PDZ domains at its carboxyl-terminus. In addition, MAGI-1 possesses two WW domains rather than the SH3 domain of DLG. Three MAGI-1 isoforms (*a*, *b* and *c*), identical except for sequences carboxyl-terminal to PDZ5, have been identified (Fig. 1). The presence of a consensus bipartite nuclear localization signal within the unique carboxyl-terminal sequences of MAGI-1c hints that this particular isoform may under certain conditions have functions in the nucleus.

To show binding of MAGI-1 to the 9ORF1 protein, we subjected extracts of COS-7 cells expressing HA epitope-tagged mouse MAGI-1b (HAMAGI-1b) or MAGI-1c (HAMAGI-1c) to GST-pulldown assays with a wild-type 9ORF1 fusion protein. We found that wild-type 9ORF1 complexed similarly with both MAGI-1b (data not shown) and MAGI-1c (Fig. 2A). Like 9ORF1, the related E4-ORF1 transforming proteins of adenovirus types 5 (5ORF1) and 12 (12ORF1) also possess carboxyl-terminal PDZ domain-binding motifs (Table 1) and likewise bound to both MAGI-1b and MAGI-1c in these assays (data not shown; Fig 2A). With the use of MAGI-1-specific antibodies (Dobrosotskaya *et al.*, 1997), we also showed that 9ORF1 is similarly able to associate with endogenous MAGI-1 protein derived from extracts of CREF rat embryo fibroblasts (Fig. 2B). Which MAGI-1 isoform(s) is expressed in CREF cells was not determined, but the size of the detected polypeptide is most consistent with that of MAGI-1c. Also notable was that MAGI-1 and 9ORF1-associated protein p180 co-migrated in protein gels, suggesting that these proteins are the same (Fig. 3).

The specificity of the binding results described above was demonstrated by inclusion of transformation-defective 9ORF1 mutant proteins in the same experiments. The PDZ domain-binding motif of severely transformation-defective 9ORF1 mutant IIIA is disrupted by deletion (Table 1), which renders this mutant unable to complex with any 9ORF1-associated proteins (Weiss *et al.*, 1997a; Weiss and Javier, 1997). In contrast, the PDZ domain-binding motifs of the weak-transforming 9ORF1 mutants IIIC and IIID have less disruptive missense mutations (Table 1), which permit these mutants to bind a subset of 9ORF1-associated proteins, albeit at substantially reduced levels in most cases (Weiss *et al.*, 1997a; Weiss and Javier, 1997). In GST-pulldown assays, we found that MAGI-1 failed to complex with mutant IIIA, yet complexed with mutant IIIC at approximately wild-type levels or with mutant IIID at

substantially reduced levels (Fig. 2). The fact that this binding profile of MAGI-1 to wild-type and mutant 9ORF1 proteins was identical to that previously observed for 9ORF1-associated protein p180 (Weiss and Javier, 1997) provided further support for the idea that these proteins are the same. More important, these findings indicated that 9ORF1 binding to MAGI-1 is specific and depends on a functional 9ORF1 PDZ domain-binding motif.

We next performed reciprocal co-immunoprecipitation assays with extracts of COS-7 cells co-expressing HAMAGI-1c and either wild-type or mutant 9ORF1 protein. We found that MAGI-1 co-precipitated with wild-type 9ORF1 but failed to co-precipitate with mutant IIIA (Fig. 4). MAGI-1 also co-precipitated with mutants IIIC and IIID, but at levels slightly below or substantially below, respectively, that of the wild-type 9ORF1 protein (Fig. 4). These results were concordant with those of the GST-pulldown assays (see Fig. 2) and also indicated that 9ORF1 and MAGI-1 form specific complexes in cells.

9ORF1 interacts primarily with MAGI-1 PDZ1 and PDZ3

The fact that disrupting the PDZ domain-binding motif of 9ORF1 impairs its binding to MAGI-1 implies that this viral protein binds one or more MAGI-1 PDZ domains. To verify this prediction, we performed protein blotting assays by incubating membrane-immobilized fusion proteins of individual MAGI-1 PDZ domains with a radiolabeled 9ORF1 protein probe. In these assays, the wild-type 9ORF1 protein probe bound strongly with PDZ1 and PDZ3, weakly with PDZ2, but failed to bind either PDZ4 or PDZ5 (Fig. 5A). Additionally, none of these MAGI-1 PDZ domains reacted with a mutant IIIA protein probe (data not shown), indicating that the detected binding was specific and dependent on a functional 9ORF1 PDZ domain-binding motif.

As 9ORF1 mutants IIIC and IIID displayed nearly wild-type or reduced binding, respectively, to MAGI-1 (see Figs. 2 and 4), these mutant proteins were also used as probes in

protein blotting assays. In these experiments, mutants IIIC and IIID displayed reciprocal defects in binding to MAGI-1 PDZ1 and PDZ3. Specifically, mutant IIIC reacted with PDZ3 but not with PDZ1 and mutant IIID reacted with PDZ1 but not with PDZ3 (Fig. 5A). Also, mutant IIID bound to MAGI-1 PDZ2, but mutant IIIC did not interact detectably with this domain. These results revealed that, although they are able to bind MAGI-1, mutants IIIC and IIID both have impaired domain interactions with this PDZ protein.

To confirm that MAGI-1 PDZ1 and PDZ3 primarily determine binding of 9ORF1 to the full-length MAGI-1 polypeptide, we constructed a MAGI-1 double-deletion mutant missing both PDZ1 and PDZ3 (HAMAGI-1 Δ PDZ1+3) (Fig. 5B). In agreement with the results of protein blotting assays (see Fig. 5A), 9ORF1 failed to bind HAMAGI-1 Δ PDZ1+3 in GST-pulldown assays (Fig. 5C). The weak interaction of 9ORF1 with MAGI-1 PDZ2 observed in protein blotting assays (see Fig. 5A) was presumably too low to detect in these experiments. These findings showed that MAGI-1 PDZ1 and PDZ3, and no other region of MAGI-1, largely mediate binding to 9ORF1.

Contrary to results obtained with the HAMAGI-1 Δ PDZ1+3 double-deletion mutant, MAGI-1 single-deletion mutants missing either only PDZ1 (HAMAGI-1 Δ PDZ1) or only PDZ3 (HAMAGI-1 Δ PDZ3) (Fig. 5B) associated with 9ORF1 at approximately wild-type levels (Fig. 5C), demonstrating that either PDZ1 alone or PDZ3 alone is sufficient to confer upon MAGI-1 wild-type binding to 9ORF1. This finding also suggested that the strong binding of mutant IIIC to MAGI-1 (see Figs. 2 and 4) is due to this mutant retaining approximately wild-type affinity for PDZ3 and that the weak binding of mutant IIID to MAGI-1 (see Figs. 2 and 4) is due to this mutant having reduced affinity for PDZ1. The reason that the predicted reduced affinity of mutant IIID for PDZ1 was not revealed in protein blotting assays (see

Fig. 5A) is not clear, but it may be due to differences in the specific activity of each protein probe.

9ORF1 aberrantly sequesters MAGI-1 in the cytoplasm of cells

Indirect immunofluorescence (IF) microscopy assays were used to ascertain the subcellular distribution of MAGI-1 in cells. We found that, in normal CREF fibroblasts, MAGI-1 was primarily distributed diffusely within the cytoplasm (Fig. 6A). Other PDZ proteins also localize in the cytoplasm (Wu *et al.*, 1998; Yang *et al.*, 1998), although these polypeptides more often associate with the plasma membrane at sites of cell-cell contact in epithelial cells (Fanning and Anderson, 1999). Because 9ORF1 is present within punctate bodies in the cytoplasm of CREF cells (Weiss *et al.*, 1996), we hypothesized that the subcellular distribution of MAGI-1 seen in normal CREF cells would be altered in 9ORF1-expressing CREF cells. As predicted, MAGI-1 was redistributed within punctate bodies in the cytoplasm of the CREF cell line expressing wild-type 9ORF1 (CREF-9ORF1) (Fig. 6A). This aberrant localization of MAGI-1 was due to association of 9ORF1 with MAGI-1, as these proteins co-localized in the same cytoplasmic bodies (Fig. 6B).

We also examined the subcellular distribution of MAGI-1 in CREF cell lines stably expressing mutant 9ORF1 proteins (see Table 1) which, similar to wild-type 9ORF1, exhibit punctate cytoplasmic staining in CREF cells (Weiss *et al.*, 1997a). Despite the fact that each of the different CREF cell lines expressed 9ORF1 protein at comparable levels (Fig. 7, *upper panel*), the staining pattern of MAGI-1 in the CREF cell line expressing mutant IIIA (CREF-IIIA; Fig. 6A), which fails to bind MAGI-1 (see Fig. 2), was similar to that of normal CREF cells, whereas substantially reduced amounts of aberrant punctate staining for MAGI-1 were detected in the cytoplasm of the CREF cell line expressing mutant IIID (CREF-IIID;

Fig. 6A), which binds weakly to MAGI-1 (see Fig. 2). Interestingly, the CREF cell line expressing mutant IIIC (CREF-IIIC), which binds MAGI-1 at nearly wild-type levels (see Fig. 2), showed a MAGI-1 staining pattern similar to that of normal CREF cells (Fig. 6A). Therefore, in addition to having defective PDZ-domain interactions with MAGI-1 (see Fig. 5A), mutants IIIC and IIID also either failed or showed a substantially reduced capacity, respectively, to sequester MAGI-1 within punctate bodies in the cytoplasm of CREF cells.

To confirm the aberrant sequestration of MAGI-1 by 9ORF1 detected in IF assays, we performed crude cell-fractionation assays with the same CREF cell lines. In these experiments, cells lysed in RIPA buffer were separated by centrifugation into RIPA buffer-soluble supernatant and RIPA buffer-insoluble pellet fractions, each of which was immunoblotted for the presence of MAGI-1 protein. In normal CREF cells, the majority of MAGI-1 protein was detected in the RIPA buffer-soluble fraction but, in CREF-9ORF1 cells, MAGI-1 was exclusively present within the RIPA buffer-insoluble fraction (Fig. 7, *lower panel*). It was this inability to recover soluble MAGI-1 protein from extracts of CREF-9ORF1 cells that prevented us from showing co-immunoprecipitation of 9ORF1 and MAGI-1 with this particular cell line. More important, the results of crude cell-fractionation assays with CREF cells expressing mutant 9ORF1 proteins were in accordance with the IF findings because MAGI-1 protein was recovered primarily in the RIPA buffer-soluble fraction of the CREF-IIIA, CREF-IIIC, and CREF-IIID cell lines (Fig. 7, *lower panel*).

High-risk human papillomavirus E6 oncoproteins also complex with MAGI-1

We (Lee *et al.*, 1997) and others (Kiyono *et al.*, 1997) previously showed that, like 9ORF1, high-risk but not low-risk HPV E6 oncoproteins contain functional PDZ domain-binding motifs at their carboxyl-termini (Table 1) and bind DLG. To determine whether high-risk HPV E6

oncoproteins also bind MAGI-1, we performed GST-pulldown assays with lysates of COS-7 cells expressing the HAMAGI-1c protein. The results indicated that wild-type high-risk 16E6 and 18E6, but not low-risk HPV-11 E6 (11E6), bind MAGI-1 in these assays (Fig. 8). Moreover, the mutants 16E6-T149D/L151A and 18E6-V158A, which have disrupted PDZ domain-binding motifs (Table 1), failed to bind MAGI-1, indicating that the interactions between wild-type high-risk E6 oncoproteins and MAGI-1 were specific and required a functional PDZ domain-binding motif. We further demonstrated that a 16 aa-residue carboxyl-terminal 18E6 peptide (18E6-CT16) containing the PDZ domain-binding motif was sufficient to mediate binding to MAGI-1 (Fig. 8).

High-risk HPV E6 oncoproteins target MAGI-1 for degradation

High-risk HPV E6 oncoproteins promote degradation of the p53 tumor suppressor protein in cells by ubiquitin-dependent proteolysis (Scheffner *et al.*, 1990). As we recently showed that DLG is also targeted for degradation by high-risk HPV E6 proteins (Gardioli *et al.*, 1999), it was of interest to determine whether MAGI-1 is similarly affected by these viral proteins. This possibility was initially examined by mixing and incubating *in vitro*-translated FLAG epitope-tagged MAGI-1 (FLAGMAGI-1c) with wild-type or mutant 18E6 and 16E6 proteins. MAGI-1 protein levels were substantially reduced after a brief incubation with wild-type 18E6 or 16E6 but remained unchanged following longer incubations with either mutant 18E6-V158A or 16E6-T149D/L151A, or water-primed *in vitro*-translation reactions (Fig. 9).

To determine whether high-risk HPV E6 proteins also specifically target MAGI-1 for degradation in cells, we compared the steady-state protein levels of MAGI-1 in COS-7 cells either expressing MAGI-1 alone or co-expressing MAGI-1 and wild-type or mutant E6 proteins. Consistent with our *in vitro* results, MAGI-1 protein levels were substantially reduced in cells

expressing either wild-type 18E6 or 16E6 (Fig. 10A). The results of additional experiments indicated that the reduction of MAGI-1 protein levels in cells expressing these wild-type E6 proteins was specific and due to proteolysis. First, no decrease in MAGI-1 protein levels was detected in cells expressing either the 18E6-V158A or 16E6-T149D/L151A mutant protein, or the low-risk 11E6 protein (Fig. 10A). Second, consistent with our inability to detect binding of 18E6 to a truncated MAGI-1 protein lacking all five PDZ domains (MAGI-1 Δ 5PDZ) (see Fig. 5B) or to the wild-type MAGUK-family PDZ-protein ZO-2 (Jesaitis and Goodenough, 1994) (Fig. 10B), 18E6 failed to reduce the protein levels of either polypeptide in cells (Fig. 10C). Finally, the results of pulse-chase experiments in COS-7 cells expressing MAGI-1 alone or co-expressing MAGI-1 and 18E6 demonstrated that the half-life of the MAGI-1 protein is drastically decreased from approximately 24 h in normal cells to approximately 1 h in 18E6-expressing cells (Fig. 11). From these results, we conclude that high-risk HPV E6 oncoproteins specifically target the PDZ-protein MAGI-1 for degradation in cells.

Discussion

Interactions of the 9ORF1 oncoprotein with the MAGUK-protein DLG and with several other unidentified cellular factors (p220, p180, p160, p155) correlate with the ability of this viral protein to transform cells (Weiss and Javier, 1997). Thus, identification and characterization of the unidentified cellular proteins is expected to aid in fully revealing the mechanisms of 9ORF1-induced transformation. In this study, we showed that, in addition to DLG, 9ORF1 also binds to the related MAGUK-protein MAGI-1 and that this cellular PDZ protein likely represents the previously unidentified 9ORF1-associated protein p180. Particularly noteworthy is that all transformation-defective 9ORF1 mutants having an altered PDZ domain-binding motif displayed impaired interactions with MAGI-1. For example, the severely transformation-defective mutant IIIA and the weak-transforming mutant IIID failed or showed a substantially reduced capacity, respectively, to bind MAGI-1. In addition, although the weak-transforming mutant IIIC bound to MAGI-1 at nearly wild-type levels in cells, this mutant protein was impaired both for interacting with certain MAGI-1 PDZ domains and for aberrantly sequestering MAGI-1 within RIPA buffer-insoluble complexes in the cytoplasm of cells. With respect to the latter observation, we noted that, in contrast to wild-type 9ORF1, substantial amounts of mutant IIIC protein exist in the RIPA buffer-soluble fraction of cells, suggesting that this mutant may be inherently unable to sequester PDZ proteins in the cytoplasm of cells. Taken together, results with transformation-defective 9ORF1 mutants suggest that the ability of 9ORF1 to bind and aberrantly sequester MAGI-1 in cells contributes to 9ORF1-mediated cellular transformation.

It is also noteworthy that, among six different PDZ proteins examined, only MAGI-1 was found to interact with 9ORF1. This finding indicates that 9ORF1 targets only select PDZ

proteins in cells. This idea is further evidenced by the select interaction of 9ORF1 with two of the five PDZ domains of MAGI-1 and two of the three PDZ domains of DLG (Lee *et al.*, 1997). These observations, coupled with the fact that 9ORF1 mutants IIIC and IIID bind only one MAGI-1 PDZ domain, argue that precise sequence requirements both within the PDZ domain-binding motif of 9ORF1 and within each PDZ domain of the 9ORF1-associated targets determine these highly specific protein-protein interactions.

The fact that MAGI-1 is a MAGUK-family protein suggests that this PDZ protein functions to assemble numerous cellular targets into large signaling complexes in cells. In contrast to many PDZ proteins, however, MAGI-1 was found to localize predominantly in the cytoplasm of CREF fibroblasts. Although we cannot discount the possibility that a minor fraction of MAGI-1 is present at the membrane of CREF cells, this finding may indicate that MAGI-1 functions primarily in the cytoplasm. Alternatively, it is feasible that MAGI-1 does function at the membrane, but its translocation to this site occurs only following specific cellular stimuli. Besides possible cytoplasmic and membrane activities, the MAGI-1c isoform, which contains a consensus bipartite nuclear localization signal (Dobrosotskaya *et al.*, 1997), may additionally function in the nucleus, perhaps to regulate the transcription of certain cellular genes. Again, we did not detect MAGI-1 in the nucleus of cells, but nuclear localization may occur only under specific conditions, as has been reported for the related MAGUK-family protein ZO-1 (Gottardi *et al.*, 1996). Regardless of where in the cell MAGI-1 functions, however, this cellular factor would likely be inactivated in 9ORF1-expressing cells, as we found that 9ORF1 sequesters MAGI-1 in the cytoplasm of cells. Also considering that 9ORF1 binds strongly to MAGI-1 PDZ1 and PDZ3, 9ORF1 would be expected to block MAGI-1 from complexing with the normal cellular targets of these PDZ domains. Therefore, aberrant

sequestration and disruption of protein complexes, as well as perturbation of associated protein activities, may all be envisioned as possible mechanisms by which 9ORF1 could inhibit the normal functions of MAGI-1 in cells.

Like 9ORF1, all known high-risk HPV E6 oncoproteins also possess a carboxyl-terminal PDZ domain-binding motif (Lee *et al.*, 1997). Significantly, disruption of the PDZ domain-binding motif of 16E6 renders this viral protein transformation-defective in rat 3Y1 fibroblasts (Kiyono *et al.*, 1997). As infections with high-risk HPV-16 and HPV-18 are associated with approximately 75% of cervical carcinomas (Bosch *et al.*, 1995), our finding that both the 16E6 and 18E6 oncoproteins, but not the low-risk 11E6 protein, utilize their carboxyl-terminal PDZ domain-binding motif to bind the PDZ-protein MAGI-1 is also likely to be important. This idea is further underscored by the facts that 16E6 and 18E6 mutant proteins having disrupted PDZ domain-binding motifs fail to bind MAGI-1 and that the wild-type 18E6 protein does not complex with the related MAGUK proteins ZO-1 (unpublished results) and ZO-2. Such specific and selective interactions suggest that the ability of high-risk HPV E6 oncoproteins to associate with MAGI-1 in cells may contribute to the development of HPV-associated cancers in people.

A common mechanism by which the oncoproteins of DNA tumor viruses promote cell proliferation is to inactivate cellular tumor suppressor proteins. For example, both the adenovirus E1B and high-risk HPV E6 oncoproteins functionally inactivate the tumor suppressor protein p53, yet by distinct mechanisms. In this regard, E1B sequesters p53 in an inactive state (Shenk, 1996), whereas high-risk HPV E6 targets p53 for ubiquitin-mediated proteolysis (Howley, 1996). Likewise, we found that the 9ORF1 oncoprotein sequesters MAGI-1 in the cytoplasm of cells whereas the high-risk HPV E6 proteins target MAGI-1 for degradation in

cells. These findings argue that adenovirus E4-ORF1 and high-risk HPV E6 oncoproteins similarly inactivate MAGI-1 by distinct mechanisms. As MAGI-1 is related to DLG and both proteins are selectively targeted by two otherwise unrelated viral oncoproteins, it seems plausible that these PDZ proteins have related functions in cells. Therefore, we hypothesize that MAGI-1 similarly functions to suppress inappropriate cellular proliferation and, consequently, represents a new candidate tumor suppressor protein.

Materials and methods

Cells and cell extracts

CREF (Fisher *et al.*, 1982), TE85 (McAllister *et al.*, 1971), and COS-7 (Gluzman, 1981) cell lines were maintained in culture medium [Dulbecco's Modified Eagle Medium supplemented with gentamicin (20 µg/ml) and 6% or 10% fetal bovine serum (FBS)]. CREF cell pools (group 16) stably expressing wild-type or mutant 9ORF1 protein (Weiss *et al.*, 1997a), as well as a CREF cell pool stably expressing an influenza hemagglutinin (HA) epitope-tagged 9ORF1 protein (Weiss *et al.*, 1997b), were maintained in culture medium supplemented with G418.

Cell extracts were prepared in either RIPA buffer [50 mM Tris-HCl pH 8.0, 150 mM NaCl, 1% (vol/vol) Nonidet P-40, 0.5% (wt/vol) sodium deoxycholate, 0.1% (wt/vol) sodium dodecyl sulfate (SDS)] or NETN buffer [20 mM Tris, pH 8.0, 100 mM NaCl, 1 mM EDTA, 0.5% Nonidet P-40 (vol/vol)] as described previously (Lee *et al.*, 1997). Alternatively, cells were lysed directly in sample buffer [0.15 M Tris-HCl pH 6.8, 2% (wt/vol) SDS, 10% (vol/vol) glycerol, 1% (vol/vol) β-mercaptoethanol, 0.0015% (wt/vol) bromophenol blue]. For crude cell-fractionation assays, the pellet obtained after centrifugation of RIPA buffer-lysed cells was solubilized in sample buffer using the same volume originally used to lyse the cells in RIPA buffer. Protein concentrations of cell extracts were determined by the Bradford assay (Bradford, 1976).

Plasmids

pCDNA3 (Invitrogen) plasmids coding for amino-terminal FLAG epitope-tagged mouse MAGI-1 isoform b (MAGI-1b), MAGI-1 isoform c (MAGI-1c), and MAGI-1b missing either PDZ1 (aa 453-549; MAGI-1bΔPDZ1), PDZ2 (aa 625-702; MAGI-1bΔPDZ2), or PDZ3

(aa 796-875; MAGI-1b Δ PDZ3), as well as pGEX-KG (Pharmacia) plasmids coding for MAGI-1 PDZ1 (aa 431-545), PDZ2 (aa 601-702), PDZ4 (aa 925-1034), or PDZ5 (aa 1013-1116) were generously provided by Guy James. cDNA sequences coding for MAGI-1 PDZ3 (aa 763-880) were amplified by PCR and introduced in-frame with the glutathione *S*-transferase (GST) gene of pGEX-2T to make pGEX-MAGI-1PDZ3. pGEX-2T and pGEX-2TK plasmids coding for wild-type Ad5 and Ad12 E4-ORF1 proteins (5ORF1 and 12ORF1, respectively), as well as for wild-type or mutant 9ORF1 proteins were described previously (Weiss and Javier, 1997). The cDNAs of HPV-18 E6 (18E6) mutant 18E6-V158A, wild-type HPV-16 E6 (16E6), and mutant 16E6-T149D/L151A were introduced into the *Hind*III and *Eco*RI sites of pSP64 (Promega) to generate pSP64-18E6-V158A, pSP64-16E6, and pSP64-16E6-T149D/L151A. An HA-epitope tag was introduced at the amino-terminus of MAGI-1b, MAGI-1c, MAGI-1 Δ 5PDZ (aa 1-424), 16E6, mutant 16E6-T149D/L151A, and canine ZO-2 by PCR methods. cDNAs coding for the HA-epitope-tagged MAGI-1 and 16E6 proteins were introduced between the *Hind*III and *Eco*RI sites of CMV expression plasmid GW1 (British Biotechnology) to generate GW1-HAMAGI-1b, GW1-HAMAGI-1c, GW1-HAMAGI-1 Δ 5PDZ, GW1-HA16E6, and GW1-HA16E6-T149D/L151A. The HA-epitope-tagged ZO-2 cDNA was introduced into the *Sma*I site of GW1 to generate GW1-HAZO-2. The deletions of pCDNA3-FLAGMAGI-1b Δ PDZ1 and pCDNA3-FLAGMAGI-1b Δ PDZ3 were subcloned individually or in combination into GW1-HAMAGI-1b to generate GW1-HAMAGI-1b Δ PDZ1, GW1-HAMAGI-1b Δ PDZ3, and GW1-HAMAGI-1b Δ PDZ1+3. PCR reactions were performed with *Pfu* polymerase (Stratagene), and plasmids were verified by restriction enzyme and limited sequence analyses. Plasmids GW1-HA18E6, GW1-HA18E6-V158A, GW1-HA11E6,

GW1-9ORF1wt, GW1-9ORF1IIIA, GW1-9ORF1IIIC, GW1-9ORF1IIID, and pSP64-18E6 were described elsewhere (Gardiol *et al.*, 1999).

Antisera and antibodies

Rabbit polyclonal antiserum raised to the unique amino-terminal region of MAGI-1 (aa 2-140) was generously provided by Guy James (Dobrosotskaya *et al.*, 1997). 9ORF1 antiserum was described previously (Javier, 1994). Commercially-available FLAG antibodies (Santa Cruz Biotechnology), 12CA5 HA monoclonal antibodies (BABCO; Boehringer Mannheim), normal rabbit IgG, peroxidase-conjugated goat anti-rabbit or goat anti-mouse IgG (Southern Biotechnology Associates), FITC-conjugated goat anti-rabbit or goat anti-mouse IgG (Gibco BRL), or Texas red-conjugated goat anti-mouse IgG (Molecular Probe) were used.

GST-pulldown, immunoprecipitation, and immunoblot assays

GST-pulldown and immunoprecipitation assays were performed with cell extracts in RIPA buffer as described previously (Lee *et al.*, 1997). Immunoblot assays were carried out as described previously (Weiss *et al.*, 1996) using either 9ORF1 (1:5000), HA (0.2 µg/ml), or MAGI-1 (1 µg/ml) primary antibodies and either horseradish peroxidase-conjugated goat anti-rabbit IgG or goat anti-mouse IgG (1:5000) secondary antibodies. Immunoblotted assays were developed by enhanced chemiluminescence (Pierce).

Protein blotting assays

Individual MAGI-1 PDZ domains were expressed as GST-fusion proteins in bacteria, purified on glutathione sepharose beads (Pharmacia) (Smith and Corcoran, 1994), separated by SDS-polyacrylamide gel electrophoresis (PAGE), and transferred to a nitrocellulose membrane.

Methods for preparing radiolabeled GST fusion protein probes and for performing protein blotting assays with such probes have been described (Lee *et al.*, 1997).

Immunofluorescence microscopy assays

For indirect immunofluorescence (IF) microscopy assays (Harlow and Lane, 1988), cells were grown on coverslips, fixed in methanol for 20 min at -20°C, blocked in IF buffer [TBS (50 mM Tris-HCl pH 7.5, 200 mM NaCl) containing 10% goat serum (Sigma)] for 1 h at RT and, then, incubated with either MAGI-1 antibodies (5 µg/ml), HA antibodies (0.24 mg/ml) or normal rabbit IgG (5 µg/ml) for 3 h at 37°C. Cells were subsequently washed with TBS, blocked as described above, incubated with either FITC-conjugated goat anti-rabbit or goat anti-mouse IgG antibodies (1:250) or Texas red-conjugated goat anti-mouse IgG antibodies (1:250) for 1 h at 37°C, and washed with TBS. All antibodies were diluted in IF buffer. Cells were visualized by fluorescence microscopy using a Zeiss Axiophot microscope, and images were processed using Adobe PhotoShop software.

In vitro-degradation assays

pCDNA3-FLAGMAGI-1c, pSP64-18E6, pSP64-18E6-V158A, pSP64-16E6, and pSP64-16E6-T149D/L151A plasmids were transcribed and translated *in vitro* using the TnT coupled rabbit reticulocyte lysate system (Promega) and 50 µCi [³⁵S]-cysteine (1200 Ci/mmol) (Amersham), according to the manufacturer's instructions. The amount of radioactivity introduced into *in vitro*-translated proteins per microliter of reaction was determined by resolving an aliquot of each reaction by SDS-PAGE and quantifying CPM within relevant protein bands using a Storm Molecular Dynamics phosphorimager. For *in vitro*-degradation assays, a reaction volume equivalent to 50 CPM of *in vitro*-translated FLAGMAGI-1c protein was mixed with a

reaction volume equivalent to 250 CPM of *in vitro*-translated 18E6, 18E6-V158A, 16E6, or 16E6-T149D/L151A protein. All assay volumes were equalized with a water-primed *in vitro*-translation reaction and, at selected time points, an aliquot from each assay mixture was removed and subjected to immunoprecipitation analysis. Recovered proteins were resolved by SDS-PAGE and visualized by autoradiography.

Pulse-chase labeling of proteins in cells

At 48 h post-transfection, COS-7 cells were incubated with methionine- and cysteine-free DMEM containing 5% dialyzed FBS [5% FBS-DMEM-MC] for 30 min and, then, pulse labeled for 15 min in the same medium containing 0.2 mCi/ml [³⁵S] EXPRESS protein label (Dupont). Following several washes with 5% FBS-DMEM-MC, pulse radiolabelled cells were chased by incubation with culture medium containing five-fold excess methionine (15 mg/L) for various times, harvested, and lysed in RIPA buffer. Cell extracts were subjected to immunoprecipitation with HA antibodies, and recovered proteins were resolved by SDS-PAGE and visualized by autoradiography. Amounts of protein immunoprecipitated were quantified using a phosphorimager.

Acknowledgements

We are indebted to Guy James (University of Texas Health Sciences Center, San Antonio) for generously providing MAGI-1 reagents. We also thank Bruce Stevenson for providing the canine ZO-2 expression plasmid. B.G. and S.S.L. were recipients of a Molecular Virology Training Grant (T32 AI07471) and the U.S. Army Breast Cancer Training Grant (DAMD17-94-J4204), respectively. This work was supported by grants from the National Institutes of Health (RO1 CA58541), the American Cancer Society (RPG-97-668-01-VM), and the U.S. Army (DAMD17-97-1-7082) to R.T.J. and an Associazione Italiana per la Ricerca sul Cancro grant to L.B.

References

- Bosch, F.X., Manos, M.M., Munoz, N., Sherman, M., Jansen, A.M., Peto, J., Schiffman, M.H., Moreno, V., Kurman, R. and Shah, K.V. (1995) Prevalence of human papillomavirus in cervical cancer: a worldwide perspective. International biological study on cervical cancer (IBSCC) Study Group. *J. Natl. Cancer Inst.*, **87**, 796-802.
- Bradford, M.M. (1976) A rapid and sensitive method for the quantitation of microgram quantities of protein utilizing the principle of protein-dye binding. *Anal. Biochem.*, **72**, 248-254.
- Craven, S.E. and Bretz, D.S. (1998) PDZ proteins organize synaptic signaling pathways. *Cell*, **93**, 495-498.
- Dobrosotskaya, I., Guy, R.K. and James, G.L. (1997) MAGI-1, a membrane-associated guanylate kinase with a unique arrangement of protein-protein interaction domains. *J. Biol. Chem.*, **272**, 31589-31597.
- Fanning, A.S. and Anderson, J.M. (1999) PDZ domains: fundamental building blocks in the organization of protein complexes at the plasma membrane. *J. Clin. Invest.*, **103**, 767-772.
- Fisher, P.B., Babiss, L.E., Weinstein, I.B. and Ginsberg, H.S. (1982) Analysis of type 5 adenovirus transformation with a cloned rat embryo cell line (CREF). *Proc. Natl. Acad. Sci. USA*, **79**, 3527-3531.
- Gardioli, D., Kuhne, C., Glaunsinger, B., Lee, S., Javier, R. and Banks, L. (1999) Oncogenic papillomavirus E6 proteins target the discs large tumour suppressor for proteasome-mediated degradation. *Oncogene*, **18**, 5487-5496.
- Gluzman, Y. (1981) SV40-transformed simian cells support the replication of early SV40 mutants. *Cell*, **23**, 175-182.

- Gottardi, C.J., Arpin, M., Fanning, A.S. and Louvard, D. (1996) The junction-associated protein, zonula occludens-1, localizes to the nucleus before the maturation and during the remodeling of cell-cell contacts. *Proc. Natl. Acad. Sci. U S A*, **93**, 10779-10784.
- Harlow, E. and Lane, D. (1988) Cell staining. In Harlow, E. and Lane, D. (eds.), *Antibodies: a laboratory manual*. Cold Spring Harbor Laboratory, Cold Spring Harbor, N.Y., pp. 359-420.
- Haskins, J., Gu, L., Wittchen, E.S., Hibbard, J. and Stevenson, B.R. (1998) ZO-3, a novel member of the MAGUK protein family found at the tight junction, interacts with ZO-1 and occludin. *J. Cell. Biol.*, **141**, 199-208.
- Howley, P.M. (1996) Papillomavirinae: the viruses and their replication. In Fields, B.N., Knipe, D.M. and Howley, P.M. (eds.), *Fields Virology*. Lippincot-Raven, Philadelphia, Vol. 2, pp. 2045-2076.
- Javier, R., Raska, K., Jr., Macdonald, G.J. and Shenk, T. (1991) Human adenovirus type 9-induced rat mammary tumors. *J. Virol.*, **65**, 3192-3202.
- Javier, R.T. (1994) Adenovirus type 9 E4 open reading frame 1 encodes a transforming protein required for the production of mammary tumors in rats. *J. Virol.*, **68**, 3917-3924.
- Jesaitis, L.A. and Goodenough, D.A. (1994) Molecular characterization and tissue distribution of ZO-2, a tight junction protein homologous to ZO-1 and the *Drosophila* discs-large tumor suppressor protein. *J. Cell. Biol.*, **124**, 949-961.
- Kiyono, T., Hiraiwa, A., Fujita, M., Hayashi, Y., Akiyama, T. and Ishibashi, M. (1997) Binding of high-risk human papillomavirus E6 oncoproteins to the human homologue of the *Drosophila* discs large tumor suppressor protein. *Proc. Nat. Acad. Sci. USA*, **94**, 11612-11616.

- Lee, S.S., Weiss, R.S. and Javier, R.T. (1997) Binding of human virus oncoproteins to hDlg/SAP97, a mammalian homolog of the Drosophila discs large tumor suppressor protein. *Proc. Natl. Acad. Sci. USA*, **94**, 6670-6675.
- Lue, R.A., Marfatia, S.M., Branton, D. and Chishti, A.H. (1994) Cloning and characterization of hdlg: the human homologue of the Drosophila discs large tumor suppressor binds to protein 4.1. *Proc. Natl. Acad. Sci. USA*, **91**, 9818-9822.
- McAllister, R.M., Filbert, J.E., Nicolson, M.O., Rongey, R.W., Gardner, M.B., Gilden, R.V. and Huebner, R.J. (1971) Transformation and productive infection of human osteosarcoma cells by a feline sarcoma virus. *Nat. New. Biol.*, **230**, 279-282.
- Muller, B.M., Kistner, U., Veh, R.W., Cases-Langhoff, C., Becker, B., Gundelfinger, E.D. and Garner, C.C. (1995) Molecular characterization and spatial distribution of SAP97, a novel presynaptic protein homologous to SAP90 and the Drosophila discs-large tumor suppressor protein. *J. Neurosci.*, **15**, 2354-2366.
- Nevins, J.R. and Vogt, P.K. (1996) Cell transformation by viruses. In Fields, B.N., Knipe, D.M. and Howley, P.M. (eds.), *Fields Virology*. Lippincott-Raven Publishers, Philadelphia, Vol. 1, pp. 301-343.
- Philipp, S. and Flockerzi, V. (1997) Molecular characterization of a novel human PDZ domain protein with homology to INAD from Drosophila melanogaster. *FEBS Lett.*, **413**, 243-248.
- Prasad, R., Gu, Y., Alder, H., Nakamura, T., Canaani, O., Saito, H., Huebner, K., Gale, R.P., Nowell, P.C., Kuriyama, K. and et al. (1993) Cloning of the ALL-1 fusion partner, the AF-6 gene, involved in acute myeloid leukemias with the t(6;11) chromosome translocation. *Cancer Res.*, **53**, 5624-5628.

- Sato, T., Irie, S., Kitada, S. and Reed, J.C. (1995) FAP-1: a protein tyrosine phosphatase that associates with Fas. *Science*, **268**, 411-415.
- Scheffner, M., Werness, B.A., Huibregtse, J.M., Levine, A.J. and Howley, P.M. (1990) The E6 oncoprotein encoded by human papillomavirus types 16 and 18 promotes the degradation of p53. *Cell*, **63**, 1129-1136.
- Shenk, T. (1996) Adenoviridae: the viruses and their replication. In Fields, B.N., Knipe, D.M. and Howley, P.M. (eds.), *Fields Virology*. Lippincott-Raven Publishers, Philadelphia, Vol. 2, pp. 2111-2148.
- Smith, D.B. and Corcoran, L.M. (1994) Expression and purification of glutathione-S-transferase fusion proteins. In Ausubel, F.M., Brent, R., Kingston, R.E., Moore, D.D., Seidman, J.G., Smith, J.A. and Struhl, K. (eds.), *Current Protocols in Molecular Biology*. John Wiley & Sons, Inc., New York, Vol. 2, pp. 16.17.11-16.17.17.
- Thomas, D.L., Shin, S., Jiang, B.H., Vogel, H., Ross, M.A., Kaplitt, M., Shenk, T.E. and Javier, R.T. (1999) Early region 1 transforming functions are dispensable for mammary tumorigenesis by human adenovirus type 9. *J. Virol.*, **73**, 3071-3079.
- Thomas, U., Phannavong, B., Muller, B., Garner, C.C. and Gundelfinger, E.D. (1997) Functional expression of rat synapse-associated proteins SAP97 and SAP102 in *Drosophila* dlg-1 mutants: effects on tumor suppression and synaptic bouton structure. *Mech. Dev.*, **62**, 161-174.
- Weiss, R.S., Gold, M.O., Vogel, H. and Javier, R.T. (1997a) Mutant adenovirus type 9 E4 ORF1 genes define three protein regions required for transformation of CREF cells. *J. Virol.*, **71**, 4385-4394.

- Weiss, R.S. and Javier, R.T. (1997) A carboxy-terminal region required by the adenovirus type 9 E4 ORF1 oncoprotein for transformation mediates direct binding to cellular polypeptides. *J. Virol.*, **71**, 7873-7880.
- Weiss, R.S., Lee, S.S., Prasad, B.V.V. and Javier, R.T. (1997b) Human adenovirus early region 4 open reading frame 1 genes encode growth-transforming proteins that may be distantly related to dUTP pyrophosphatase enzymes. *J. Virol.*, **71**, 1857-1870.
- Weiss, R.S., McArthur, M.J. and Javier, R.T. (1996) Human adenovirus type 9 E4 open reading frame 1 encodes a cytoplasmic transforming protein capable of increasing the oncogenicity of CREF cells. *J. Virol.*, **70**, 862-872.
- Willott, E., Balda, M.S., Fanning, A.S., Jameson, B., Van Itallie, C. and Anderson, J.M. (1993) The tight junction protein ZO-1 is homologous to the Drosophila discs-large tumor suppressor protein of septate junctions. *Proc. Natl. Acad. Sci. USA*, **90**, 7834-7838.
- Woods, D.F. and Bryant, P.J. (1991) The discs-large tumor suppressor gene of Drosophila encodes a guanylate kinase homolog localized at septate junctions. *Cell*, **66**, 451-464.
- Wu, H., Reuver, S.M., Kuhlendahl, S., Chung, W.J. and Garner, C.C. (1998) Subcellular targeting and cytoskeletal attachment of SAP97 to the epithelial lateral membrane. *J. Cell Sci.*, **111**, 2365-2376.
- Yang, N., Higuchi, O. and Mizuno, K. (1998) Cytoplasmic localization of LIM-kinase 1 is directed by a short sequence within the PDZ domain. *Exp. Cell Res.*, **241**, 242-252.

Figure legends

Fig. 1. Three isoforms of MAGI-1. MAGI-1 has an inverted MAGUK domain structure with a guanylate kinase-homology domain (GuK) at its amino-terminus and PDZ domains at its carboxyl-terminus. MAGI-1a, -1b, and -1c isoforms are identical except that their sequences diverge carboxyl-terminal to PDZ5. WW, WW domain; NLS, putative bipartite nuclear localization signal.

Fig. 2. Binding of 9ORF1 to MAGI-1 *in vitro*. (A) 9ORF1 protein binding to mouse MAGI-1c detected in GST-pulldown assays. Extracts of RIPA buffer-lysed COS-7 cells transfected with 5 µg of empty GW1 or 5 µg of GW1-HAMAGI-1c plasmid were used in GST-pulldown reactions with the indicated GST fusion protein, and recovered proteins were immunoblotted with HA antibodies. *Upper panel*, MAGI-1 binding to wild-type and mutant 9ORF1 proteins (see Table 1). *Lower panel*, MAGI-1 binding to the wild-type E4-ORF1 proteins of Ad9, Ad5 (5ORF1), and Ad12 (12ORF1). COS-7 extracts representing one-half the amount used in GST pulldown reactions were also directly immunoblotted with HA antibodies as a control. (B) 9ORF1 binding to endogenous rat MAGI-1 of CREF cells using GST-pulldown assays. CREF cell extracts in RIPA buffer were subjected to GST-pulldown assays and then immunoblotted with MAGI-1 antibodies.

Fig. 3. Co-migration of MAGI-1 and 9ORF1-associated protein p180 in a protein gel. GST-pulldown reactions using GST or GST-9ORF1 protein were performed with extracts of human TE85 cells in RIPA buffer. Recovered proteins from duplicate GST-pulldown reactions were separated in parallel by SDS-PAGE and transferred to a membrane, and membranes were either blotted with a radiolabeled 9ORF1 protein probe (*left*) or with MAGI-1 antibodies (*right*).

Fig. 4. Binding of 9ORF1 to MAGI-1 *in vivo*. Co-immunoprecipitation assays were performed with extracts of COS-7 cells transfected with 4 μ g of GW1-HAMAGI-1 plasmid and either 4 μ g empty GW1 or 4 μ g of GW1 plasmid expressing wild-type or the indicated mutant 9ORF1 protein. COS-7 extracts in RIPA buffer were subjected to immunoprecipitation with either HA antibodies (*upper panel*) or 9ORF1 antibodies (*lower panel*), and recovered proteins were separately immunoblotted with the same two antibodies. In the lower panel, immunoprecipitation of the COS-7 extract with pre-immune serum (pre) was included as a negative control.

Fig. 5. Binding of 9ORF1 to MAGI-1 PDZ1 and PDZ3. (A) Strong binding of 9ORF1 to two of five MAGI-1 PDZ domains. GST proteins fused to individual MAGI-1 PDZ domains were separated by SDS-PAGE, immobilized on duplicate membranes, and either stained with coomassie or protein blotted with the indicated wild-type or mutant 9ORF1 fusion protein probe. (B) Illustration of MAGI-1 deletion mutants. (C) Deletion of both PDZ1 and PDZ3 from MAGI-1 abolishes its interaction with 9ORF1. Extracts of RIPA buffer-lysed COS-7 cells transfected with 5 μ g of GW1 plasmid expressing either HA-tagged wild-type or the indicated mutant MAGI-1 protein were subjected to GST-pulldown reactions with either GST or GST-9ORF1 fusion protein, and recovered proteins were immunoblotted with HA antibodies. COS-7 extracts representing one-tenth the amount used in GST pulldown reactions were also directly immunoblotted with HA antibodies as a control.

Fig. 6. Aberrant sequestration of MAGI-1 in the cytoplasm of 9ORF1-expressing CREF cells. (A) Localization of MAGI-1 in normal CREF cells or CREF cells expressing wild-type or mutant 9ORF1 proteins. Indirect immunofluorescence assays were performed with normal CREF cells (*panels a and c*) or CREF cells stably expressing wild-type 9ORF1 (*panels b and d*),

mutant IIIA (*panel e*), mutant IIIC (*panel f*), or mutant IIID (*panel g*). Cells were reacted with either normal rabbit IgG (*panels a and b*) or MAGI-1 antibodies (*panels c-g*) and visualized by fluorescence microscopy. **(B)** Co-localization of 9ORF1 and MAGI-1 proteins in CREF cells. Double-label indirect immunofluorescence assays were performed by reacting CREF cells stably expressing HA epitope-tagged 9ORF1 (CREF-HA9ORF1) with both HA and MAGI-1 antibodies. Each of the three panels represents the same field containing a single representative cell stained for 9ORF1 (*left panel*), MAGI-1 (*center panel*), or the merged images (*right panel*).

Fig. 7. Aberrant sequestration of MAGI-1 within RIPA buffer-insoluble complexes in 9ORF1-expressing CREF cells. Normal CREF cells or CREF cells stably expressing wild-type or mutant 9ORF1 protein were lysed either in sample buffer (*upper panel*) or in RIPA buffer and subsequently centrifuged to yield RIPA buffer-soluble supernatant (S) and RIPA buffer-insoluble pellet (I) fractions (*lower panel*). Extracts of sample buffer-lysed cells or equal volumes of the S and I fractions from RIPA buffer-lysed cells were separately immunoblotted with MAGI-1 antibodies or 9ORF1 antiserum.

Fig. 8. Binding of high-risk HPV E6 oncoproteins to MAGI-1 *in vitro*. Extracts of COS-7 cells transfected with 5 μ g of empty GW1 or 5 μ g of GWI-HAMAGI-1c plasmid were subjected to GST-pulldown reactions with the indicated GST fusion protein, and recovered proteins were immunoblotted with HA antibodies. GST pulldown assays with the indicated GST fusion protein were performed with COS-7 extracts in RIPA buffer or NETN buffer. COS-7 extracts representing one-tenth the amount used in GST pulldown reactions were also directly immunoblotted with HA antibodies as a control.

Fig. 9. HPV-18 E6-induced degradation of MAGI-1 *in vitro*. *In vitro*-translated FLAG epitope-tagged MAGI-1c (FLAGMAGI-1c) was mixed with *in vitro*-translated wild-type 18E6, 18E6-V158A, wild-type 16E6, 16E6-T149D/L151A, or control water-primed lysates and incubated at 30°C for the indicated times. At each time point, reactions were immunoprecipitated with FLAG antibodies, and recovered proteins were separated by SDS-PAGE and visualized by autoradiography (*left panel*). The amount of *in vitro*-translated E6 protein used in each assay is shown (*right panel*).

Fig. 10. Selective reduction in MAGI-1 protein levels *in vivo* by high-risk HPV E6 proteins.

(A) Decrease in the steady-state protein levels of MAGI-1 induced by high-risk HPV E6 oncoproteins. Extracts of RIPA buffer-lysed COS-7 cells, which were transfected with GW1-HAMAGI-1c plasmid alone or in combination with a GW1 plasmid expressing the indicated wild-type or mutant HPV E6 protein, were immunoblotted with HA antibodies.

(B) Failure of 18E6 to bind a MAGI-1 deletion mutant missing all five PDZ domains (MAGI-1Δ5PDZ) or the wild-type ZO-2 protein. Extracts of RIPA buffer-lysed COS-7 cells were transfected with 5 μg of the indicated GW1 expression plasmid and, then, were subjected to GST-pulldown reactions with either GST or GST-18E6 protein. Recovered proteins were immunoblotted with HA antibodies. COS-7 extracts representing one-tenth the amount used in GST pulldown reactions were also directly immunoblotted with HA antibodies as a control.

(C) Inability of 18E6 to reduce the steady-state protein levels of MAGI-1Δ5PDZ or ZO-2 in cells. Extracts of RIPA buffer-lysed COS-7 cells transfected with either GW1-HAMAGIΔ5PDZ plasmid alone (*upper panel*) or GW1-HAZO-2 plasmid alone (*lower panel*), or either the former or latter plasmid in combination with GW1 plasmid expressing wild-type or mutant HA18E6 (*upper and lower panels*), were immunoblotted with HA antibodies.

Fig. 11. Decrease in MAGI-1 protein half-life induced by the high-risk HPV-18 E6 protein.

COS-7 cells, which were transfected with either empty GW1 plasmid, GW1-HAMAGI-1c alone or in combination with the GW1-HA18E6, were pulse-labeled for 15 min with [³⁵S] EXPRESS protein label and, then, chased with unlabeled culture medium for the indicated times. At each time point, cell extracts were immunoprecipitated with HA antibodies. Recovered MAGI-1 protein was visualized by autoradiography and quantified by phosphorimager analysis.

Table I. Carboxyl-terminal amino-acid sequences of wild-type and mutant adenovirus E4-ORF1 and human papillomavirus (HPV) E6 proteins*

Protein	Carboxyl-terminal amino-acid sequence			
	Consensus type I PDZ domain-binding motif			
	X	(S/T)	X	(V/I/L)-COOH
<u>Adenovirus E4-ORF1</u>				
<i>wt</i> 9ORF1	A	T	L	V
mutant IIIA	A	P		
mutant IIIC	D	T	L	V
mutant IIID	A	T	P	V
<i>wt</i> 5ORF1	A	S	N	V
<i>wt</i> 12ORF1	A	S	L	I
<u>HPV E6</u>				
<i>wt</i> 18E6	E	T	Q	V
mutant 18E6-V158A	E	T	Q	A
<i>wt</i> 16E6	E	T	Q	L
mutant 16E6-T149D/L151A	E	D	Q	A
<i>wt</i> 11E6	D	L	L	P

*The carboxyl-terminal sequences of Ad9 E4 ORF1 (9ORF1), HPV-18 E6 (18E6), and HPV-16 E6 (16E6) define a type I PDZ domain-binding motif, which is not present at the carboxyl-terminus of HPV-11 E6 (11E6). Substitution mutations are indicated by bolded amino-acid residues.

Figure 1.

MAGI-1a



MAGI-1b



MAGI-1c



Figure 2 A.

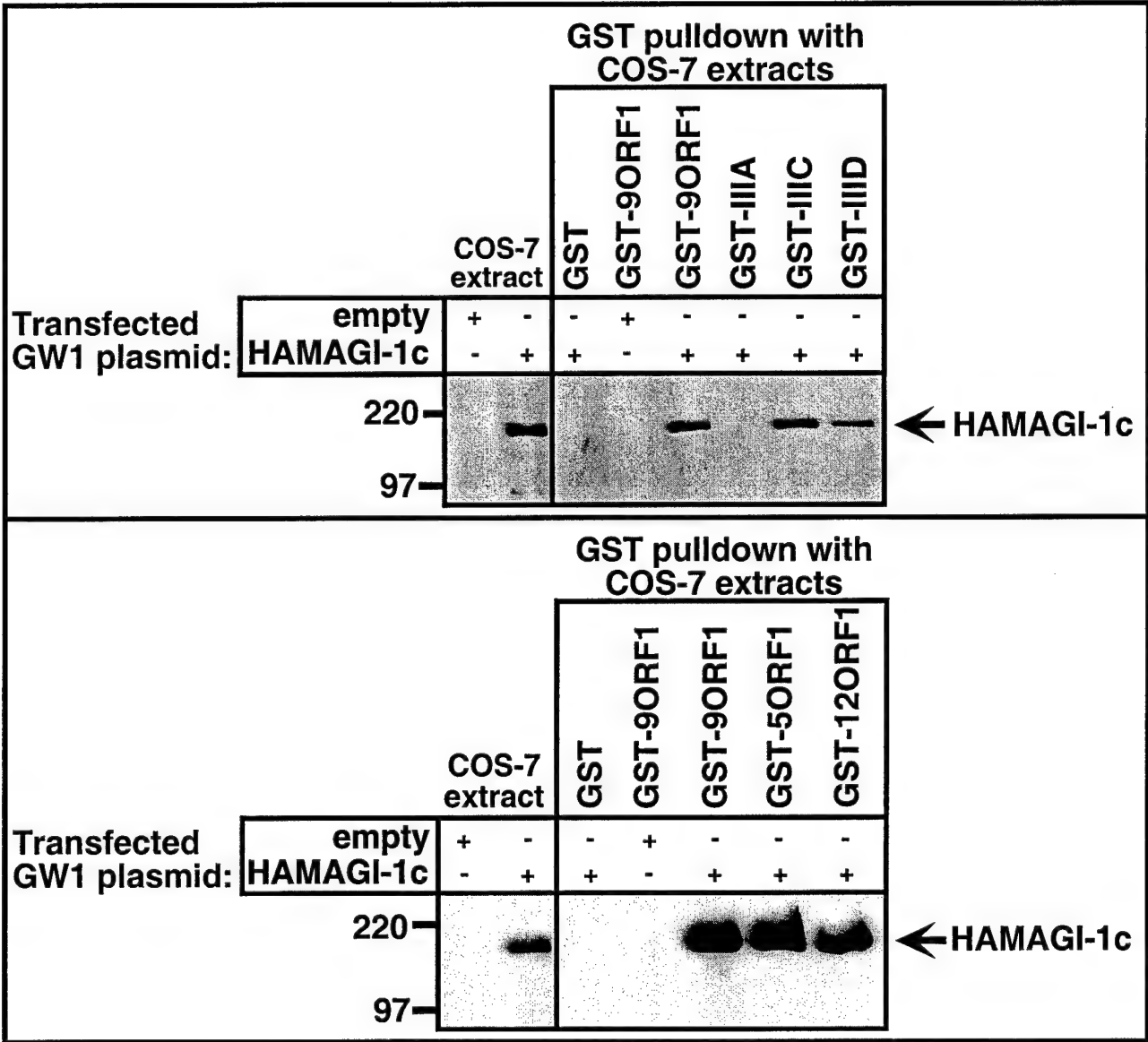


Figure 2 B.

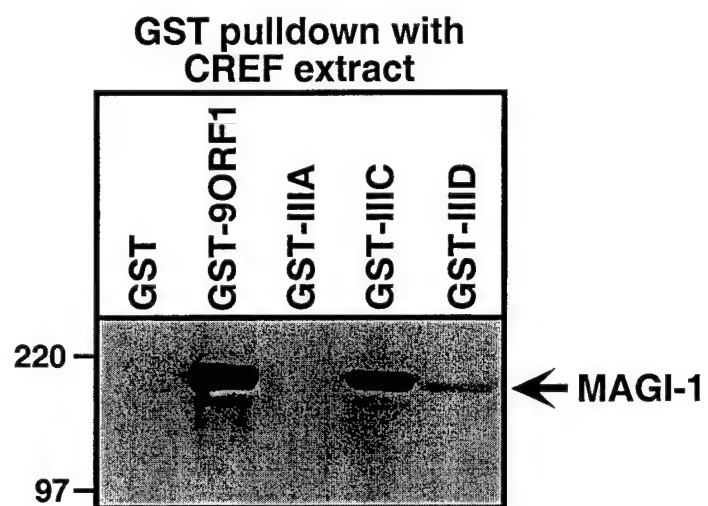


Figure 3.

GST-pulldown with extracts of TE85 cells

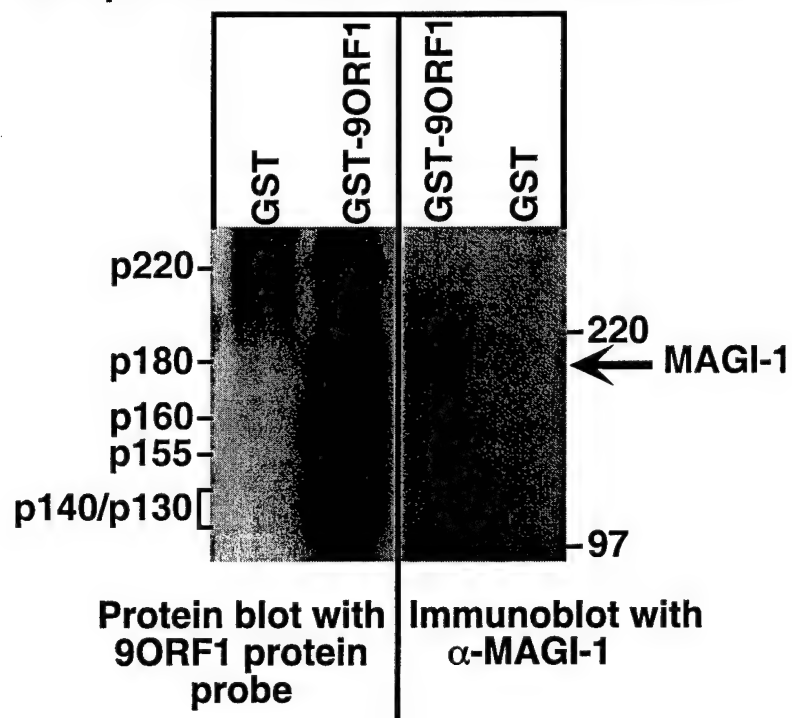


Figure 4.

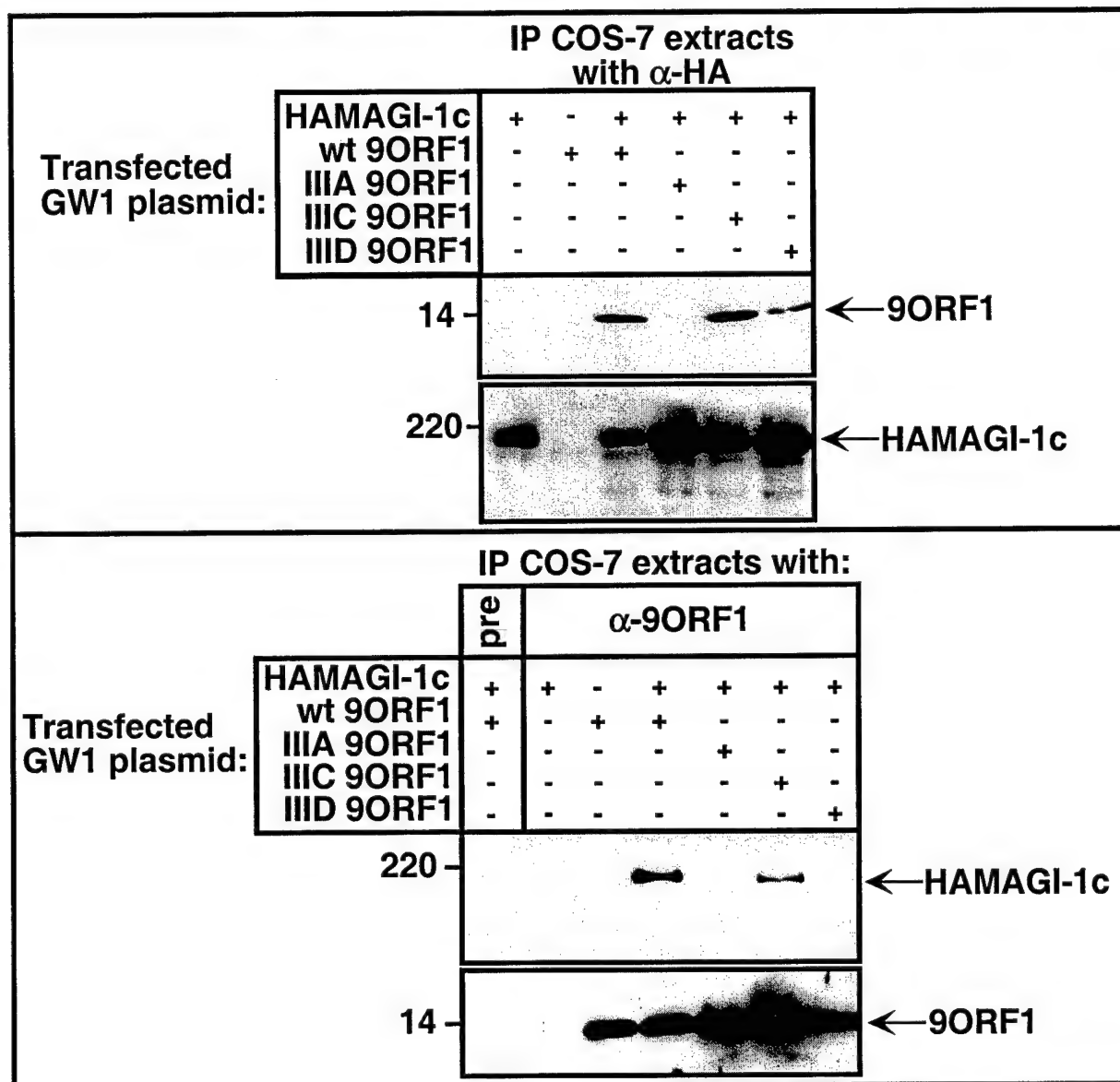


Figure 5 A.

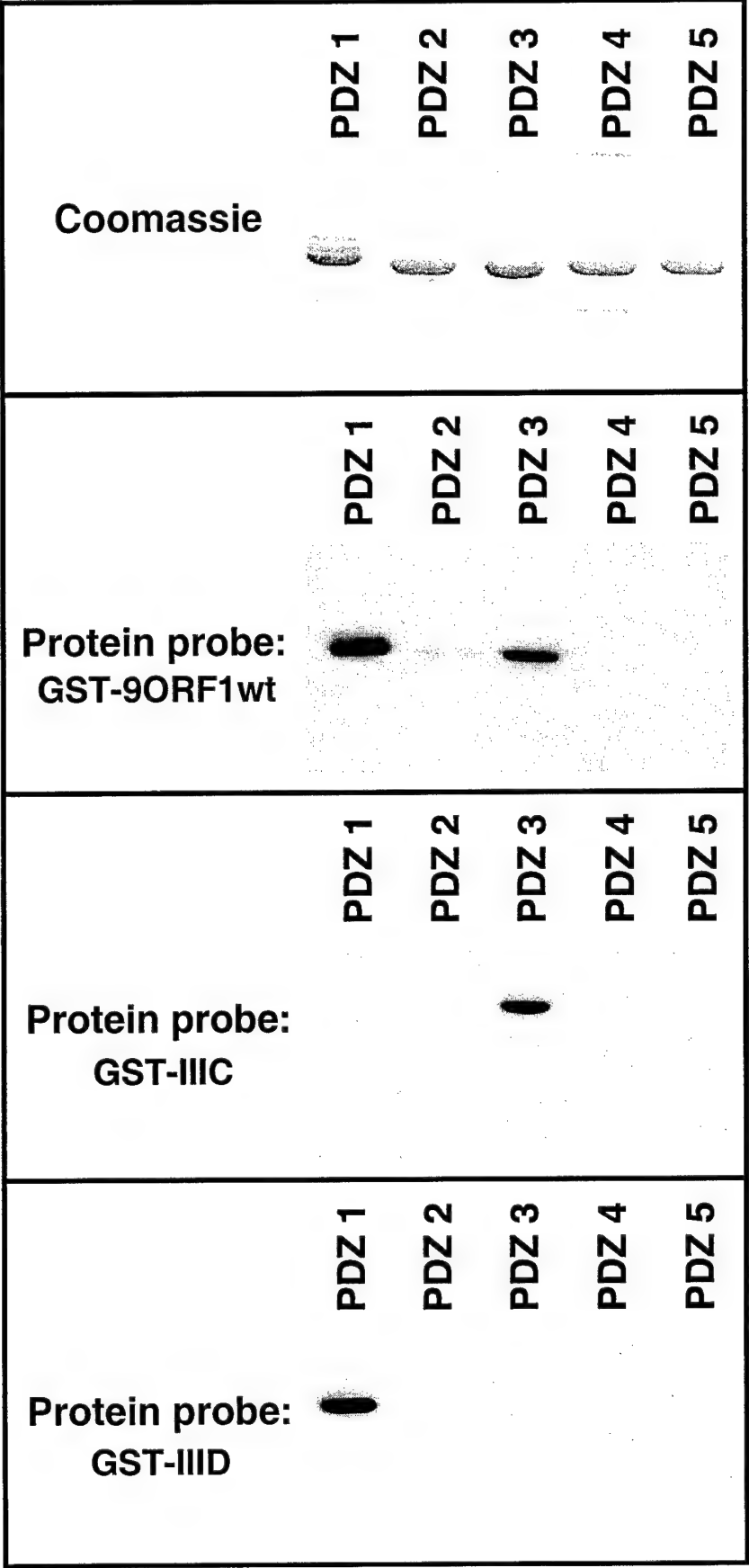


Figure 5 B.

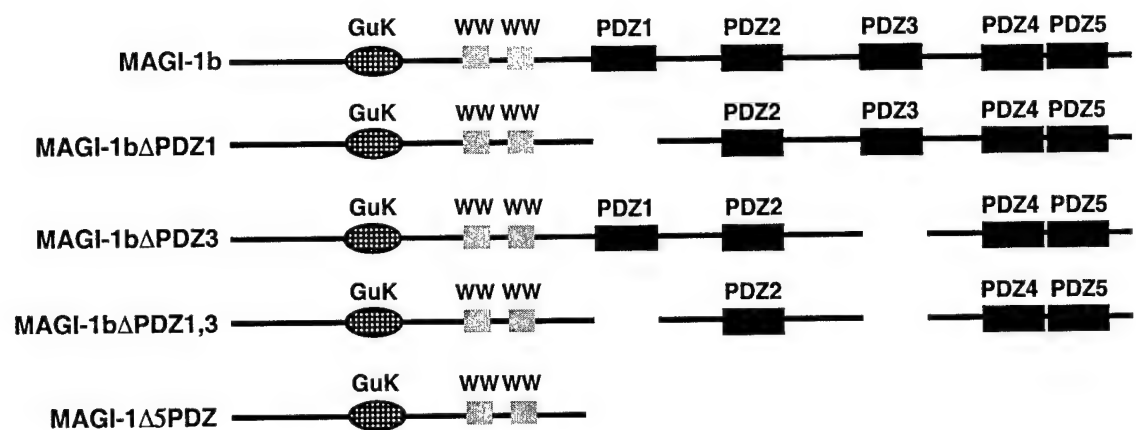


Figure 5 C.

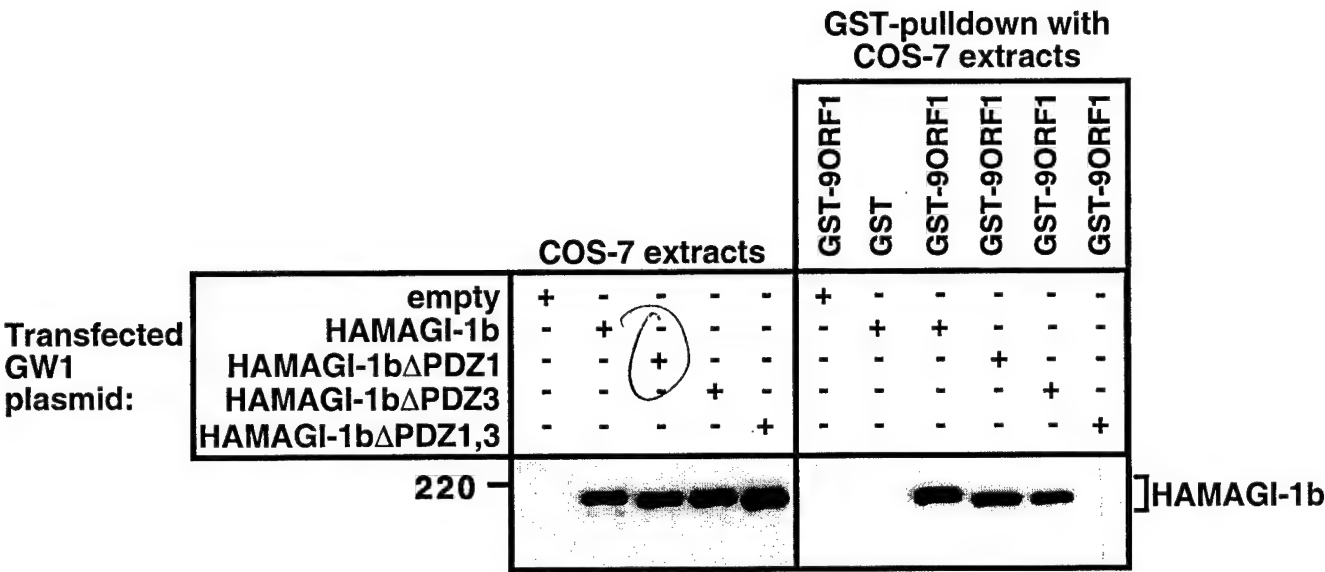


Figure 5D.

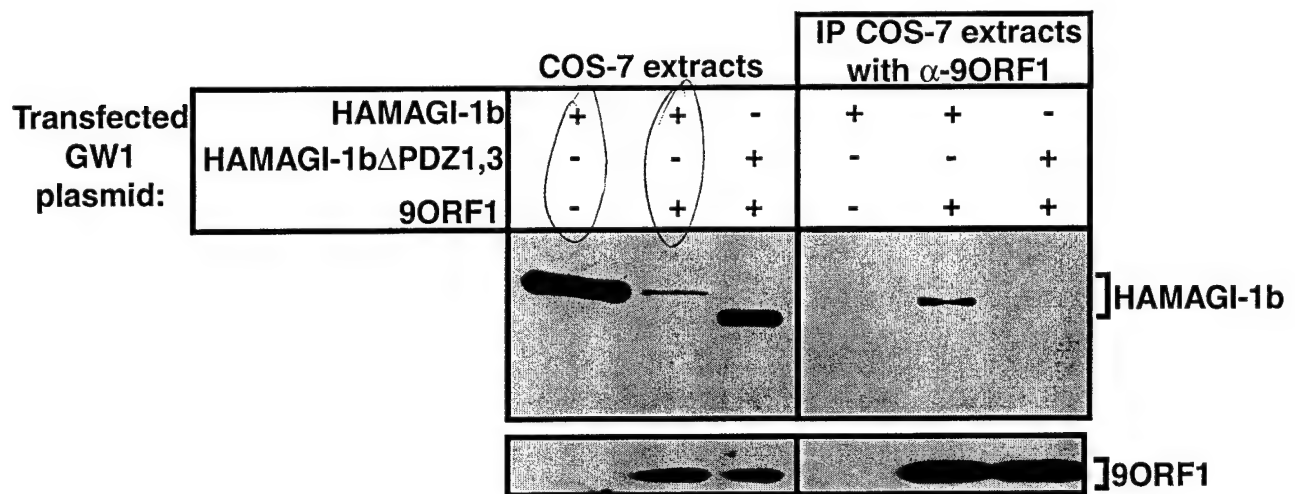
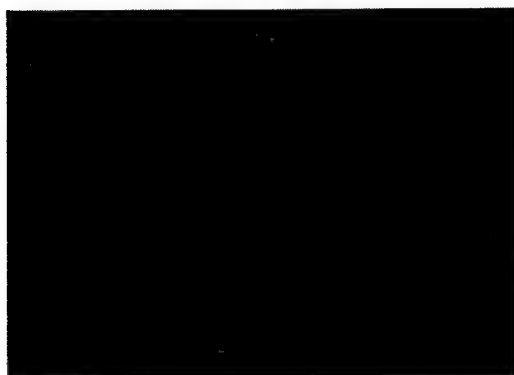
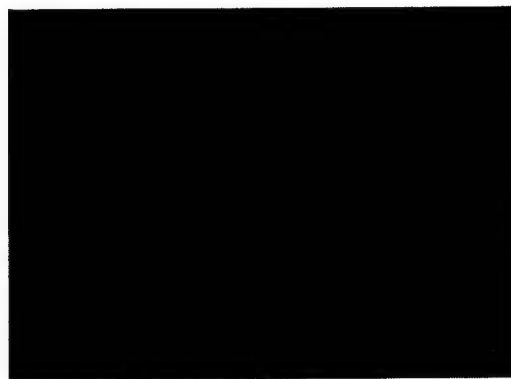


Figure 6 A.



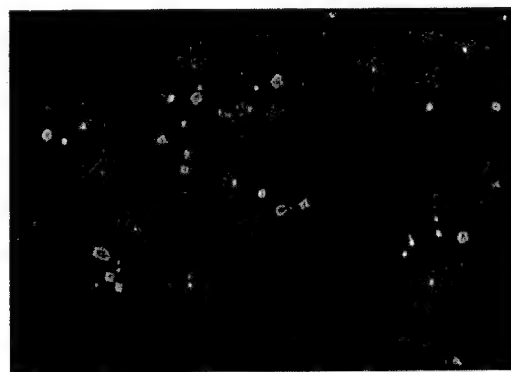
(a) CREF-vector/normal IgG



(b) CREF-9ORF1/normal IgG



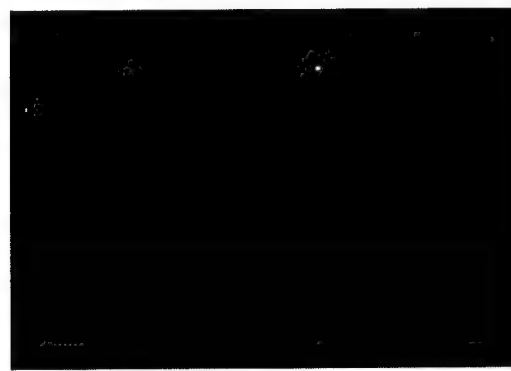
(c) CREF-vector/ α -MAGI



(d) CREF-9ORF1/ α -MAGI



(e) CREF-IIIA/ α -MAGI



(f) CREF-IIIC/ α -MAGI



(g) CREF-IIID/ α -MAGI

Figure 6 B.

CREF-HA9ORF1

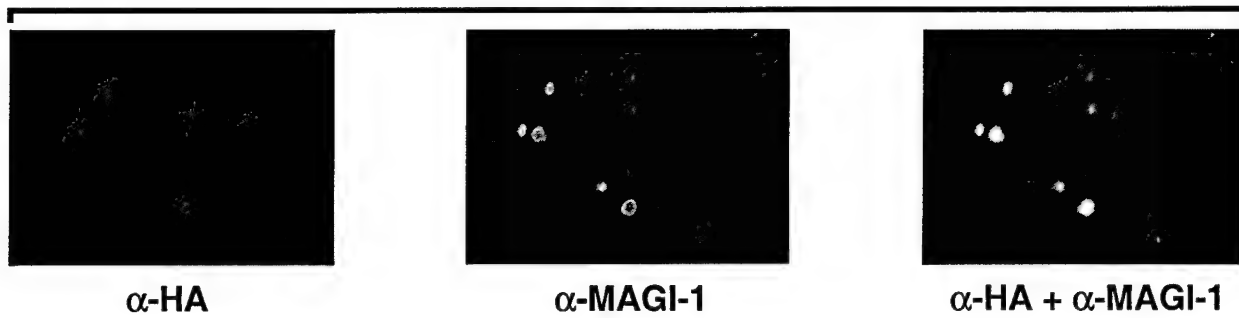


Figure 7.

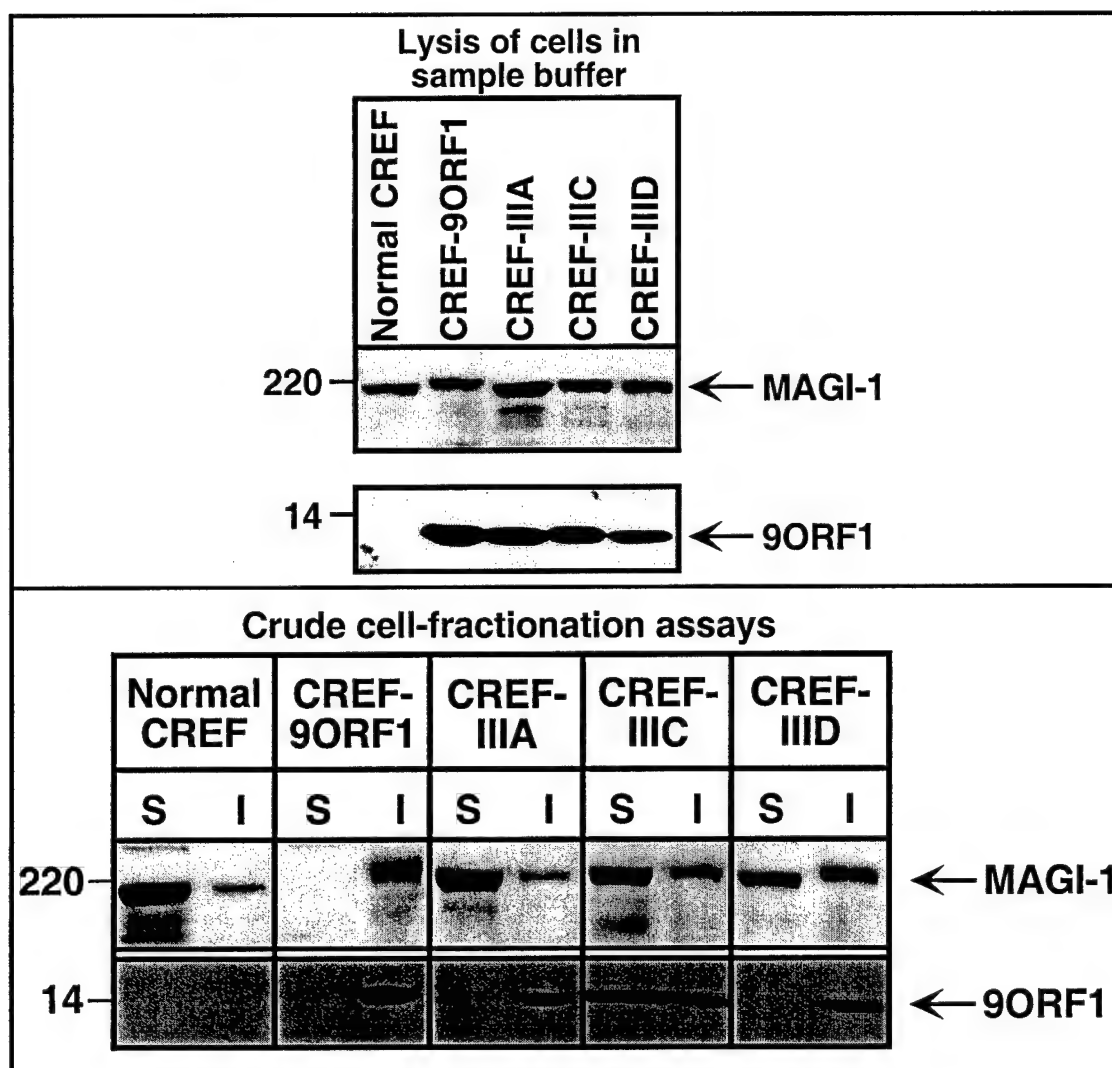


Figure 8.

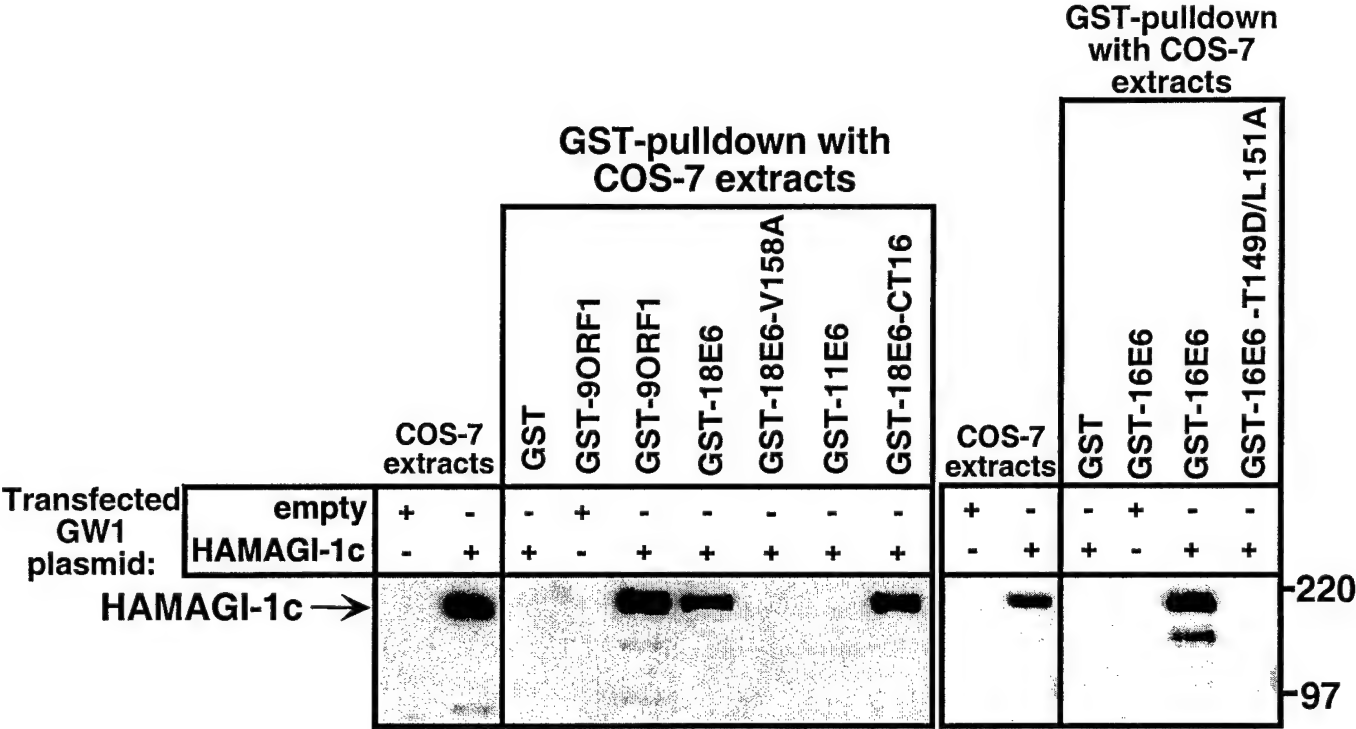


Figure 9.

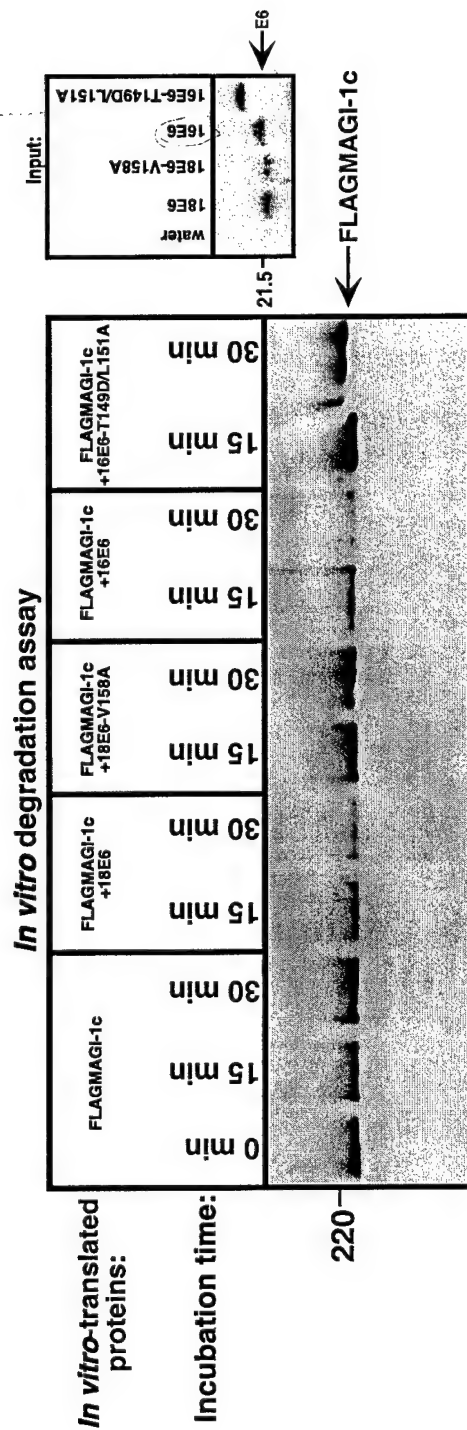


Figure 10 A.

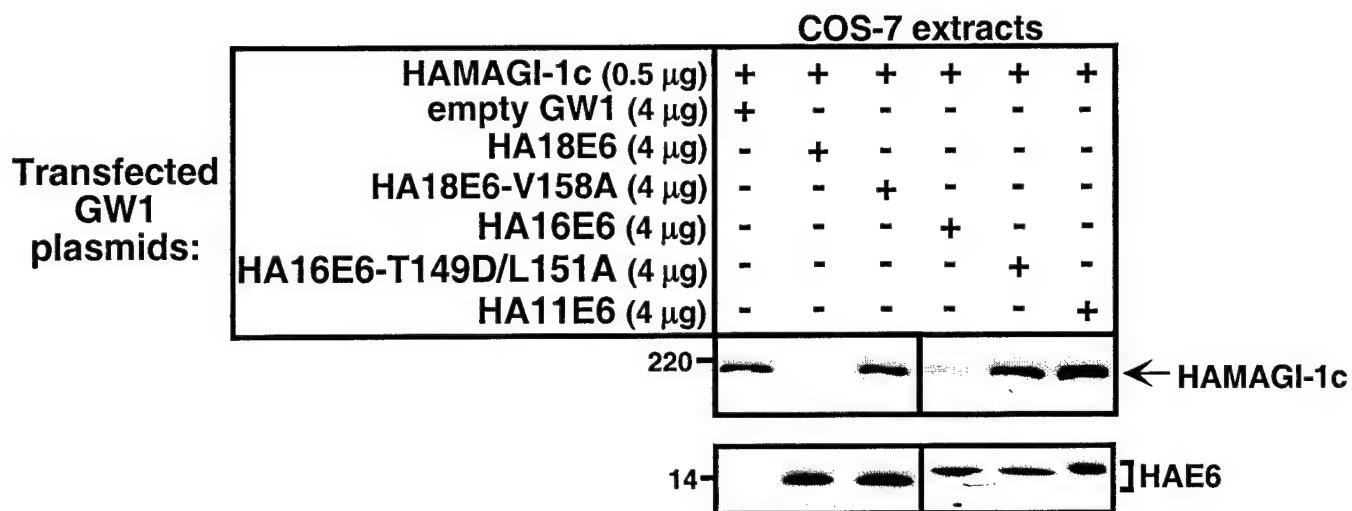


Figure 10 B.

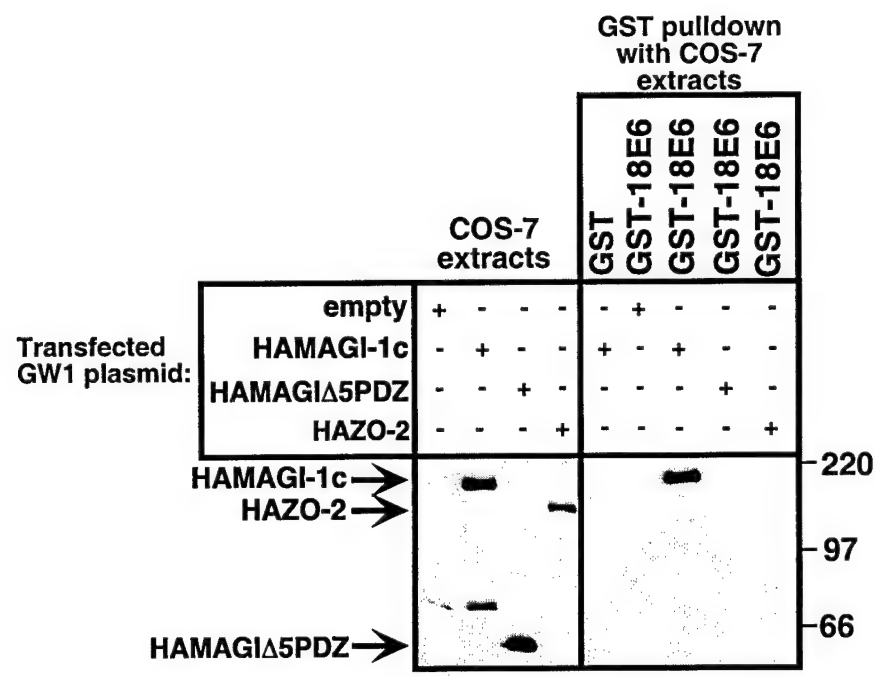


Figure 10 C.

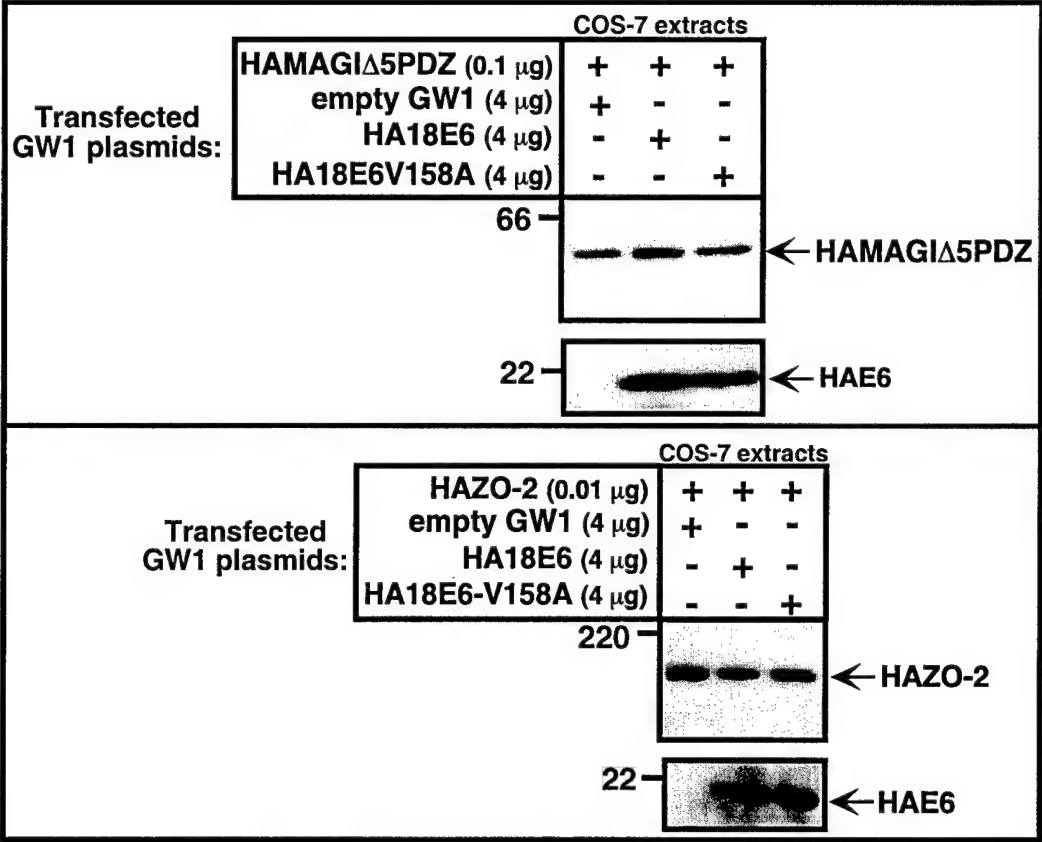
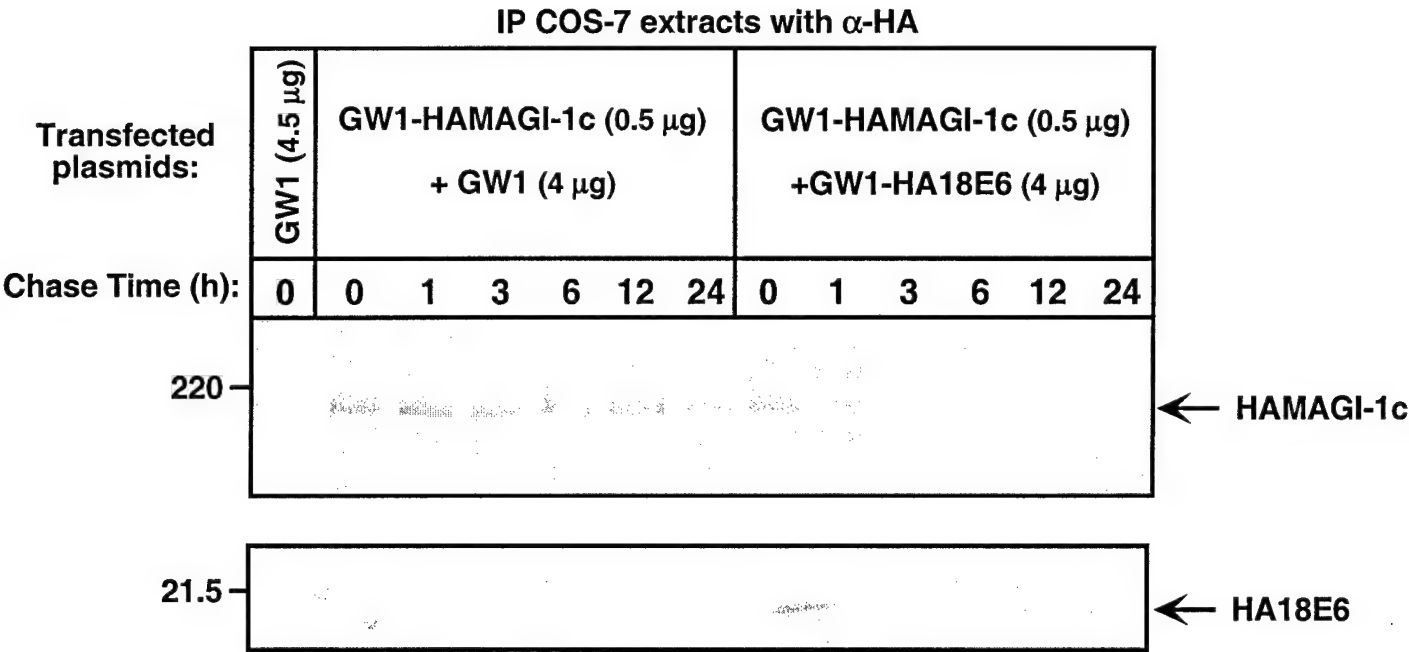


Figure 11.



**The Multi-PDZ Domain Protein MUPP1 Is a Cellular Target for Both
Adenovirus E4-ORF1 and High-Risk Papillomavirus Type 18 E6
Oncoproteins**

Siu Sylvia Lee¹, Britt Glaunsinger¹, Fiamma Mantovani², Lawrence Banks² and Ronald T. Javier^{1*}

¹Department of Molecular Virology and Microbiology, Baylor College of Medicine, Houston,
Texas 77030, USA; ²International Center for Genetic Engineering and Biotechnology, Padriciano
99, I-34012 Trieste, Italy

Running Title: Viral oncoproteins bind the multi-PDZ domain protein MUPP1

*Corresponding footnote: Ronald T. Javier, Department of Molecular Virology and
Microbiology, Baylor College of Medicine, One Baylor Plaza,
Houston, Texas 77030, U.S.A.

Phone: (713) 798-3898

Fax: (713) 798-3586

E-mail: rjavier@bcm.tmc.edu

Abstract

A general theme that has emerged from studies of DNA tumor viruses is that otherwise unrelated oncoproteins encoded by these viruses often target the same important cellular factors. Major oncogenic determinants for human adenovirus type 9 (Ad9) and high-risk human papillomaviruses (HPV) are the E4-ORF1 and E6 oncoproteins, respectively, and although otherwise unrelated, both of these viral proteins possess a functional PDZ domain-binding motif that is essential for their transforming activity and for binding to the PDZ domain-containing and putative tumor suppressor protein DLG. We report here that the PDZ domain-binding motifs of Ad9 E4-ORF1 and high-risk HPV-18 E6 also mediate binding to the widely-expressed cellular factor MUPP1, a large multi-PDZ domain protein predicted to function as an adapter in signal transduction. With regard to the consequences of these interactions in cells, we showed that Ad9 E4-ORF1 aberrantly sequesters MUPP1 within the cytoplasm of cells, whereas HPV-18 E6 targets this cellular protein for degradation. These effects were specific because mutant viral proteins unable to bind MUPP1 lack these activities. From these results, we propose that the multi-PDZ domain protein MUPP1 is involved in negatively regulating cellular proliferation and that the transforming activities of two different viral oncoproteins depend, in part, on their ability to inactivate this cellular factor.

Introduction

Human adenovirus type 9 (Ad9) is a unique oncogenic virus that generates estrogen-dependent mammary tumors in rats (24). Whereas the viral E1A and E1B oncoproteins are responsible for tumorigenesis by most human adenoviruses (46), the primary oncogenic determinant for Ad9 is its E4-ORF1 (9ORF1) transforming protein (23, 25, 54, 61). Mutational analyses of the 125 amino-acid (aa) residue 9ORF1 protein implicate three separate regions (Regions I, II, and III) as being critical for transformation (58). Although the activities associated with Regions I and II have not been determined, Region III at the extreme carboxyl-terminus of 9ORF1 mediates interactions with multiple cellular polypeptides (p220, p180, p160, p155, p140/p130) (59). This carboxyl-terminal 9ORF1 domain was recently discovered to define a functional PDZ-domain binding motif (30) and, consistent with this finding, 9ORF1-associated protein p140/130 was identified as the cellular PDZ-protein DLG (30), a mammalian homolog of the *Drosophila* discs large tumor suppressor protein dlg-A (31, 35).

In humans, infections with human T-cell leukemia virus type 1 (HTLV-1) and high-risk human papillomaviruses (HPV) are associated with the development of adult T-cell leukemia and cervical carcinoma, respectively (5, 45). Finding a functional PDZ domain-binding motif at the carboxyl-terminus of 9ORF1 subsequently led us to discover that HTLV-1 Tax and high-risk but not low-risk HPV E6 oncoproteins possess similar binding motifs at their carboxyl-termini and, in addition, bind DLG (30). Although it is well established that transformation by high-risk HPV E6 proteins depends, in part, on an ability to target the tumor suppressor protein p53 for degradation (44), other E6 functions are also known to be important (29, 40, 49). In this regard, high-risk HPV-16 E6 mutant proteins having a disrupted PDZ domain-binding motif lose the

capacity to oncogenically transform rat 3Y1 fibroblasts (28). Moreover, we recently showed that high-risk HPV E6 proteins target the PDZ-protein DLG for degradation in cells (11). Therefore, a common ability of several different human virus oncoproteins to complex with cellular PDZ-domain proteins likely contributes to their transforming potentials.

PDZ domains are approximately 80 aa-residue modular units that mediate protein-protein interactions (6, 7). PDZ domain-containing proteins represent a diverse family of polypeptides that contain single or multiple PDZ domains, other types of protein-protein interaction modules including SH3, WW, PTB or pleckstrin-homology domains, as well as protein kinase or phosphatase domains (37, 42). Consistent with such domain structures, many PDZ proteins have been found to play a role in signal transduction. In this capacity, these cellular factors serve to localize receptors and cytosolic signaling proteins to specialized membrane sites in cells and, in addition, to act as scaffolding proteins to organize these cellular targets into large supramolecular complexes (6, 8, 39). The PDZ domains of these cellular factors typically recognize specific peptide sequence motifs located at the extreme carboxyl-termini of their target proteins (50), although PDZ domains can also mediate other types of protein interactions (3, 32, 65). To date, three different types of carboxyl-terminal PDZ domain-binding motifs have been identified (33, 50, 52) and, at their extreme carboxyl-termini, the adenovirus 9ORF1, HTLV-1 Tax, and high-risk HPV E6 oncoproteins possess a type I binding motif having the consensus sequence -(S/T)-X-(V/I/L)-COOH (X, any aa residue) (30).

Although our findings (30, 58, 59) and those of others (28) suggest that DLG is an important cellular target for transformation by both human adenovirus E4-ORF1 and high-risk HPV E6 oncoproteins, our previous results with the 9ORF1 protein also argue for the existence

of additional important cellular PDZ-protein targets. Specifically, disruption of the 9ORF1 PDZ domain-binding motif abolishes interaction of 9ORF1 with DLG, as well as with several other unidentified cellular proteins (p220, p180, p160, p155) (59). Consistent with this observation, we now report that 9ORF1-associated protein p220 is the multi-PDZ domain protein MUPP1 (57) and that 9ORF1 abnormally sequesters this cellular factor within the cytoplasm of cells. We further show that the high-risk HPV-18 E6 (18E6) oncoprotein likewise complexes with MUPP1 but instead targets this cellular factor for degradation in cells. These findings suggest that the transforming potentials of the human adenovirus E4-ORF1 and 18E6 proteins depend on their ability to block the function of MUPP1, a large multi-PDZ domain protein predicted to function as a scaffolding factor in cell signaling.

Materials and Methods

Cells. 3T3 (22), CREF (9), COS7 (13), TE85 (34), and 293 (14) cell lines, as well as the Ad9-induced rat mammary tumor cell line 20-8, were maintained in culture medium (Dulbecco's Modified Eagle Medium supplemented with 10% fetal bovine serum) under a 5% CO₂ atmosphere in a humidified incubator at 37°C. CREF cell pools (group 16) stably expressing wild-type or mutant 9ORF1 protein (58) and a CREF cell pool stably expressing an influenza virus hemagglutinin (HA) epitope-tagged 9ORF1 protein (60) were maintained in culture medium supplemented with G418 (Gibco BRL).

Plasmids. The partial murine 9BP-1 cDNA (30) encoding the carboxyl-terminal 526 aa-residues of 9BP-1 was inserted between the *Bam*HI and *Hind*III sites of plasmid pQE9 (Qiagen) to make plasmid pQE9-9BP1-CT526. The full-length rat MUPP1 cDNA from pBSK-MUPP1 (57) was introduced between either the *Sac*II and *Eco*RV sites of plasmid pSL301 (Invitrogen) or the *Hind*III and *Eco*RI sites of CMV expression-plasmid GW1 (British Biotechnology) to create plasmid pSL301-MUPP1 or GW1-MUPP1, respectively. Plasmid GW1-HAMUPP1 was derived from GW1-MUPP1 by introducing an HA-epitope tag at the amino-terminus of MUPP1 by PCR methods. Plasmids GW1-HAMUPP1 Δ PDZ7, GW1-HAMUPP1 Δ PDZ10, or GW1-HAMUPP1 Δ PDZ7/10 were derived from GW1-HAMUPP1 by deletion of MUPP1 sequences coding for either PDZ7 (aa-residues 1166-1232) or PDZ10 (aa-residues 1616-1656), or for both of these PDZ domains, respectively, by PCR methods.

Plasmids GW1-9ORF1wt, GW1-9ORF1IIIA, GW1-9ORF1IIIC, GW1-9ORF1IIID, or GW1-18E6 contain the respective wild-type or mutant 9ORF1 (58) or wild-type 18E6 gene inserted between the *Hind*III and *Eco*RI sites of plasmid GW1. The wild-type 18E6 cDNA was

also introduced between the *Hind*III and *Eco*RI sites of plasmid pSP64 (Promega) to make plasmid pSP64-18E6. Substitution of 18E6 valine residue 158 for alanine (18E6-V158A) or threonine and valine residues 156 and 158 for aspartic acid and alanine (18E6-T156D/V158A), as well as introduction of an HA-epitope tag at the amino-termini of 18E6, HPV-11 E6 (11E6), rat DLG (35), and human ZO-1 (63) proteins, were accomplished by PCR methods. Altered E6 and DLG cDNAs were introduced between the *Hind*III and *Eco*RI sites of plasmid GW1 to make plasmids GW1-HA18E6, GW1-HA18E6-V158A, GW1-HA18E6-T156D/V158A, GW1-HA11E6, and GW1-HADLG, whereas the HAZO-1 cDNA was inserted between the *Kpn*I and *Bgl*II sites of plasmid GW1 to make plasmid GW1-HAZO-1. Plasmids pcDNA3-DLG and pSP64-p53 were described previously (11, 38).

For the construction of glutathione-S-transferase (GST) fusion protein expression plasmids, cDNA sequences coding for 9BP1-US9/10 (aa-residues 179-251), MUPP1-NT (aa-residues 1-123), MUPP1-PDZ1-3 (aa-residues 118-504), MUPP1-PDZ4-5 (aa-residues 489-785), MUPP1-US5/6 (aa-residues 780-990), MUPP1-PDZ6 (aa-residues 985-1110), MUPP1-PDZ7 (aa-residues 1105-1312), MUPP1-PDZ8-9 (aa-residues 1307-1611), MUPP1-PDZ10 (aa-residues 1606-1706), MUPP1-PDZ11 (aa-residues 1701-1830), MUPP1-PDZ12-13 (aa-residues 1825-2054), 18E6-V158A, and 18E6-T156D/V158A were PCR amplified and introduced in-frame with the GST gene of plasmid pGEX-2T or pGEX-4T-1 (Pharmacia). pGEX-2T plasmids containing wild-type or mutant E4-ORF1 genes have been described (59). pGEX-2T plasmids containing wild-type 18E6 and 11E6 cDNAs were kindly provided by P. Howley.

PCR amplifications were performed with *pfu* polymerase (Stratagene), and plasmids were verified by restriction enzyme and limited sequence analyses.

Lambda phage cDNA library screening. A DNA fragment from the 9BP-1 cDNA (nts 134-544) (30) was radiolabeled by the random-priming method (53) and used to screen the mouse pancreatic cell λ gt11 cDNA library kindly provided by S. Tsai, according to standard methods (51).

Antisera and antibodies. The 6xHis-tagged 9BP1-CT526, GST-9BP1-US9/10 and GST-MUPP1-US5/6 fusion proteins were expressed in bacteria and purified with either Ni-NTA agarose (Qiagen) or glutathione beads (Pharmacia) (48), as recommended by the manufacturers. Rabbits were immunized with purified 9BP1-CT526 or MUPP1-US5/6 fusion proteins to generate polyclonal antisera by standard methods (18). The purified GST-9BP1-US9/10 fusion protein was covalently linked to Affi-Gel 10 beads (BioRad) and used to affinity-purify 9BP-1 antibodies by standard methods (19). Commercially-available HA (12CA5) monoclonal antibodies (BABCO), horseradish peroxidase-conjugated goat anti-rabbit IgG or goat anti-mouse IgG antibodies (Southern Biotechnology Associates), fluorescein isothiocyanate-conjugated goat anti-rabbit IgG (Gibco BRL), and Texas Red-conjugated goat anti-mouse IgG antibodies (Molecular Probe; Eugene, OR) were utilized. p53, DLG, and 9ORF1 antisera were described previously (1, 11, 25).

Transfections and cell extracts. COS7 cells were transfected with lipofectin or lipofectamine (Gibco BRL) according to manufacturer's recommendations and harvested 48 h post-transfection. For preparation of cell extracts, cells were washed with ice-cold PBS (4.3 mM Na_2HPO_4 , 1.4 mM KH_2PO_4 , 137 mM NaCl, 2.7 mM KCl) and either lysed in sample buffer (0.065 M Tris-

HCl pH 6.8, 2% [w/v] sodium dodecyl sulfate (SDS), 10% [v/v] β -mercaptoethanol, 0.005% bromophenol blue) and boiled immediately or lysed for 10 min on ice in RIPA buffer (50 mM Tris-HCl pH 8.0, 150 mM NaCl, 1% [v/v] Nonidet P-40, 0.5% [w/v] sodium deoxycholate, 0.1% [w/v] SDS) containing protease inhibitors (300 μ g/ml phenylmethylsulfonyl fluoride, 6 μ g/ml each aprotinin and leupeptin) and phosphatase inhibitors (50 mM NaF, 0.1 mM Na_3VO_4). RIPA buffer-lysed cells were cleared by centrifugation (14,000 X g, 20 min, 4°C), and protein concentrations were determined by the Bradford method (47). For crude cell-fractionation assays, the pellet recovered after centrifugation of RIPA buffer-lysed cells was solubilized in sample buffer using an equivalent volume as was used originally to lyse the cells in RIPA buffer.

GST pulldown, immunoprecipitation, and immunoblot assays. For both GST pulldown and immunoprecipitation assays, glutathione- or protein A-sepharose beads (Pharmacia) bound to GST fusion proteins or antibodies, respectively, were incubated with cell extracts in RIPA buffer (3 h, 4°C), washed extensively with RIPA buffer, and boiled in sample buffer. Recovered proteins were separated by SDS-polyacrylamide gel electrophoresis (SDS-PAGE). For each GST pulldown reaction, 5 μ g of each GST fusion protein was used and verified in each experiment by staining relevant portions of the protein gel with Coomassie brilliant blue dye. Each immunoprecipitation reaction was carried out with 1 μ g or 12 μ g of p53 or HA antibodies, respectively, 1 μ l of DLG antiserum, or 5 μ l of either 9ORF1, 9BP-1, or MUPP1 antiserum, or the corresponding matched pre-immune serum.

For immunoblot assays, proteins separated by SDS-PAGE were electrotransferred to a polyvinylidene fluoride (PVDF) membrane, which was incubated with blocking buffer (TBST

buffer {50 mM Tris-HCl pH 7.5, 200 mM NaCl, 0.2% [v/v] Tween-20} containing 5% non-fat dry milk) for 1 h, with the appropriate primary antiserum or antibody (1:5000 dilution of either 9ORF1, 9BP-1, or MUPP1 antiserum, or 1.2 µg/ml of HA antibodies) for 2 h and, then, with horseradish peroxidase-conjugated goat anti-rabbit IgG or goat anti-mouse IgG secondary antibodies (1:5000) (Southern Biotechnology Associates Inc.) for 1 h. Antibodies were diluted in TBST containing 0.5% non-fat dry milk, and incubations were performed at RT. After extensive washes in TBST buffer, membranes were developed by enhanced chemiluminescence methods (Pierce).

Protein blotting assays. Protein blotting assays and preparation of [³²P]-radiolabeled 9ORF1 fusion protein probes were performed as described (59). Briefly, MUPP1 fusion proteins were separated by SDS-PAGE and electrotransferred to a PVDF membrane. The membranes were incubated with blocking buffer and, then, with the [³²P]-labeled GST-9ORF1 protein probe (5 X 10⁵ cpm/ml) in TBST (12 h, 4°C), washed extensively with RIPA buffer, and developed by autoradiography.

***In vitro* translation and degradation assays.** Plasmid pcDNA3-DLG, pSP64-p53, pSL301-MUPP1, or pSP64-18E6 was transcribed and translated *in vitro* using the TNT-coupled rabbit reticulocyte system (Promega) and 10 µCi of [³⁵S]-cysteine (1000Ci/mmol) (Amersham), according to the manufacturer's instructions. *In vitro* degradation assays were performed as described (11). Briefly, the specified *in vitro* translation reactions were mixed and incubated at 30°C for the indicated times, and proteins were immunoprecipitated, separated by SDS-PAGE, and detected by autoradiography.

Pulse-chase labeling of cell proteins. Transfected COS7 cells were pre-incubated in culture medium lacking methionine and cysteine for 30 min, metabolically labeled for 10 min with 0.4 mCi EXPRE³⁵S³⁵S [³⁵S] protein labeling mix (New England Nuclear) in 1.5 ml of culture medium lacking methionine and cysteine and, then, chased with culture medium containing excess unlabeled methionine (15 mg/L) (2). At various times post-chase, cells were harvested, lysed in RIPA buffer, and cell proteins were immunoprecipitated with HA antibodies, separated by SDS-PAGE, and developed by autoradiography. The amount of radioactivity present within each protein band of interest was quantified using a Storm Molecular Dynamics phosphorimager.

Indirect immunofluorescence microscopy. Indirect immunofluorescence (IF) microscopy assays were performed by standard methods (17). Cells were grown on glass coverslips, fixed in methanol for 20 min at -20°C, blocked with IF buffer (TBS {50 mM Tris-HCl pH 7.5, 200 mM NaCl} containing 10% goat serum), and reacted first with either pre-immune serum or MUPP1 antiserum (1:500) and, then, with fluorescein isothiocyanate-conjugated goat anti-rabbit IgG secondary antibodies (1:250) (Gibco BRL). For double-labeling IF experiments, cells on coverslips were incubated with both MUPP1 antiserum (1:500) and HA monoclonal antibodies (66 µg/ml) and, then, with both fluorescein isothiocyanate-conjugated goat anti-rabbit IgG (1:250) (Gibco BRL) and Texas Red-conjugated goat anti-mouse IgG secondary antibodies (1:300) (Molecular Probe). All antibodies were diluted in IF buffer, and incubations were performed at 37°C. Coverslips with attached cells were rinsed briefly in a 0.5 mg/ml 4', 6-diamidino-2-phenylindole solution to stain nuclei and affixed to slides with mounting medium (VectorShield). Images were collected with a Zeiss Axiophot fluorescence microscope and digitally processed using the Adobe PhotoShop software.

Sequence alignment. Pairwise sequence alignments were performed using the Align algorithm of the BCM Search Launcher web browser (<http://dot.imgen.bcm.tmc.edu:9331/seq-search/alignment.html>). Mouse, rat, and human MUPP1 sequences (accession numbers AJ131869, AJ001320, and AJ001319, respectively) were obtained from GenBank.

Results

9BP-1 and 9ORF1-associated protein p220 have similar characteristics. By screening λ gt11 cDNA expression libraries with a 9ORF1 protein probe, we previously isolated a partial cDNA coding for the carboxyl-terminal 526 aa-residues of the novel mouse multi-PDZ domain protein 9BP-1 (30). Subsequent re-screening of the same λ gt11 library with a 9BP-1 DNA probe led to the isolation of a cDNA coding for a larger partial carboxyl-terminal 688 aa-residue 9BP-1 polypeptide that contains five PDZ-homology domains (Fig. 1A).

To assess initially whether 9BP-1 may represent one of the unidentified 9ORF1-associated cellular proteins (p220, p180, p160, or p155), we raised polyclonal antisera to the carboxyl-terminal 526 aa-residues of this partial polypeptide (30). By immunoblot analysis, two independent 9BP-1 antisera specifically recognized an approximately 250 kD protein which, in cell lines derived from various species, exhibited slightly different gel mobilities (Fig. 2A; data not shown). The latter observation presumably reflects species-specific differences for this polypeptide. More important, 9BP-1 was found to be complexed with 9ORF1 in lysates of 9ORF1-expressing cells (see below; data not shown). Additionally, comparison of the gel mobility of 9BP-1 with that of each 9ORF1-associated protein showed that 9BP-1 and 9ORF1-associated protein p220 co-migrate and exhibit identical species-specific gel mobilities (Fig. 2A), suggesting that these proteins are the same.

9BP-1 is the multi-PDZ domain protein MUPP1. From BLAST searches of protein sequence databases, we subsequently found that the partial mouse 9BP-1 polypeptide exhibits 99% aa-sequence identity with the carboxyl-terminal region of the 2055 aa-residue mouse multi-PDZ domain protein MUPP1 (Figs. 1A and 1B), as well as 94% or 82% aa-sequence identity with the

carboxyl-terminal region of rat MUPP1 (2054 aa residues) or human MUPP1 (2042 aa residues), respectively (data not shown). MUPP1 is a widely-expressed polypeptide, containing thirteen PDZ domains and no other recognizable protein motifs, and was isolated by virtue of its ability to bind the cytoplasmic domain of the 5-HT_{2C} serotonin receptor in yeast two-hybrid screens (57).

To confirm that 9BP-1 and MUPP1 are indeed the same polypeptides, we generated polyclonal antisera to a unique 210 aa-residue rat MUPP1 region that lies between PDZ5 and PDZ6 and that lacks sequence similarity with other known proteins (see Fig. 1A). As with the 9BP-1 antisera, these MUPP1 antisera specifically recognized an approximately 250 kD cellular protein in cell lysates (data not shown) and, in addition, cross-reacted with 9BP-1 protein immunoprecipitated from human, rat, and mouse cell lines (Fig. 2B).

9ORF1 binds MUPP1. We utilized GST pulldown assays to show that the wild-type 9ORF1 protein can bind to MUPP1. In these assays, we found that the GST-9ORF1 fusion protein bound both to HA epitope-tagged rat MUPP1 (HAMUPP1) transiently expressed in COS7 cells (Fig. 3) and to endogenous MUPP1 from CREF rat embryo fibroblasts (data not shown), as did GST fusion proteins of the related wild-type adenovirus types 5 and 12 E4-ORF1 transforming proteins (GST-5ORF1 and GST-12ORF1, respectively) (60). To assess whether these binding results with 9ORF1 were specific, we also examined in these same assays three different transformation-defective 9ORF1 mutant proteins having disrupted (mutant IIIA) or altered (mutants IIIC and IIID) carboxyl-terminal PDZ domain-binding motifs (Table 1) (30, 58). With respect to the residues mutated in 9ORF1 mutants IIIC and IIID, such sequences surrounding the conserved residues of type I PDZ domain-binding motifs are known to influence binding to some

PDZ domains (50). In GST pulldown assays with the three 9ORF1 mutant proteins, we found that only mutant IIID was able to bind to MUPP1, albeit at substantially reduced levels compared to that of wild-type 9ORF1 (Fig. 3). This binding profile of MUPP1 to these 9ORF1 mutants is distinct from that of DLG (30) and, as expected, is identical to that previously observed for 9ORF1-associated protein p220 (59).

The physical association between 9ORF1 and MUPP1 in cells was examined by performing co-immunoprecipitation assays. From lysates of COS7 cells transiently expressing HAMUPP1 and either wild-type or mutant 9ORF1 protein, we found that MUPP1 co-immunoprecipitated with wild-type 9ORF1 and with mutant IIID 9ORF1 at reduced levels, but failed to co-immunoprecipitate with either mutant IIIA or IIIC 9ORF1 (Fig. 4A). Identical results were obtained for endogenous MUPP1 from CREF cell lines stably expressing comparable levels of wild-type or mutant 9ORF1 protein (Fig. 4B). These findings with COS7 and CREF cells were fully concordant with the GST pulldown assay results (see Fig. 3). It was also noteworthy that MUPP1 similarly co-immunoprecipitated with wild-type 9ORF1 from lysates of an Ad9-induced rat mammary tumor cell line (Fig. 4C). Taken together, the results of GST pulldown and co-immunoprecipitation assays demonstrated that 9ORF1 utilizes its PDZ domain-binding motif to mediate a specific interaction with the multi-PDZ domain protein MUPP1 in cells.

9ORF1 binds selectively to MUPP1 PDZ7 and PDZ10. To reveal which of the thirteen MUPP1 PDZ domains interacts with 9ORF1, we constructed a panel of fusion proteins containing ten different non-overlapping MUPP1 protein fragments (Fig. 5A), which collectively represented the entire full-length MUPP1 polypeptide. A similar quantity of each MUPP1

fusion protein was immobilized on a membrane (data not shown) and blotted with a radiolabeled 9ORF1 protein probe. In these experiments, 9ORF1 bound to MUPP1 PDZ7 and PDZ10, but not to any other region of this cellular protein (Fig. 5B). A functional 9ORF1 PDZ domain-binding motif was required for these interactions, as a mutant GST-III A 9ORF1 protein probe failed to react with any of the MUPP1 fusion proteins in similar assays (data not shown).

To relate the *in vitro* binding results to formation of 9ORF1-MUPP1 protein complexes in cells, we constructed MUPP1 deletion mutants lacking PDZ7 (HAMUPP1 Δ PDZ7), PDZ10 (HAMUPP1 Δ PDZ10), or both domains (HAMUPP1 Δ PDZ7/10) and tested these MUPP1 mutants for their ability to co-immunoprecipitate with 9ORF1 from COS7 cell lysates. The results showed that HAMUPP1 Δ PDZ7 co-immunoprecipitated with 9ORF1 at wild-type levels, that HAMUPP1 Δ PDZ10 co-immunoprecipitated with 9ORF1 at slightly reduced levels, but that HAMUPP1 Δ PDZ7/10 failed to co-immunoprecipitate with 9ORF1 in these assays (Fig. 5C). These findings corroborated our *in vitro* binding results in showing that, among the thirteen MUPP1 PDZ domains, only PDZ7 and PDZ10 are capable of mediating binding of MUPP1 to 9ORF1 *in vivo*.

9ORF1 aberrantly sequesters MUPP1 within punctate bodies in the cytoplasm of cells.

Using indirect immunofluorescence (IF) microscopy assays, we sought to ascertain the subcellular distribution of MUPP1 in normal CREF cells, as well as CREF cell lines stably expressing wild-type or mutant 9ORF1 protein. In normal CREF cells, we found that MUPP1 displayed mostly diffuse and somewhat perinuclear staining in the cytoplasm, although some MUPP1 protein was also detected at discrete points of cell-cell contact (Fig. 6A). The latter

finding is consistent with the observation that PDZ proteins frequently localize to membranes at specialized regions of cell-cell contact in epithelial cells (8). Because 9ORF1 exists primarily within punctate bodies in the cytoplasm of cells (61), we reasoned that the subcellular localization of MUPP1 may be perturbed in 9ORF1-expressing CREF cells. Significantly, in contrast to results obtained with normal CREF cells, MUPP1 was found to be sequestered within punctate bodies in the cytoplasm of greater than 95% of CREF cells expressing wild-type 9ORF1 (Fig. 6A), similar to the staining pattern previously observed for 9ORF1. Using a CREF cell line stably expressing an HA epitope-tagged 9ORF1 protein, we were able to demonstrate that 9ORF1 and MUPP1 co-localize within these cytoplasmic bodies (Fig. 6B).

Additional IF assay results indicated that the cytoplasmic sequestration of MUPP1 by 9ORF1 depended on an ability of 9ORF1 to complex with this cellular PDZ protein. Specifically, CREF cell lines expressing 9ORF1 mutants IIIA and IIIC, which fail to bind MUPP1, showed a MUPP1 staining pattern similar to that seen in normal CREF cells. Moreover, the CREF cell line expressing 9ORF1 mutant IIID, which exhibits weak binding to MUPP1, showed some cytoplasmic punctate staining for MUPP1, although substantially less than that observed in the CREF cell line expressing wild-type 9ORF1 (Fig. 6A). It is worth mentioning that, similar to the wild-type 9ORF1 protein, these three 9ORF1 mutant proteins also display punctate staining in the cytoplasm of CREF cells (58).

To corroborate the IF assay results, we performed crude cell-fractionation experiments in the same CREF cell lines. Following direct lysis in 2% SDS, each cell line was found to express comparable levels of both MUPP1 and 9ORF1 proteins (Fig. 7A). CREF cell lysates were also prepared in RIPA buffer and separated by centrifugation into a RIPA buffer-soluble supernatant

fraction and a RIPA buffer-insoluble pellet fraction. Immunoblot analyses of these two different fractions with MUPP1 antiserum revealed that wild-type 9ORF1-expressing CREF cells contain substantially less RIPA buffer-soluble MUPP1 protein and concomitantly more RIPA buffer-insoluble MUPP1 protein than do normal CREF cells (Fig. 7B). The fact that the portion of MUPP1 protein retained in the RIPA buffer-soluble fraction of the wild-type 9ORF1-expressing cells could be depleted by quantitative immunoprecipitation of 9ORF1 (Fig. 7C) indicated that the vast majority of MUPP1 protein in these cells is complexed with 9ORF1.

The redistribution of MUPP1 into the RIPA buffer-insoluble fraction of wild-type 9ORF1-expressing CREF cells was also related to the ability of 9ORF1 to bind this cellular protein because mutant IIIA and IIIC 9ORF1 largely failed to aberrantly redistribute MUPP1 in CREF cells whereas mutant IIID 9ORF1 retained a reduced capacity to induce this effect (Fig. 7B). These differences are not likely to be due to the lower amounts of RIPA buffer-insoluble mutant IIIA and IIIC 9ORF1 proteins present in these CREF cells (see Fig. 7B), as transiently-transfected 293 cells contained equivalent amounts of RIPA buffer-insoluble wild-type and mutant 9ORF1 proteins but still yielded a pattern of MUPP1 redistribution similar to that of the CREF cell lines (Fig. 7D). That 9ORF1 redistributed MUPP1 into the RIPA buffer-insoluble fraction of 293 cells more effectively than it did in CREF cells may be due to the higher protein levels attained for 9ORF1 and MUPP1 in transient transfections of the 293 cells. Together, the results of IF and crude cell-fractionation assays argued that 9ORF1 aberrantly sequesters MUPP1 within RIPA buffer-insoluble complexes in the cytoplasm of cells.

The high-risk HPV type 18 E6 (18E6) oncoprotein binds MUPP1 and targets this cellular protein for degradation in cells. Because, like 9ORF1, high-risk HPV E6 oncoproteins also

possess a functional PDZ domain-binding motif and complex with DLG (28, 30), we next explored the possibility that such HPV E6 proteins likewise bind to MUPP1. In GST pulldown assays, the wild-type high-risk 18E6 protein associated both with HAMUPP1 protein expressed in COS7 cells (Fig. 8) and with endogenous MUPP1 from CREF cells (data not shown). This binding was specific and dependent on a functional PDZ domain-binding motif because in these assays the 18E6-V158A and 18E6-T156D/V158A mutant proteins, which have disrupted PDZ-domain binding motifs (Table 1), failed to complex with MUPP1 (Fig. 8; data not shown), as did the wild-type low-risk HPV type 11 E6 (11E6) protein which lacks a PDZ domain-binding motif (Table 1). It is notable that HPV-16 E6 mutants having functionally disrupted PDZ domain-binding motifs, like those of 18E6-V158A and 18E6-T156D/V158A, are no longer able to oncogenically transform rodent fibroblasts (28).

The fact that high-risk HPV E6 oncoproteins promote degradation of several cellular factors (10, 15, 55), including the tumor suppressor protein p53 (44) and DLG (11), prompted us to test whether 18E6 has similar effects on MUPP1. Incubation of *in vitro*-translated high-risk HPV E6 proteins with p53 leads to degradation of this cellular factor (44), so we first examined MUPP1 in similar assays. Although 18E6-induced degradation of both p53 and DLG was more efficient, a modest reduction in MUPP1 protein levels was reproducibly observed following a 3 h incubation with 18E6 (Fig. 9). This effect was also consistently greater than that observed in control water-primed *in vitro* translation reactions.

Whether 18E6 may target MUPP1 for degradation in cells was examined by expressing HAMUPP1 alone or together with 18E6 in COS7 cells. In these assays, we found that,

compared to cells expressing MUPP1 alone, cells co-expressing MUPP1 and 18E6 showed substantially lower steady-state levels of MUPP1 protein (Fig. 10A). It is important to mention that this effect is distinct from that seen in the RIPA buffer-soluble fraction of 9ORF1-expressing cells (see Figs. 7B and 7D), as MUPP1 was not sequestered within the RIPA buffer-insoluble fraction of 18E6-expressing cells (data not shown). To produce this effect, 18E6 required a functional PDZ domain-binding motif because mutants 18E6-V158A and 18E6-T156D/V158A, as well as wild-type 11E6, failed to reduce MUPP1 protein levels in COS7 cells. Additionally, only specific cellular PDZ proteins were affected by 18E6, as 18E6 neither bound the DLG-related PDZ-protein ZO-1 (Fig. 10B) (63) nor reduced its protein levels in these cells (Fig. 10C).

To verify that the 18E6-mediated reduction in MUPP1 steady-state protein levels was due to decreased stability of this cellular protein in cells, we performed pulse-chase experiments with COS7 cells either expressing HAMUPP1 alone or co-expressing both HAMUPP1 and 18E6. The results showed that MUPP1 protein levels modestly declined after a 6 h chase period in the absence of 18E6 whereas, in the presence of 18E6, MUPP1 protein levels were more reduced after only a 3 h chase period (Fig. 11). By quantifying amounts of radioactivity present in MUPP1 protein bands at each time point, we estimated that the half-life of the MUPP1 protein was shortened from 5.7 h in control COS7 cells to 1.3 h in 18E6-expressing COS7 cells. This greater than four-fold decrease in the half-life of the MUPP1 protein argues that 18E6 targets this cellular factor for degradation in cells.

Discussion

The results presented in this paper demonstrate that the widely-expressed multi-PDZ protein MUPP1 is a direct cellular target for the Ad9 E4-ORF1 oncoprotein (9ORF1), as well as for the related E4-ORF1 transforming proteins derived from Ad5 and Ad12 (5ORF1 and 12ORF1, respectively) (Fig. 3). We also showed that interactions between 9ORF1 and MUPP1 are mediated by the carboxyl-terminal PDZ domain-binding motif of 9ORF1 and the PDZ7 and PDZ10 domains of MUPP1 (Figs. 3 - 5). As 5ORF1 and 12ORF1 also possess carboxyl-terminal PDZ domain-binding motifs, these viral proteins likely complex with MUPP1 in a similar fashion. More important, the fact that transformation-defective 9ORF1 mutants with altered PDZ domain-binding motifs either fail or have reduced capacities to complex with MUPP1 in cells argues that binding of 9ORF1 to MUPP1 is critical for 9ORF1-induced transformation (Figs. 3 and 4). Our finding that 9ORF1 associates with MUPP1 in an Ad9-induced mammary tumor cell line (Fig. 4C) further suggests that this interaction also contributes to Ad9-induced mammary tumorigenesis in rats. With the findings presented in this paper, 9ORF1 has now been shown to complex with two different cellular PDZ-proteins, MUPP1 and DLG (30). As the weakly-transforming 9ORF1 mutants IIIC and IIID bind only one of these two PDZ proteins whereas the completely transformation-defective 9ORF1 mutant IIIA fails to bind either PDZ protein, we believe that interaction of 9ORF1 with both MUPP1 and DLG is important for full 9ORF1 transforming activity.

It is also worth noting that we have failed to detect binding of 9ORF1 to several other cellular PDZ proteins (BG and RJ, unpublished results), suggesting that 9ORF1 interacts with

only a select group of these cellular factors. We hypothesize that such selective binding of 9ORF1 is achieved through sequences surrounding its PDZ domain-binding motif. In this model, specific amino-acid residues adjacent to the 9ORF1 PDZ domain-binding motif would play differential roles in mediating binding to each 9ORF1-associated PDZ protein. Consistent with this idea, 9ORF1 mutant IIIC retains wild-type binding to DLG (30) but fails to bind MUPP1 and, conversely, 9ORF1 mutant IIID fails to bind DLG (30) but retains an ability to bind MUPP1 (see Table 1 and Figs. 3 and 4).

The domain structure of MUPP1 suggests that this cellular factor functions as an adapter protein in signal transduction (57). Moreover, having the largest number of PDZ domains (thirteen) yet reported in a polypeptide, MUPP1 has the capacity to assemble a large array of cellular targets into a multitude of different signaling complexes. As further support for a presumed role in cell signaling, MUPP1 was isolated in yeast two-hybrid screens for its ability to interact with the cytoplasmic carboxyl-terminal domain of the 5-HT_{2C} serotonin receptor (57) which, in the central nervous system, is implicated in a variety sensory, motor, and behavioral processes (20). The putative interaction between the 5-HT_{2C} receptor and MUPP1 in cells is suspected to involve a type I PDZ domain-binding motif at the extreme carboxyl-terminus of the 5-HT_{2C} receptor and at least one MUPP1 PDZ domain (57). The fact that overexpression of the 5-HT_{2C} receptor has been shown to confer a transformed state to 3T3 fibroblasts (62) also suggests a possible link between MUPP1 and signaling pathways involved in regulating cellular proliferation.

We found that most of the MUPP1 protein in CREF fibroblasts is present within the cytoplasm, although some MUPP1 protein is also detected at discrete regions of cell-cell contact

(Fig. 6). Consistent with the notion that MUPP1 functions in signal transduction, PDZ proteins that have known roles in cell signaling also localize to membranes at regions of cell-cell contact in epithelial cells (8) and, in some cases, within the cytoplasm (64, 66). With respect to how MUPP1 may function in cells, studies with the *Drosophila* MUPP1-related multi-PDZ protein InaD are likely to provide the most useful paradigm. The polypeptide InaD, consisting of five PDZ domains, functions to regulate the rhodopsin light-activated signaling pathway in retinal neurons. Each of the InaD PDZ domains mediates binding to a different signaling protein, among which include the calcium channel TRP, phospholipase C- β , and protein kinase C. InaD serves to organize these cellular targets into large signaling complexes and localize them to specialized cell membranes and, in so doing, allows rapid and efficient activation and deactivation of the light response (56). Although the PDZ protein-regulated signaling pathways perturbed by 9ORF1 in cells have yet to be identified, we previously showed that two prominent transformed properties of 9ORF1-expressing CREF cells in culture are anchorage-independent growth and an ability to grow to high saturation densities (61). As proliferation of normal cells is inhibited by either detachment from a substrate matrix or formation of extensive cell-cell contacts (12, 16), one intriguing possibility is that 9ORF1 interferes with MUPP1's ability to regulate cell-growth-controlling signaling cascades that emanate from these important plasma membrane contact points.

Among the thirteen MUPP1 PDZ domains, 9ORF1 specifically targets only two of these domains, namely PDZ7 and PDZ10 (Fig. 5). This selective interaction may serve to block MUPP1 from associating with cellular targets of these particular domains or, alternatively, to bring 9ORF1 into close proximity with other MUPP1 cellular targets in order to modify their

activities. A recently discovered activity for some PDZ proteins is the ability to direct their cellular targets to the proper location within cells (4, 26, 41, 56). One notable example comes from studies of vulval development in *Caenorhabditis elegans*. In this system, LET-23, an EGF receptor-like protein, must be localized to the basolateral membrane of the vulval epithelial cells in order for this receptor to associate with its growth factor ligand (27). Three different PDZ domain-containing proteins LIN-7, LIN-2, and LIN-10, which complex with LET-23, are responsible for directing this receptor to its proper site in cells (26). Therefore, considering that 9ORF1 aberrantly sequesters MUPP1 in the cytoplasm of cells (Figs. 6 and 7), it is reasonable to assume that 9ORF1 completely abolishes the function of MUPP1 by preventing this PDZ protein, and its cellular targets, from reaching their proper destinations in the cell.

We also showed that the high-risk 18E6 oncoprotein utilizes a PDZ domain-binding motif to complex with and promote degradation of the MUPP1 protein in cells (Figs. 8 - 11). Whether 18E6 targets MUPP1 for ubiquitin-mediated, proteasome-dependent proteolysis, as it does for p53 (43), was not determined. The modest 18E6-induced MUPP1 degradation observed after mixing *in vitro* translated proteins (Fig. 9) may indicate that 18E6 utilizes a different mechanism to degrade MUPP1 than it does to degrade p53 and DLG. Nevertheless, the degradation of MUPP1 protein that we observed in 18E6-expressing COS7 cells implies that MUPP1 function is abrogated in cells infected by HPV-18. Because the carboxyl-terminal PDZ domain-binding motif sequence of high-risk HPV types 31, 39, 45 and 51 E6 proteins is identical to that of 18E6 (30), MUPP1 is also likely to be targeted for degradation by these and probably other high-risk HPV E6 oncoproteins. Our additional finding that the low-risk 11E6 protein neither binds MUPP1 nor targets this cellular protein for degradation in cells (Figs. 8 and 10) provides

additional support for the idea that binding of high-risk E6 proteins to MUPP1 may contribute to HPV-induced carcinogenesis.

Our results argue that an ability to bind cellular PDZ proteins contributes to the transforming activities of both the adenovirus E4-ORF1 and high-risk HPV E6 oncoproteins. With respect to possible roles in the life cycles of adenovirus and HPV, these interactions are expected to help create an optimal environment for viral replication within infected host cells by overcoming normal defense mechanisms that block abnormal progression into S phase. Such an activity is common to the oncoproteins of DNA tumor viruses and is invariably mediated by their interactions with host cell factors intimately involved in regulating cellular proliferation and differentiation (36). In this regard, the fact that two unrelated viral oncoproteins, adenovirus E4-ORF1 and high-risk HPV E6, have both evolved to target the MUPP1 protein in cells strengthens the hypothesis that interactions with this cellular factor are pertinent to transformation. It is well known that the Ad5 E1B oncoprotein sequesters the tumor suppressor protein p53 in cells (46), whereas the unrelated high-risk HPV E6 oncoproteins promote degradation of this same cellular factor (21). In these examples, functional inactivation of p53 is the ultimate outcome for these interactions, but the mechanisms by which these viral oncoproteins accomplish this effect are distinct. Our findings suggest that the adenovirus E4-ORF1 and HPV E6 oncoproteins likewise inactivate MUPP1 by different mechanisms. This interesting parallel with the tumor suppressor protein p53, together with the fact that the PDZ-protein DLG is a putative tumor suppressor protein, hint that MUPP1 may function to negatively regulate cellular proliferation and, thus, may represent a novel tumor suppressor

protein. Consequently, revealing the cellular functions for this multi-PDZ domain adaptor protein may provide new insights into mechanisms that contribute to the development of human malignancies.

Acknowledgments

We are grateful to Christoph Ullmer and Alan Fanning for generously providing us with the pBSK-MUPP1 and pSK-ZO-1 plasmids, respectively. We thank Richard Sutton for helpful discussions and critical reading of the manuscript. We also thank Hank Adams and Frank Herbert (Microscopy Core, Department of Cell Biology, Baylor College of Medicine) for their assistance. S.S.L. was the recipient of a U.S. Army Breast Cancer Training Grant (DAMD17-94-J4204) and B.G. was the recipient of a Molecular Virology Training Grant (T32 AI07471). This work was supported by National Institutes of Health (ROI CA58541), American Cancer Society (RPG-97-668-01-VM) and U.S. Army (DAMD17-97-1-7082) grants to R.T.J. and an Associazione Italiana per la Ricerca sul Cancro grant to L.B.

References

1. **Banks, L., G. Matlashewski, and L. Crawford.** 1986. Isolation of human-p53-specific monoclonal antibodies and their use in the studies of human p53 expression. *Eur. J. Biochem.* **159**:529-534.
2. **Bonifacino, J. S.** 1991. Biosynthetic Labeling of Proteins, p. 10.18.1-10.18.9. *In* F. M. Ausubel, R. Brent, R. E. Kingston, D. D. Moore, J. G. Seidman, J. A. Smith, and K. Struhl (ed.), *Current Protocols in Molecular Biology*, vol. 2. Greene Publishing Associates and Wiley-Interscience, New York.
3. **Brenman, J. E., D. S. Chao, S. H. Gee, A. W. McGee, S. E. Craven, D. R. Santillano, Z. Wu, F. Huang, H. Xia, M. F. Peters, S. C. Froehner, and D. S. Bredt.** 1996. Interaction of nitric oxide synthase with the postsynaptic density protein PSD-95 and alpha1-syntrophin mediated by PDZ domains. *Cell* **84**:757-767.
4. **Butz, S., M. Okamoto, and T. C. Sudhof.** 1998. A tripartite protein complex with the potential to couple synaptic vesicle exocytosis to cell adhesion in brain. *Cell* **94**:773-782.
5. **Cann, A. J., and I. S. Y. Chen.** 1996. Human T-cell leukemia virus types I and II, p. 1849-1880. *In* B. N. Fields, D. M. Knipe, and P. M. Howley (ed.), *Fields Virology*, 3rd ed, vol. 2. Lippincot-Raven, Philadelphia.
6. **Craven, S. E., and D. S. Bredt.** 1998. PDZ proteins organize synaptic signaling pathways. *Cell* **93**:495-498.
7. **Fanning, A. S., and J. M. Anderson.** 1998. PDZ domains and the formation of protein networks at the plasma membrane. *Curr. Top. Microbiol. Immunol.* **228**:209-233.

8. **Fanning, A. S., and J. M. Anderson.** 1999. PDZ domains: fundamental building blocks in the organization of protein complexes at the plasma membrane. *J. Clin. Invest.* **103**:767-772.
9. **Fisher, P. B., L. E. Babiss, I. B. Weinstein, and H. S. Ginsberg.** 1982. Analysis of type 5 adenovirus transformation with a cloned rat embryo cell line (CREF). *Proc. Natl. Acad. Sci. USA* **79**:3527-3531.
10. **Gao, Q., S. Srinivasan, S. N. Boyer, D. E. Wazer, and V. Band.** 1999. The E6 oncoproteins of high-risk papillomaviruses bind to a novel putative GAP protein, E6TP1, and target it for degradation. *Mol. Cell. Biol.* **19**:733-744.
11. **Gardioli, D., C. Kuhne, B. Glaunsinger, S. S. Lee, R. Javier, and L. Banks.** 1999. Oncogenic human papillomavirus E6 proteins target the discs large tumour suppressor for proteasome-mediated degradation. *Oncogene* **18**:5487-5496.
12. **Giancotti, F. G., and E. Ruoslahti.** 1999. Integrin signaling. *Science* **285**:1028-1032.
13. **Gluzman, Y.** 1981. SV40-transformed simian cells support the replication of early SV40 mutants. *Cell* **23**:175-182.
14. **Graham, F. L., J. Smiley, W. C. Russell, and R. Nairn.** 1977. Characteristics of a human cell line transformed by DNA from human adenovirus type 5. *J. Gen. Virol.* **36**:59-74.
15. **Gross-Mesilaty, S., E. Reinstein, B. Bercovich, K. E. Tobias, A. L. Schwartz, C. Kahana, and A. Ciechanover.** 1998. Basal and human papillomavirus E6 oncoprotein-induced degradation of Myc proteins by the ubiquitin pathway. *Proc. Natl. Acad. Sci. USA* **95**:8058-8063.

16. **Gumbiner, B. M.** 1996. Cell adhesion: the molecular basis of tissue architecture and morphogenesis. *Cell* **84**:345-357.
17. **Harlow, E., and D. Lane.** 1988. Cell staining, p. 359-420, *Antibodies. A laboratory manual.* Cold Spring Harbor Laboratory, Cold Spring Harbor.
18. **Harlow, E., and D. Lane.** 1988. Immunizations, p. 55-137, *Antibodies. A laboratory manual.* Cold Spring Harbor Laboratory, Cold Spring Harbor.
19. **Harlow, E., and D. Lane.** 1988. Storing and purifying antibodies, p. 283-318, *Antibodies. A laboratory manual.* Cold Spring Harbor Laboratory, Cold Spring Harbor.
20. **Heisler, L. K., H. M. Chu, and L. H. Tecott.** 1998. Epilepsy and obesity in serotonin 5-HT_{2C} receptor mutant mice. *Ann. N. Y. Acad. Sci.* **861**:74-78.
21. **Howley, P. M.** 1996. Papillomavirinae: the viruses and their replication, p. 2045-2076. *In* B. N. Fields, D. M. Knipe, and P. M. Howley (ed.), *Fields Virology*, 3rd ed, vol. 2. Lippincot-Raven, Philadelphia.
22. **Jainchill, J. L., S. A. Aaronson, and G. J. Todaro.** 1969. Murine sarcoma and leukemia viruses: assay using clonal lines of contact-inhibited mouse cells. *J. Virol.* **4**:549-553.
23. **Javier, R., K. Raska, Jr., and T. Shenk.** 1992. Requirement for the adenovirus type 9 E4 region in production of mammary tumors. *Science* **257**:1267-1271.
24. **Javier, R., and T. Shenk.** 1996. Mammary tumors induced by human adenovirus type 9: a role for the viral early region 4 gene. *Breast Cancer Res. Treat.* **39**:57-67.
25. **Javier, R. T.** 1994. Adenovirus type 9 E4 open reading frame 1 encodes a transforming protein required for the production of mammary tumors in rats. *J. Virol.* **68**:3917-3924.

26. **Kaech, S. M., C. W. Whitfield, and S. K. Kim.** 1998. The LIN-2/LIN-7/LIN-10 complex mediates basolateral membrane localization of the *C. elegans* EGF receptor LET-23 in vulval epithelial cells. *Cell* **94**:761-771.
27. **Kim, S. K.** 1997. Polarized signaling: basolateral receptor localization in epithelial cells by PDZ-containing proteins. *Curr. Opin. Cell Biol.* **9**:853-859.
28. **Kiyono, T., A. Hiraiwa, M. Fujita, Y. Hayashi, T. Akiyama, and M. Ishibashi.** 1997. Binding of high-risk human papillomavirus E6 oncoproteins to the human homologue of the *Drosophila* discs large tumor suppressor protein. *Proc. Natl. Acad. Sci. USA* **94**:11612-11616.
29. **Kubbutat, M. H., and K. H. Vousden.** 1998. New HPV E6 binding proteins: dangerous liaisons? *Trends Microbiol.* **6**:173-175.
30. **Lee, S. S., R. S. Weiss, and R. T. Javier.** 1997. Binding of human virus oncoproteins to hDlg/SAP97, a mammalian homolog of the *Drosophila* discs large tumor suppressor protein. *Proc. Natl. Acad. Sci. USA* **94**:6670-6675.
31. **Lue, R. A., S. M. Marfatia, D. Branton, and A. H. Chishti.** 1994. Cloning and characterization of hdlg: the human homologue of the *Drosophila* discs large tumor suppressor binds to protein 4.1. *Proc. Natl. Acad. Sci. USA* **91**:9818-9822.
32. **Maekawa, K., N. Imagawa, A. Naito, S. Harada, O. Yoshie, and S. Takagi.** 1999. Association of protein-tyrosine phosphatase PTP-BAS with the transcription-factor-inhibitory protein IkappaBalpha through interaction between the PDZ1 domain and ankyrin repeats. *Biochem. J.* **337**:179-184.

33. **Maximov, A., T. C. Sudhof, and I. Bezprozvanny.** 1999. Association of neuronal calcium channels with modular adaptor proteins. *J. Biol. Chem.* **274**:24453-24456.
34. **McAllister, R. M., M. B. Gardner, A. E. Greene, C. Bradt, W. W. Nichols, and B. H. Landing.** 1971. Cultivation in vitro of cells derived from a human osteosarcoma. *Cancer* **27**:397-402.
35. **Muller, B. M., U. Kistner, R. W. Veh, C. Cases-Langhoff, B. Becker, E. D. Gundelfinger, and C. C. Garner.** 1995. Molecular characterization and spatial distribution of SAP97, a novel presynaptic protein homologous to SAP90 and the *Drosophila* discs-large tumor suppressor protein. *J. Neurosci.* **15**:2354-2366.
36. **Nevins, J. R., and P. K. Vogt.** 1996. Cell transformation by viruses, p. 301-343. *In* B. N. Fields, D. M. Knipe, and P. M. Howley (ed.), *Fields Virology*, 3rd ed, vol. 1. Lippincott-Raven Publishers, Philadelphia.
37. **Pawson, T., and J. D. Scott.** 1997. Signaling through scaffold, anchoring, and adaptor proteins. *Science* **278**:2075-2080.
38. **Pim, D., A. Storey, M. Thomas, P. Massimi, and L. Banks.** 1994. Mutational analysis of HPV-18 E6 identifies domains required for p53 degradation in vitro, abolition of p53 transactivation in vivo and immortalisation of primary BMK cells. *Oncogene* **9**:1869-1876.
39. **Ranganathan, R., and E. M. Ross.** 1997. PDZ domain proteins: scaffolds for signaling complexes. *Curr. Biol.* **7**:R770-R773.
40. **Rapp, L., and J. J. Chen.** 1998. The papillomavirus E6 proteins. *Biochim. Biophys. Acta.* **1378**:F1-F19.

41. **Rongo, C., C. W. Whitfield, A. Rodal, S. K. Kim, and J. M. Kaplan.** 1998. LIN-10 is a shared component of the polarized protein localization pathways in neurons and epithelia. *Cell* **94**:751-759.
42. **Saras, J., and C. H. Heldin.** 1996. PDZ domains bind carboxy-terminal sequences of target proteins. *Trends Biochem. Sci.* **21**:455-458.
43. **Scheffner, M., J. M. Huibregtse, R. D. Vierstra, and P. M. Howley.** 1993. The HPV-16 E6 and E6-AP complex functions as a ubiquitin-protein ligase in the ubiquitination of p53. *Cell* **75**:495-505.
44. **Scheffner, M., B. A. Werness, J. M. Huibregtse, A. J. Levine, and P. M. Howley.** 1990. The E6 oncoprotein encoded by human papillomavirus types 16 and 18 promotes the degradation of p53. *Cell* **63**:1129-1136.
45. **Shah, K. V., and P. M. Howley.** 1996. Papillomaviruses, p. 2077-2109. *In* B. N. Fields, D. M. Knipe, and P. M. Howley (ed.), *Fields Virology*, 3rd ed, vol. 2. Lippincott-Raven, Philadelphia.
46. **Shenk, T.** 1996. Adenoviridae: the viruses and their replication, p. 2111-2148. *In* B. N. Fields, D. M. Knipe, and P. M. Howley (ed.), *Fields Virology*, 3rd ed, vol. 2. Lippincott-Raven Publishers, Philadelphia.
47. **Simonian, M. H., and J. A. Smith.** 1996. Quantitation of proteins, p. 10.1.1-10.1.10. *In* F. M. Ausubel, R. Brent, R. E. Kingston, D. D. Moore, J. G. Seidman, J. A. Smith, and K. Struhl (ed.), *Current Protocols in Molecular Biology*, vol. 2. Greene Publishing Associates and Wiley-Interscience, New York.

48. **Smith, D. B., and L. M. Corcoran.** 1994. Expression and purification of glutathione-S-transferase fusion proteins; p. 16.7.1-16.7.7. *In* F. M. Ausubel, R. Brent, R. E. Kingston, D. D. Moore, J. G. Seidman, J. A. Smith, and K. Struhl (ed.), *Current Protocols in Molecular Biology*, vol. 2. Greene Publishing Associates and Wiley-Interscience, New York.
49. **Song, S., H. C. Pitot, and P. F. Lambert.** 1999. The human papillomavirus type 16 E6 gene alone is sufficient to induce carcinomas in transgenic animals. *J. Virol.* **73**:5887-5893.
50. **Songyang, Z., A. S. Fanning, C. Fu, J. Xu, S. M. Marfatia, A. H. Chishti, A. Crompton, A. C. Chan, J. M. Anderson, and L. C. Cantley.** 1997. Recognition of unique carboxyl-terminal motifs by distinct PDZ domains. *Science* **275**:73-77.
51. **Strauss, W. M.** 1993. Hybridization with radioactive probes, p. 6.3.1-6.3.6. *In* F. M. Ausubel, R. Brent, R. E. Kingston, D. D. Moore, J. G. Seidman, J. A. Smith, and K. Struhl (ed.), *Current Protocols in Molecular Biology*, vol. 1. Greene Publishing Associates and Wiley-Interscience, New York.
52. **Stricker, N. L., K. S. Christopherson, B. A. Yi, P. J. Schatz, R. W. Raab, G. Dawes, D. E. Bassett, Jr., D. S. Bredt, and M. Li.** 1997. PDZ domain of neuronal nitric oxide synthase recognizes novel C-terminal peptide sequences. *Nat. Biotechnol.* **15**:336-342.
53. **Tabor, S., K. Struhl, S. J. Scharf, and D. H. Gelfand.** 1990. DNA-dependent DNA polymerases, p. 3.5.1-3.5.15. *In* F. M. Ausubel, R. Brent, R. E. Kingston, D. D. Moore, J. G. Seidman, J. A. Smith, and K. Struhl (ed.), *Current Protocols in Molecular Biology*, vol. 1. Greene Publishing Associates and Wiley-Interscience, New York.

54. **Thomas, D. L., S. Shin, B. H. Jiang, H. Vogel, M. A. Ross, M. Kaplitt, T. E. Shenk, and R. T. Javier.** 1999. Early region 1 transforming functions are dispensable for mammary tumorigenesis by human adenovirus type 9. *J. Virol.* **73**:3071-3079.
55. **Thomas, M., and L. Banks.** 1998. Inhibition of Bak-induced apoptosis by HPV-18 E6. *Oncogene* **17**:2943-2954.
56. **Tsunoda, S., J. Sierralta, Y. Sun, R. Bodner, E. Suzuki, A. Becker, M. Socolich, and C. S. Zuker.** 1997. A multivalent PDZ-domain protein assembles signalling complexes in a G- protein-coupled cascade. *Nature* **388**:243-249.
57. **Ullmer, C., K. Schmuck, A. Figge, and H. Lubbert.** 1998. Cloning and characterization of MUPP1, a novel PDZ domain protein. *FEBS Lett.* **424**:63-68.
58. **Weiss, R. S., M. O. Gold, H. Vogel, and R. T. Javier.** 1997. Mutant adenovirus type 9 E4 ORF1 genes define three protein regions required for transformation of CREF cells. *J. Virol.* **71**:4385-4394.
59. **Weiss, R. S., and R. T. Javier.** 1997. A carboxy-terminal region required by the adenovirus type 9 E4 ORF1 oncoprotein for transformation mediates direct binding to cellular polypeptides. *J. Virol.* **71**:7873-7880.
60. **Weiss, R. S., S. S. Lee, B. V. Prasad, and R. T. Javier.** 1997. Human adenovirus early region 4 open reading frame 1 genes encode growth-transforming proteins that may be distantly related to dUTP pyrophosphatase enzymes. *J. Virol.* **71**:1857-1870.
61. **Weiss, R. S., M. J. McArthur, and R. T. Javier.** 1996. Human adenovirus type 9 E4 open reading frame 1 encodes a cytoplasmic transforming protein capable of increasing the oncogenicity of CREF cells. *J. Virol.* **70**:862-872.

62. **Westphal, R. S., and E. Sanders-Bush.** 1996. Differences in agonist-independent and -dependent 5-hydroxytryptamine 2C receptor-mediated cell division. *Mol. Pharmacol.* **49**:474-480.
63. **Willott, E., M. S. Balda, A. S. Fanning, B. Jameson, C. Van Itallie, and J. M. Anderson.** 1993. The tight junction protein ZO-1 is homologous to the *Drosophila* discs-large tumor suppressor protein of septate junctions. *Proc. Natl. Acad. Sci. USA* **90**:7834-7838.
64. **Wu, H., S. M. Reuver, S. Kuhlendahl, W. J. Chung, and C. C. Garner.** 1998. Subcellular targeting and cytoskeletal attachment of SAP97 to the epithelial lateral membrane. *J. Cell. Sci.* **111**:2365-2376.
65. **Xia, H., S. T. Winokur, W. L. Kuo, M. R. Altherr, and D. S. Brett.** 1997. Actinin-associated LIM protein: identification of a domain interaction between PDZ and spectrin-like repeat motifs. *J. Cell Biol.* **139**:507-515.
66. **Yang, N., O. Higuchi, and K. Mizuno.** 1998. Cytoplasmic localization of LIM-kinase 1 is directed by a short sequence within the PDZ domain. *Exp. Cell Res.* **241**:242-252.

TABLE 1. Carboxyl-terminal amino-acid sequences of human adenovirus E4-ORF1 and human papillomavirus E6 proteins[†]

Protein	Carboxyl-terminal amino-acid sequence			
	<u>Consensus type I PDZ domain-binding motif</u>			
	X	(S/T)	X	(V/I/L)-COOH
<i>wt</i> 9ORF1	A	T	L	V
IIIA 9ORF1	A	P		
IIIC 9ORF1	D	T	L	V
IIID 9ORF1	A	T	P	V
<i>wt</i> 5ORF1	A	S	N	V
<i>wt</i> 12ORF1	A	S	L	I
<i>wt</i> 18E6	E	T	Q	V
18E6-V158A	E	T	Q	A
18E6-T156D/V158A	E	D	Q	A
<i>wt</i> 11E6	D	L	L	P

[†]The sequence of the last four amino-acid residues at the carboxyl-terminus of E4-ORF1 proteins from Ad9 (9ORF1), Ad5 (5ORF1), and Ad12 (12ORF1), and the HPV-18 E6 (18E6) protein define a consensus type I PDZ domain-binding motif, whereas the HPV-11 E6 (11E6) protein lacks such a motif. Also shown are 9ORF1 and 18E6 mutant proteins having altered or disrupted PDZ domain-binding motifs. Substitution mutations are depicted as bolded amino-acid residues.

Figure Legends

Fig. 1. The partial mouse protein 9BP-1 represents the carboxyl-terminus of the mouse multi-PDZ protein MUPP1. (A) PDZ-domain organizations of the partial mouse protein 9BP-1 (688 aa-residues) and the mouse multi-PDZ domain protein MUPP1 (2055 aa-residues). Note that the domain organization of 9BP-1 is identical to that of the carboxyl-terminal region of MUPP1. The unique protein region used to generate MUPP1 antisera is indicated. (B) The partial mouse protein 9BP-1 exhibits 99% amino-acid sequence identity with the carboxyl-terminal region of the mouse MUPP1 protein (aa-residues 1368-2055). Highlighted sequences denote PDZ-homology domains. Sequence alignment was performed using the Align Global Sequence Alignment algorithm from the Baylor College of Medicine Search Launcher Web site.

Fig. 2. 9ORF1-associated protein p220 displays similar properties as both 9BP-1 and MUPP1. (A) 9BP-1 and 9ORF1-associated protein p220 co-migrate and exhibit identical species-specific gel mobilities. Proteins from RIPA buffer-lysed mouse 3T3, rat CREF, human 293, and human TE85 cell lines were either immunoblotted with 9BP-1 antiserum (*left panel*) or first subjected to a GST pulldown assay with the indicated fusion protein and then blotted with a radiolabeled 9ORF1 protein probe (*right panel*). For the experiment shown in the left or right panel, 100 μ g or 2.5 mg of cell proteins was used, respectively, and the protein gels were run in parallel. Asterisks indicate 9ORF1-associated protein p220. (B) MUPP1 antiserum cross-reacts with 9BP-1 protein derived from several different species. Cell proteins (2.5 mg) in RIPA buffer from the indicated cell lines were first immunoprecipitated with either 9BP-1 antiserum (α -9BP-1) or the matched pre-immune serum (pre) and then immunoblotted with MUPP1

antiserum. Also note that the 9BP-1 protein detected above in (A) (*left panel*) and the MUPP1 protein detected here exhibited identical species-specific gel mobilities. IP, immunoprecipitation.

Fig. 3. 9ORF1 binds MUPP1 *in vitro*. GST-9ORF1 binds HA epitope-tagged rat MUPP1 protein (HAMUPP1) expressed in COS7 cells. Cells were lipofected with 4 μ g of either empty GW1 plasmid (vector) or GW1-HAMUPP1 plasmid, and cell proteins in RIPA buffer were either immunoblotted with HA antibodies (*left panel*) or first subjected to a GST pulldown assay with the indicated wild-type or mutant E4-ORF1 fusion protein (see Table 1) and then immunoblotted with HA antibodies (*right panel*). 100 μ g or 1 mg of COS7 cell proteins was used in the experiment shown in the left or right panel, respectively.

Fig. 4. 9ORF1 complexes with MUPP1 in cells. (A) 9ORF1 complexes with HA epitope-tagged rat MUPP1 protein (HAMUPP1) expressed in COS7 cells. Cells were lipofected with 6 μ g of GW1-HAMUPP1 plasmid and 2 μ g of either empty GW1 plasmid (vector) or a GW1 plasmid expressing wild-type or the indicated mutant 9ORF1 protein. Cell proteins in RIPA buffer were either immunoblotted with HA antibodies or 9ORF1 antiserum (*left panel*) or first immunoprecipitated with 9ORF1 antiserum (α -9ORF1) and then immunoblotted with HA antibodies or 9ORF1 antiserum (*right panel*). 100 μ g or 800 μ g of cell proteins was used in the experiment shown in the left or right panel, respectively. (B) 9ORF1 complexes with endogenous MUPP1 of CREF cells. Cell proteins in RIPA buffer were either immunoblotted with MUPP1 or 9ORF1 antiserum (*upper panel*) or first immunoprecipitated with 9ORF1 antiserum or the matched pre-immune serum (pre) (*lower left panel*) or, alternatively, with either MUPP1 antiserum (α -MUPP1) or the matched pre-immune serum (pre) (*lower right panel*), and

then immunoblotted with either MUPP1 or 9ORF1 antiserum. 100 μ g, 3 mg, or 3 mg of CREF cell proteins was used in the experiment shown in the upper, lower left, or lower right panel, respectively. (C) 9ORF1 complexes with MUPP1 in the Ad9-induced rat mammary tumor cell line 20-8. This tumor cell line contains a single integrated copy of the entire Ad9 viral genome (unpublished results). Cell proteins (3 mg) in RIPA buffer were first immunoprecipitated with either 9BP-1 antiserum (α -9BP-1) or the matched pre-immune serum and then immunoblotted with either 9ORF1 or 9BP-1 antiserum.

Fig. 5. MUPP1 PDZ7 and PDZ10 mediate binding to 9ORF1. (A) Illustration of the full-length MUPP1 polypeptide and ten different MUPP1 GST fusion protein constructs used in protein blotting assays. (B) 9ORF1 binds MUPP1 PDZ7 and PDZ10 *in vitro*. Approximately 1 μ g of each indicated MUPP1 GST fusion protein was immobilized on a membrane and protein blotted with a radiolabeled 9ORF1 protein probe. As a control, the membrane was stained with Coomassie brilliant blue dye to verify that an equivalent amount of each fusion protein was used in the experiment (data not shown). (C) A MUPP1 deletion mutant lacking both PDZ7 and PDZ10 fails to complex with 9ORF1 in COS7 cells. Cells were lipofected with 6 μ g of a GW1 plasmid expressing wild-type or the indicated deletion-mutant MUPP1 protein together with 2 μ g of either empty GW1 plasmid (vector) or the GW1-9ORF1wt plasmid. Cell proteins in RIPA buffer were either immunoblotted with HA antibodies (*upper panel*) or first immunoprecipitated with 9ORF1 antiserum (α -9ORF1) and then immunoblotted with HA antibodies or 9ORF1 antiserum (*lower panel*). 50 μ g or 750 μ g of cell proteins was used in the experiment shown in the upper or lower panel, respectively.

Fig. 6. 9ORF1 aberrantly sequesters MUPP1 within punctate bodies in the cytoplasm of cells. (A) Determination of the subcellular localization of MUPP1 in normal CREF cells (CREF) or CREF cell lines stably expressing wild-type (CREF-9ORF1) or the indicated mutant 9ORF1 protein (CREF-IIIA, CREF-IIIC, CREF-IIID). Indirect immunofluorescence (IF) microscopy assays were performed with either MUPP1 antiserum (α -MUPP1) or the matched pre-immune serum (pre). Despite the fact that all of the CREF cell lines expressed similar amounts of MUPP1 protein (see Fig. 7A), the MUPP1 staining for CREF-9ORF1 cells appeared brighter than that of the other CREF lines. This effect likely resulted from the large amounts of MUPP1 protein concentrated within the cytoplasmic punctate bodies. Discontinuous cell-cell contact staining for MUPP1 was most evident in normal CREF cells, and CREF-IIIA and CREF-IIIC lines, all of which exhibited similar MUPP1 staining patterns. As an example of this cell-cell contact staining, two adjacent CREF-IIIC cells within the delimited rectangular region are shown offset at higher magnification. (B) 9ORF1 and MUPP1 co-localize within punctate bodies in the cytoplasm of CREF cells. Double-labeling IF microscopy assays using both MUPP1 antiserum and HA antibodies (α -HA) were performed with CREF cells stably expressing HA epitope-tagged 9ORF1 protein (CREF-HA9ORF1). Each of the three panels shows the identical field containing the same three cells. The upper left and upper right panels show the MUPP1 and 9ORF1 staining patterns, respectively, whereas the lower panel shows the merged images.

Fig. 7. 9ORF1 aberrantly redistributes MUPP1 into the RIPA buffer-insoluble fraction of cells. (A) Similar amounts of MUPP1 and 9ORF1 proteins within CREF cell lines stably expressing wild-type and mutant 9ORF1 proteins. Cell proteins (100 μ g) extracted with sample

buffer were immunoblotted with MUPP1 antiserum or 9ORF1 antiserum. (B) Wild-type 9ORF1 specifically redistributes MUPP1 into the RIPA buffer-insoluble fraction of CREF cells. Cells from the indicated CREF lines were lysed in RIPA buffer and centrifuged to yield a RIPA buffer-soluble supernatant fraction and a RIPA buffer-insoluble pellet fraction (see *Materials and Methods*). Cell proteins from an equivalent volume of either the soluble or insoluble fraction were immunoblotted with MUPP1 or 9ORF1 antiserum. (C) Most MUPP1 protein is complexed with 9ORF1 in 9ORF1-expressing CREF cells. Cell proteins (3 mg) in the RIPA buffer-soluble fraction of normal CREF cells or wild-type 9ORF1-expressing CREF cells were subjected to five serial immunoprecipitations with 9ORF1 antiserum. Relative amounts of MUPP1 and 9ORF1 protein remaining in this fraction (100 µg of protein) "before" and "after" performing the serial immunoprecipitations was determined by immunoblot analysis. (D) Wild-type 9ORF1 also specifically redistributes HA epitope-tagged rat MUPP1 (HAMUPP1) into the RIPA buffer-insoluble fraction of 293 cells. Cells were lipofected with 1 µg of GW1-HAMUPP1 plasmid and 3 µg of either empty GW1 plasmid (vector) or a GW1 plasmid expressing wild-type or the indicated mutant 9ORF1 protein. Cell fractionation assays were performed as described above in (B), except cell proteins were immunoblotted with HA antibodies or 9ORF1 antiserum.

Fig. 8. 18E6 binds MUPP1 *in vitro*. GST-18E6 binds HA epitope-tagged rat MUPP1 (HAMUPP1) exogenously expressed in COS7 cells. Cells were lipofected with 8 µg of GW1-HAMUPP1 plasmid, and cell proteins (250 µg) in RIPA buffer were first subjected to a GST pulldown assay with the indicated fusion protein and then immunoblotted with HA antibodies.

Fig. 9. 18E6 promotes degradation of the MUPP1 protein *in vitro*. *In vitro* translated MUPP1, DLG, or p53 protein was incubated for the indicated times with a 5-fold to 10-fold molar excess of *in vitro* translated 18E6 protein (+) or with an equivalent volume of a water-primed *in vitro* translation reaction (-). Proteins from each reaction were subjected to immunoprecipitation with MUPP1, DLG, or p53 antibodies, respectively, and detected by autoradiography.

Fig. 10. 18E6 reduces the steady-state levels of MUPP1 protein in cells. (A) 18E6 reduces the steady-state levels of HA epitope-tagged rat MUPP1 (HAMUPP1) protein expressed in COS7 cells. Cells were lipofected with 1 μ g of GW1-HAMUPP1 plasmid and 4 μ g of either empty GW1 plasmid (vector) or a GW1 plasmid expressing HA epitope-tagged wild-type or the indicated mutant 18E6 protein, or expressing HA epitope-tagged wild-type 11E6 protein. Cell proteins (30 μ g) in RIPA buffer were immunoblotted with HA antibodies. (B) 18E6 does not bind HA epitope-tagged PDZ-protein ZO-1 (HAZO-1). Cells were lipofected with 3 μ g of either empty GW1 plasmid (vector), GW1-HADLG plasmid, or GW1-HAZO-1 plasmid, and cell proteins in RIPA buffer were either immunoblotted with HA antibodies (*left panel*) or first subjected to a GST pulldown assay with the indicated fusion protein and then immunoblotted with HA antibodies (*right panel*). 10 μ g or 75 μ g of COS7 cell proteins was used in the experiment shown in the left or right panel, respectively. HADLG was included as a positive control in these binding assays (30). (C) 18E6 does not reduce HAZO-1 protein levels in COS7 cells. COS7 cells were lipofected with 0.01 μ g of GW1-HAZO-1 plasmid and 4 μ g of either empty GW1 plasmid (vector) or a GW1 plasmid expressing HA epitope-tagged wild-type or the

indicated mutant 18E6 protein. Cell proteins (30 μ g) in RIPA buffer were immunoblotted with HA antibodies.

Fig. 11. 18E6 decreases the half-life of the MUPP1 protein in cells. 5.5×10^5 COS7 cells were lipofected with 5 μ g of empty GW1 plasmid (vector) or 1 μ g of GW1-HAMUPP1 plasmid and 4 μ g of either empty GW1 plasmid (HAMUPP1) or the GW1-18E6 plasmid (HAMUPP1 + 18E6). At 24 h post-transfection, cells were pulse labeled and then chased for the indicated times (see *Materials and Methods*). Cell proteins (200 μ g) were immunoprecipitated with HA antibodies (α -HA), and HAMUPP1 protein was detected by autoradiography and quantified with a phosphorimager.

Figure 1A

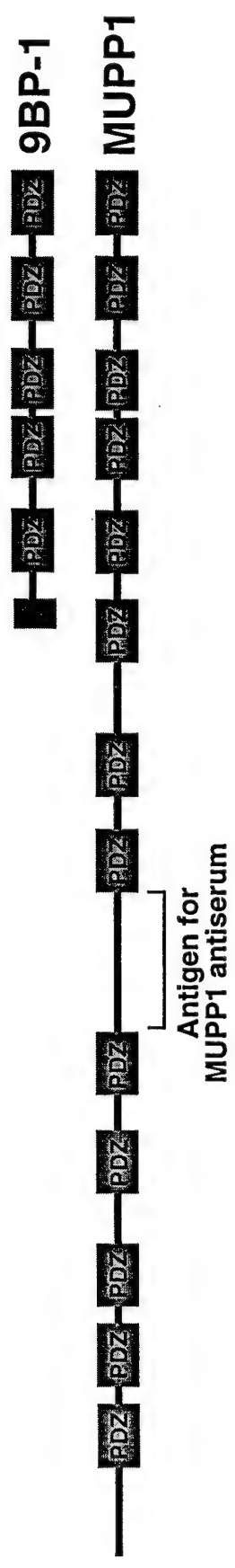


Figure 1B

9BP-1	1	IDPTGAAGRDGRLQIADELLEINGQILYGRSHONASSIIKCAPSKVKIIFIRNADAVNQTAVCPCGIAADSPSSTSDSPQN	80
MUPP1	1368	1447
9BP-1	81	KEVEPCSTTSASAADLSSI	160
MUPP1	1448	KEVEPCSTTSASAADLSSI	1527
9BP-1	161	CPVEKFIISLLKTAKATVKLIVRAENPACPAVPSSAVTVSGERKDNSQTPAVPAPDLEPIPSTSRSTPAVFASDPATCPI	240
MUPP1	1528	CPVEKFIISLLKTAKATVKLTVRAENPACPAVPSSAVTVSGERKDNSQTPAVPAPDLEPIPSPSRSTPAVFASDPATCPI	1607
9BP-1	241	IPGCETTTIEISKGTGLGLSIVGGSDTLGALIIHEVVEEGAACKDGRWLWAGDQILLEVNGIDLKATHDEAINVLRQTPQ	320
MUPP1	1608	IPGCETTTIEISKGTGLGLSIVGGSDTLGALIIHEVVEEGAACKDGRWLWAGDQILLEVNGIDLKATHDEAINVLRQTPQ	1687
9BP-1	321	RVRLTLYRDEAPYKEEDV	400
MUPP1	1688	RVRLTLYRDEAPYKEEDV	1767
9BP-1	401	ATQEAVALLLKCSLGAVTLEVGRVKAAPFHSERRPSSQSSQVSESSLSSFTPLSGINTSESLESNSKKNALASEIQRLRT	480
MUPP1	1768	ATQEAVALLLKCSLGAVTLEVGRVKAAPFHSERRPSSQSSQVSESSLSSFTPLSGINTSESLESNSKKNALASEIQRLRT	1847
9BP-1	481	VEIKKGPADSLGLSIAGGVGSPGLDVPIFIAMMHPNGVAAQTOKLRVGDRIVTICGTSTDCGTHHTQAVNLMKNASGSIEV	560
MUPP1	1848	VEIKKGPADSLGLSIAGGVGSPGLDVPIFIAMMHPNGVAAQTOKLRVGDRIVTICGTSTDCGTHHTQAVNLMKNASGSIEV	1927
9BP-1	561	QVVAGGDVSVVTGHHQQLANPCLAFGLTSSSIFPDDLGP	640
MUPP1	1928	QVVAGGDVSVVTGHHQQLANPCLAFGLTSSSIFPDDLGP	2007
9BP-1	641	GAAAEEDGRLKRGDQIIAVNGQSLGVTHEEAVAILKRTKGTVTLMVLS	688
MUPP1	2008	GAAAEEDGRLKRGDQIIAVNGQSLGVTHEEAVAILKRTKGTVTLMVLS	2055

Figure 2A

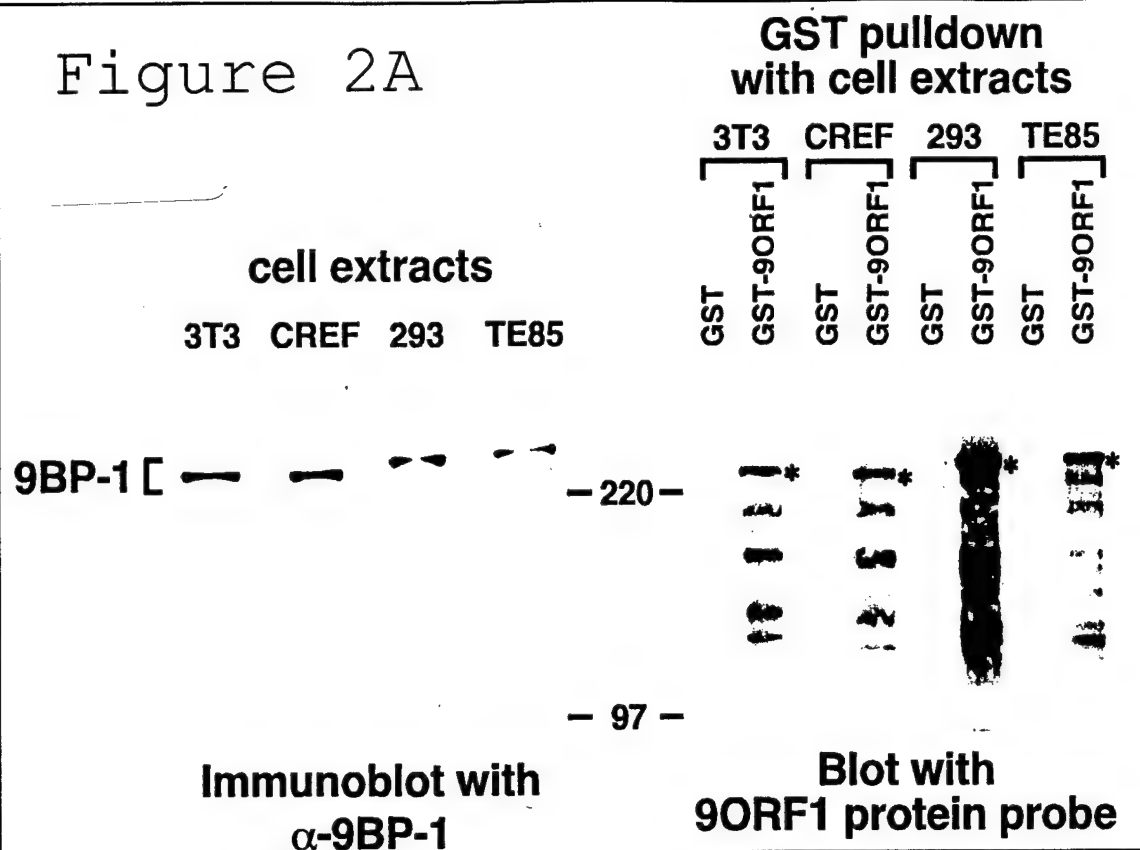


Figure 2B

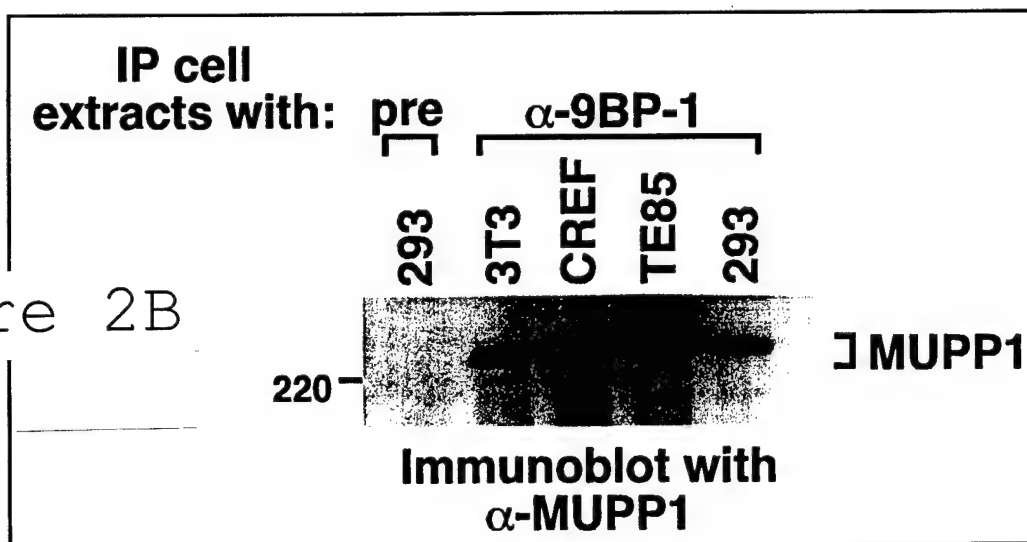


Figure 3

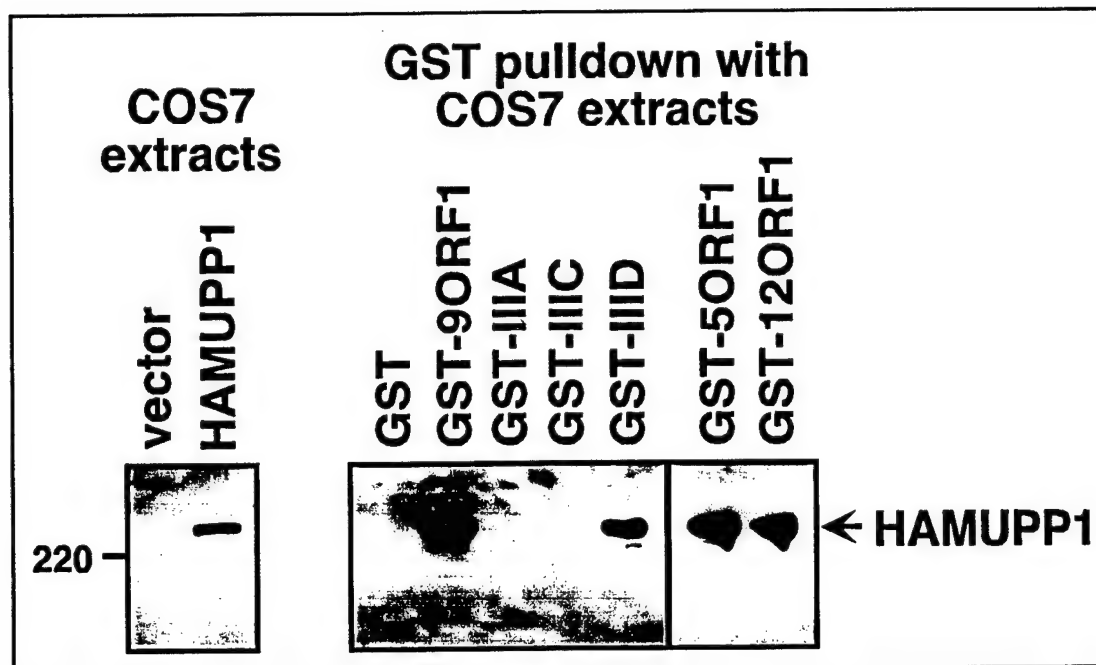


Figure 4A

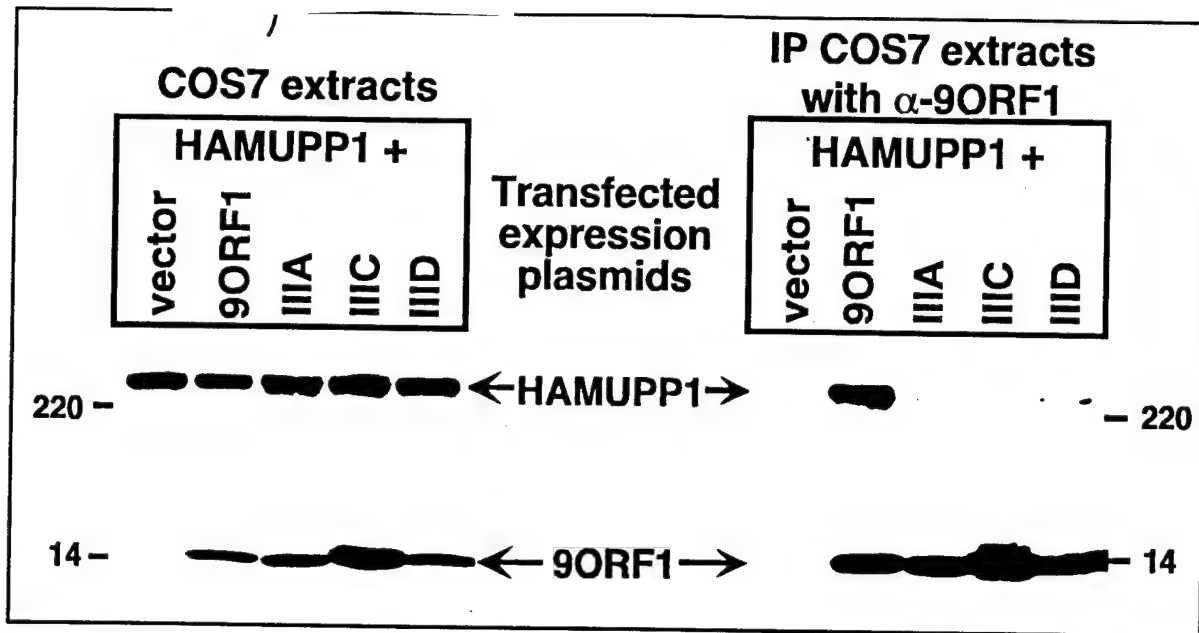


Figure 4B

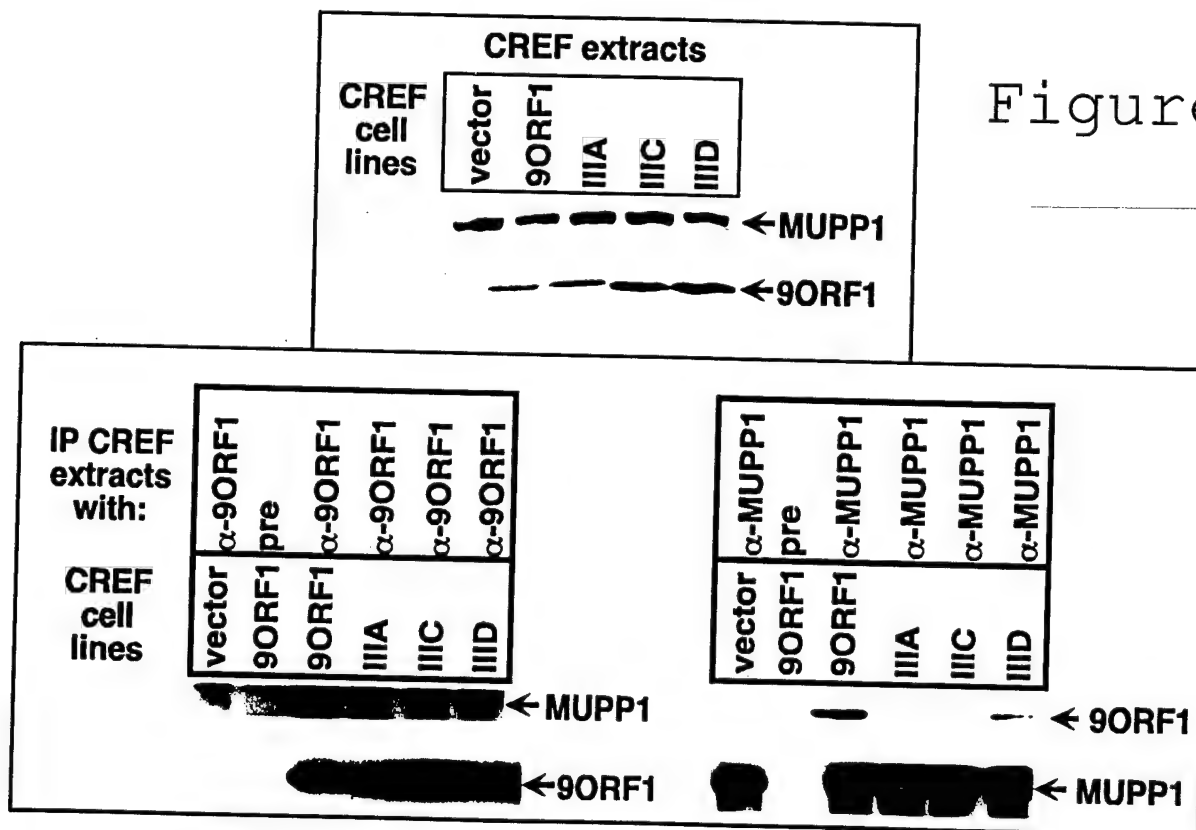


Figure 4C

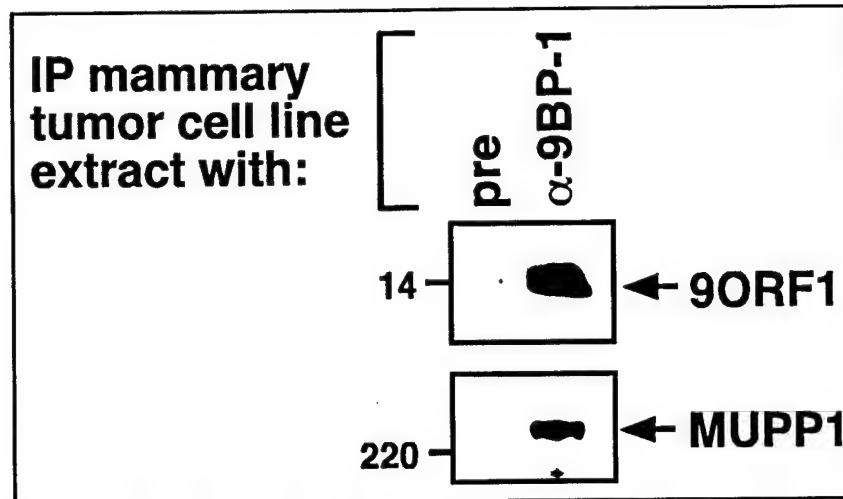


Figure 5A

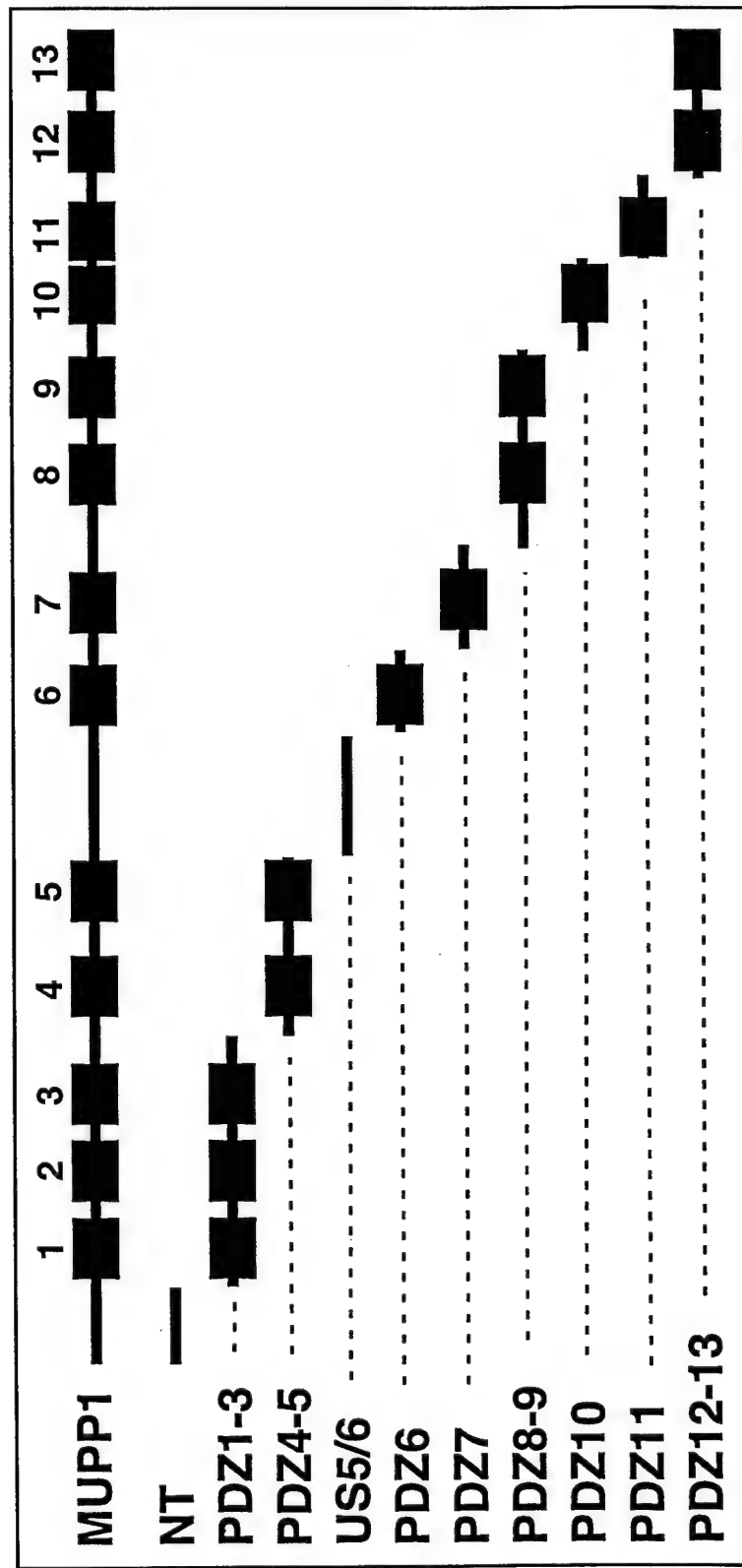


Figure 5B

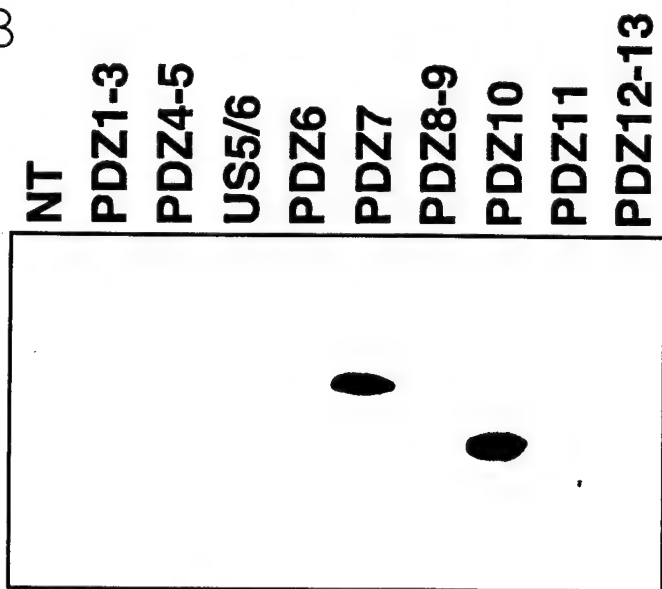


Figure 5C

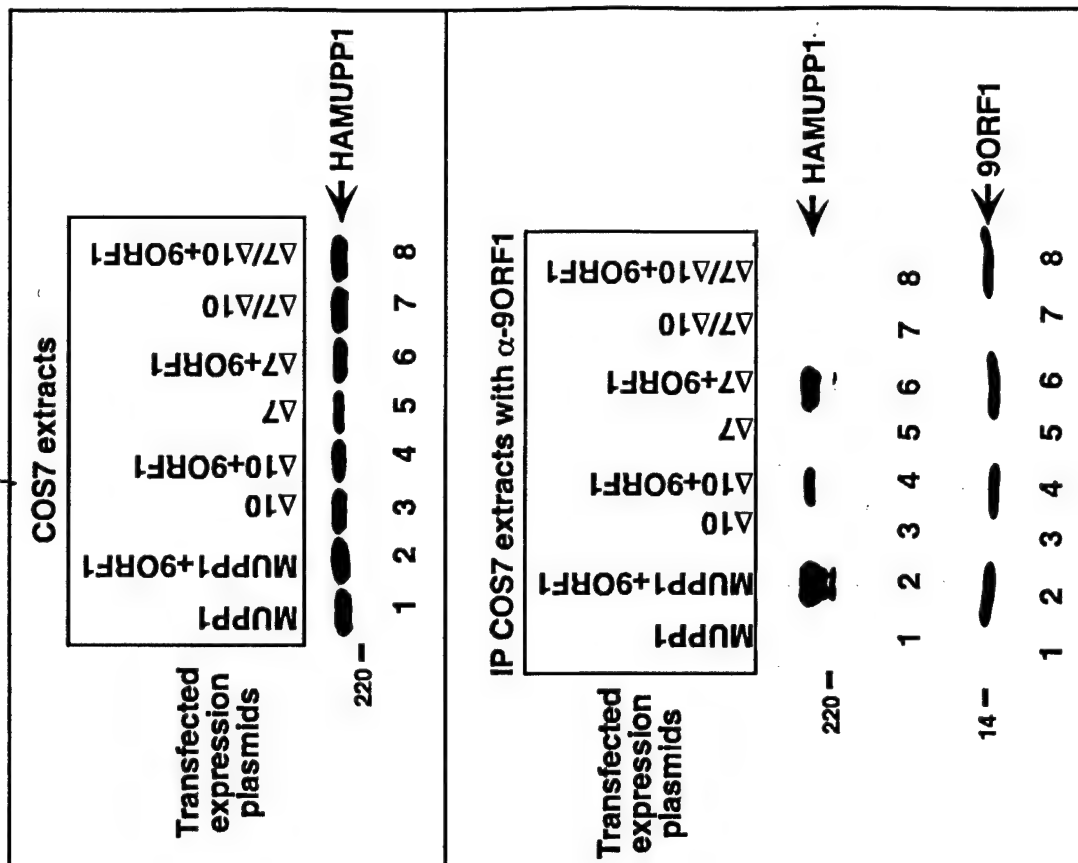


Figure 6A

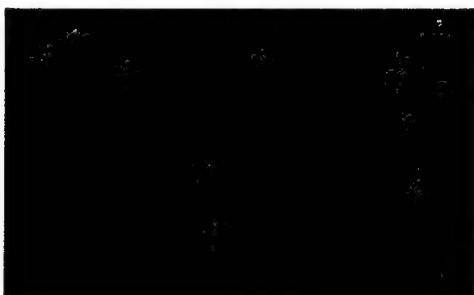
CREF/pre



CREF/ α -MUPP1



CREF-9ORF1/ α -MUPP1



CREF-IIIA/ α -MUPP1



CREF-IIIC/ α -MUPP1



CREF-IIID/ α -MUPP1



Figure 6B

CREF-HA9ORF1 cells

α -MUPP1



α -HA (9ORF1)



α -MUPP1 + α -HA



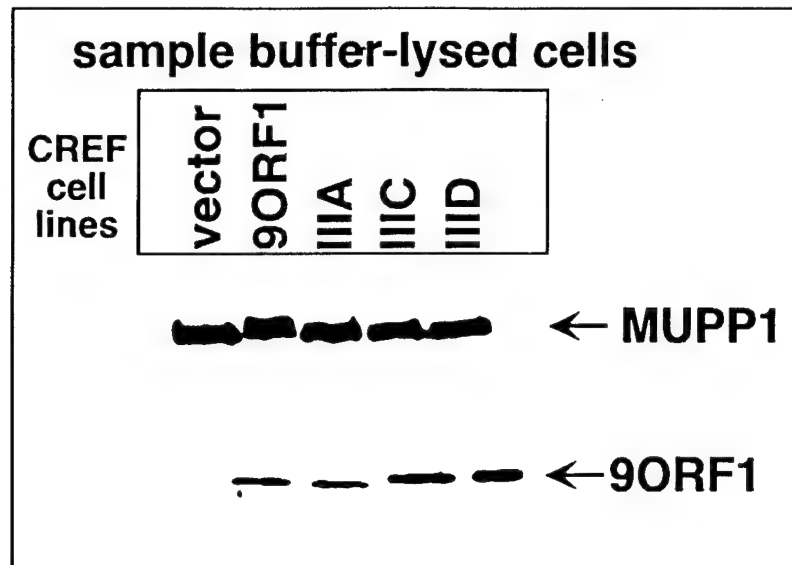
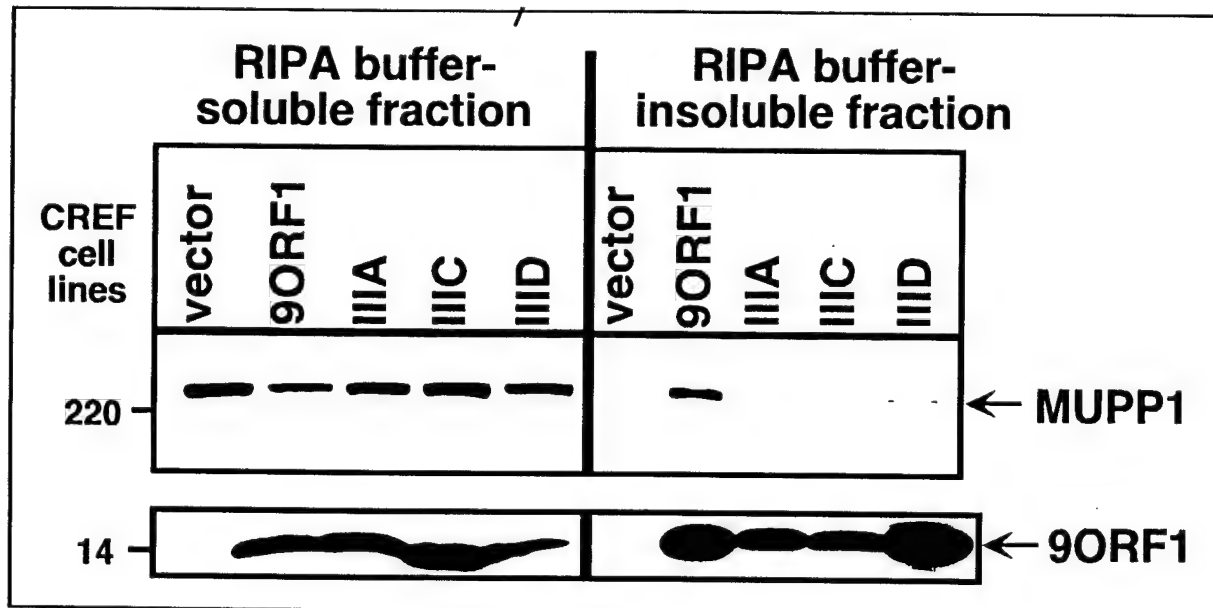


Figure 7A

Figure 7B



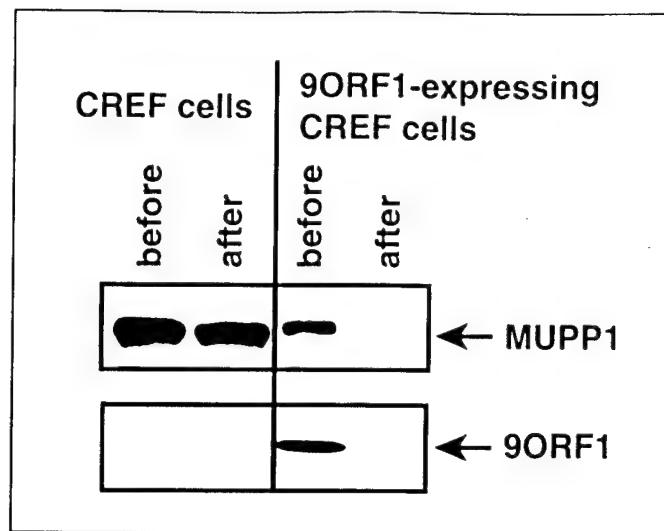


Figure 7C

Figure 7D

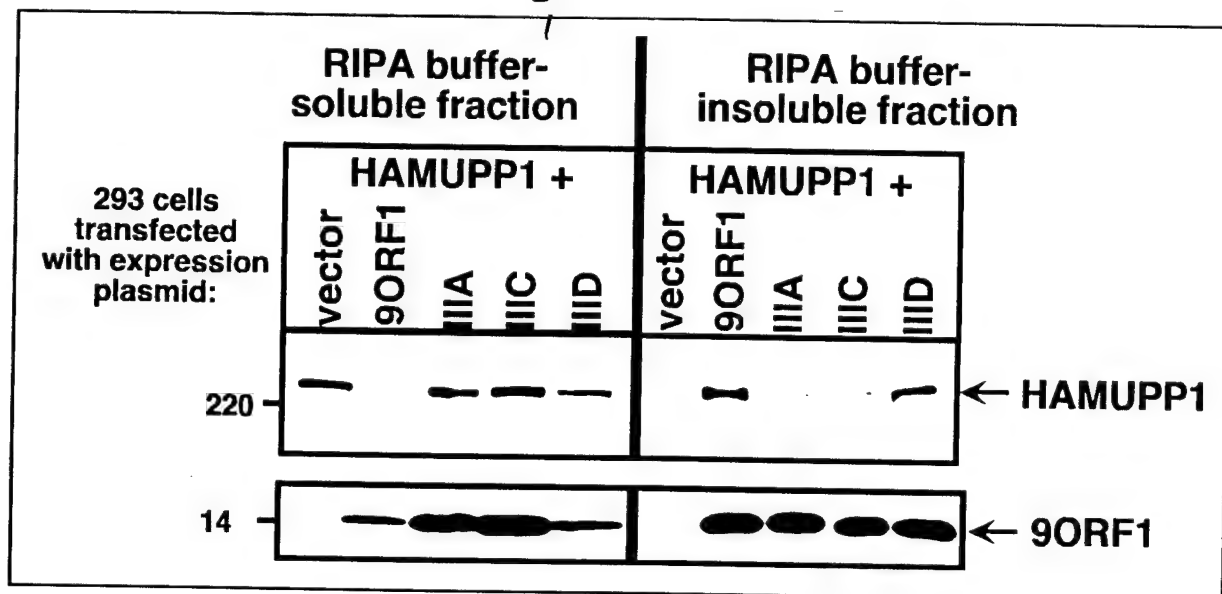


Figure 8

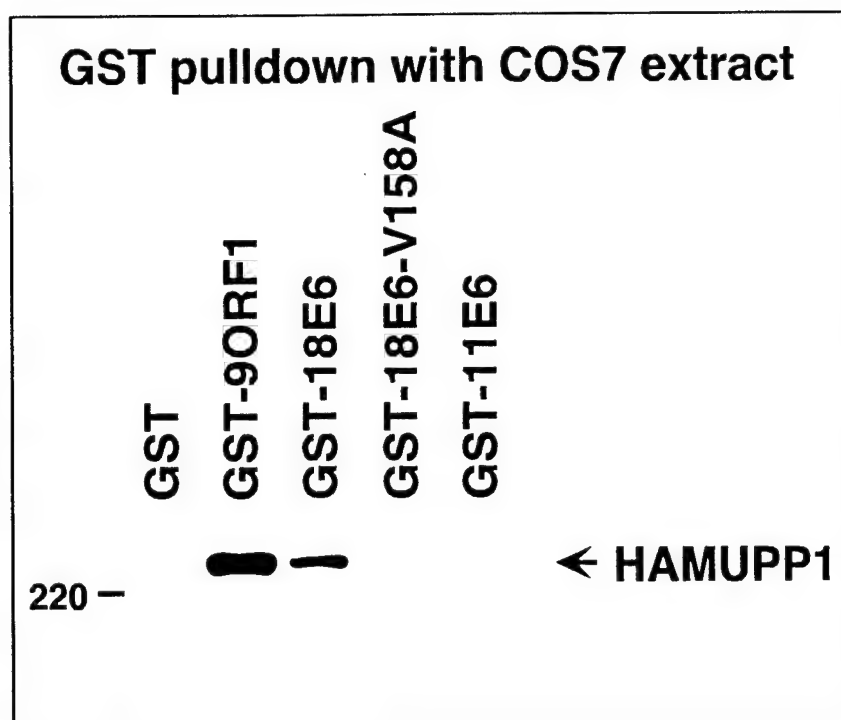
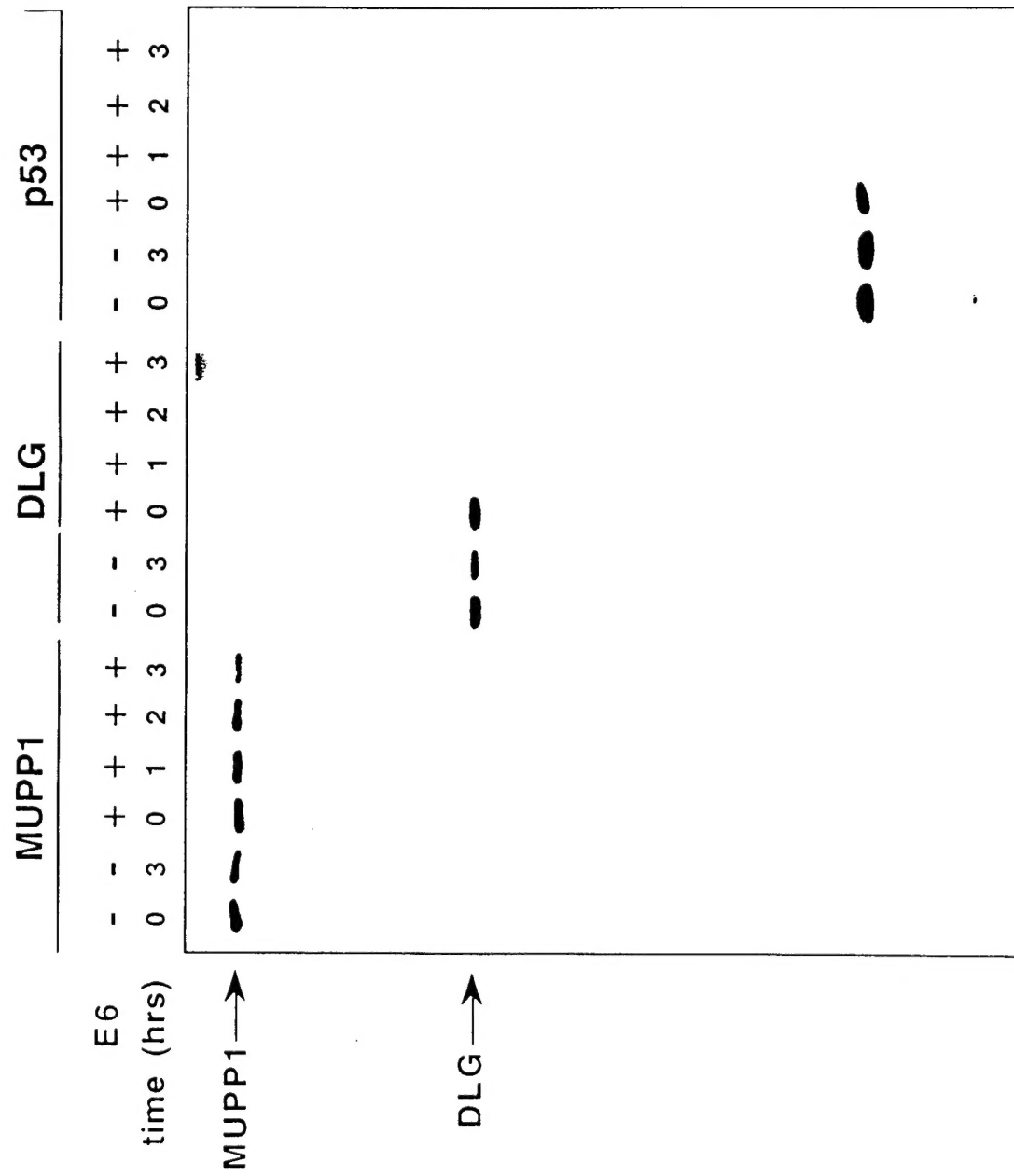


Figure 9



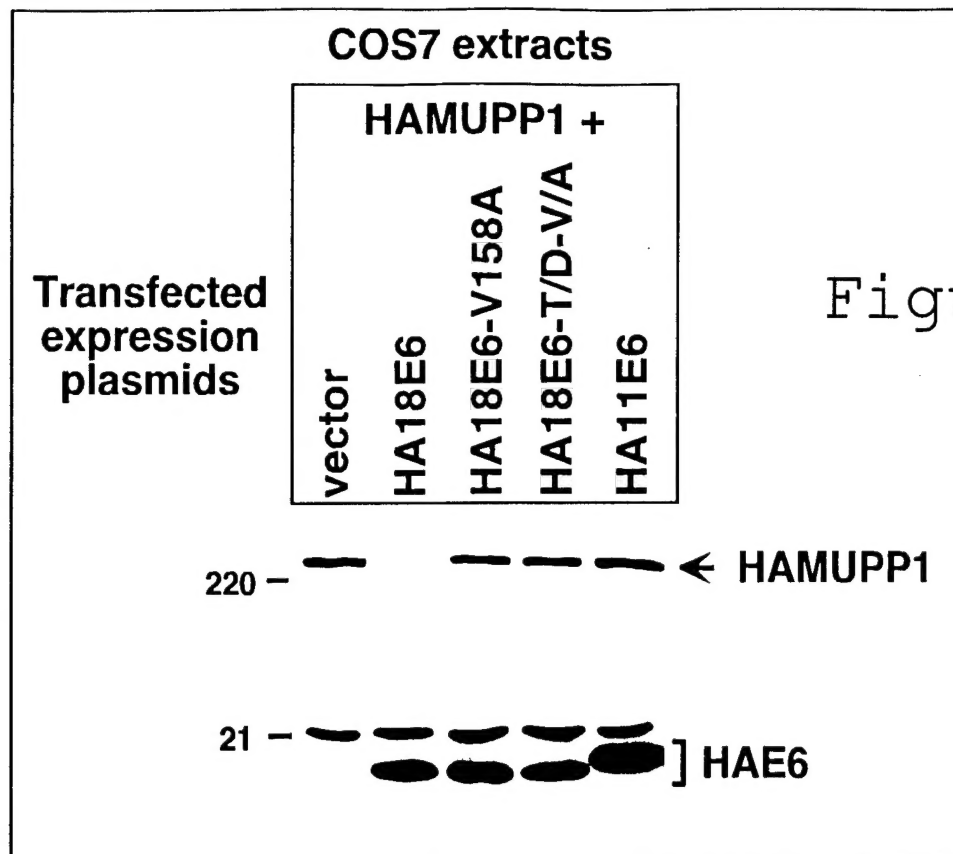
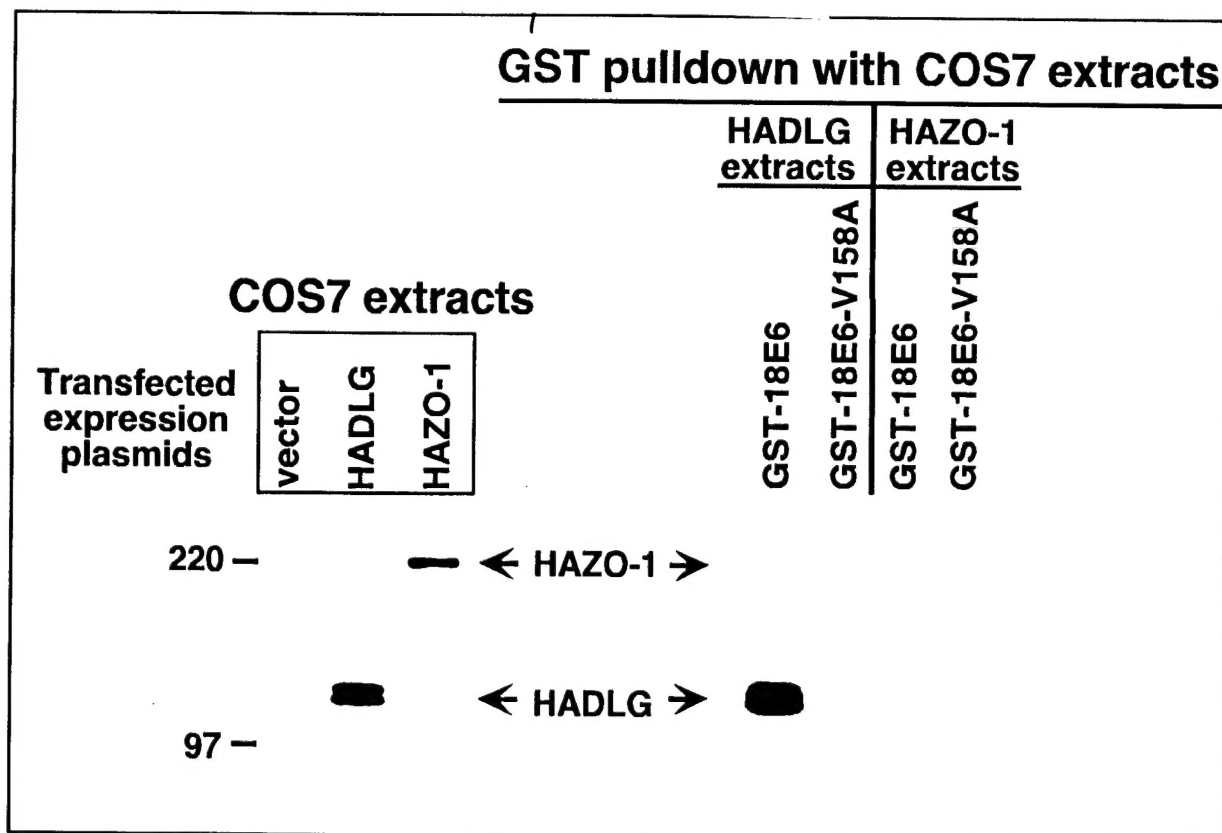


Figure 10B



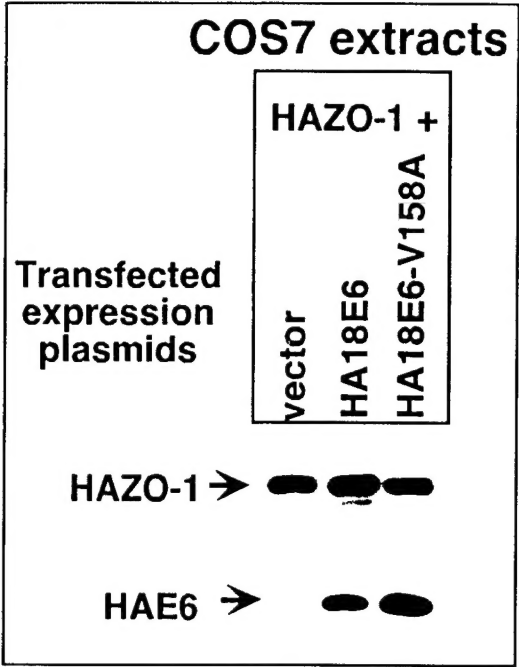


Figure 10C

— — — — —

